

QUANTUM ASPECTS
OF
EARLY UNIVERSE THERMODYNAMICS

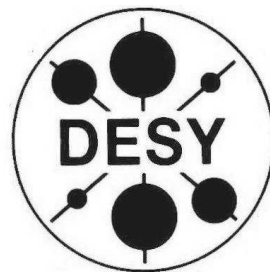
Dissertation
zur Erlangung des Doktorgrades
des Departments Physik
der Universität Hamburg

vorgelegt von

Marco Drewes

aus Hamburg

verfasst am Deutschen Elektronen Synchrotron



Hamburg

2009

Gutachter der Dissertation:	Prof. Dr. W. Buchmüller Prof. Dr. K. Fredenhagen
Gutachter der Disputation:	Prof. Dr. W. Buchmüller Prof. Dr. J. Bartels
Datum der Disputation:	27.10.2009
Vorsitzende des Prüfungsausschusses:	Prof. Dr. C. Hagner
Vorsitzender des Promotionsausschusses:	Prof. Dr. R. Klanner
Dekan der Fakultät MIN:	Prof. Dr. H. Graener

Abstract

Various features of the observable universe can be understood as the result of nonequilibrium processes during the early stages of its history, when it was filled with a hot primordial plasma. In many cases, including cosmological freezeout processes, only a few degrees of freedom were out of equilibrium and the background plasma can be viewed as a large heat bath to which these couple. We study scalar and fermionic quantum fields out of thermal equilibrium that are weakly coupled to a large thermal bath with the goal to formulate a full quantum mechanical description of such processes. The bath composition need not be specified. Our analysis is based on Kadanoff-Baym equations, which are the exact equations of motion for the correlation functions in a nonequilibrium quantum system. We solve the equations of motion for the most general Gaussian initial density matrix, without a specific ansatz or a-priori parameterisation and for arbitrarily large deviations from equilibrium. The solutions depend on integral kernels that contain memory effects. These can in good approximation be solved analytically when the field excitations have a small decay width. The full solutions are compared to results obtained by other methods. We prove that the description in terms of a stochastic Langevin equation is equivalent to the Kadanoff-Baym equations. We show the emergence of standard Boltzmann equations as a limit of the Kadanoff-Baym equations in a dilute gas when coherences play no role and discuss quantum Boltzmann equations as an intermediate step. We analyse the properties of the solutions in terms of the equation of state and investigate the validity and implications of quasiparticle approximations. We find that the equation of state can deviate significantly from that of a gas of quasiparticles even if the resonances in the plasma show quasiparticle behaviour in decays and scatterings. A detailed discussion is devoted to the influence of modified dispersion relations and widths in the plasma on gain and loss rates. We illustrate our results in two models for the bath composition, a scalar and a Yukawa model. In both cases we give analytic expressions for the imaginary parts of the self energies, which govern the gain and loss rates. Finally, we discuss applications in cosmology. Our results provide a toolkit for a full quantum mechanical description of cosmological freezeout processes. We discuss the application to thermal leptogenesis, where quantum effects are likely to be of great relevance. The scalar model can also be used to describe the late phase of reheating. In this context, we analyse under which circumstances large thermal masses can put an upper bound on the reheating temperature.

Zusammenfassung

Viele Eigenschaften des beobachtbaren Universums lassen sich als Ergebnisse von Nichtgleichgewichtsprozessen in seiner Frühgeschichte verstehen. Dabei befinden sich in vielen Fällen nur wenige Freiheitsgrade außerhalb des thermischen Gleichgewichts und der Rest des Plasmas fungiert als Wärmebad, an das diese schwach koppeln. Um eine quantenmechanische Beschreibung dieser Prozesse zu ermöglichen, untersuchen wir das Verhalten von skalaren und fermionischen Quantenfeldern außerhalb des thermischen Gleichgewichts, die schwach an ein thermisches Bad gekoppelt sind. Die Zusammensetzung des Bads muss für eine allgemeine Betrachtung nicht spezifiziert werden. Unsere Analyse basiert auf Kadanoff-Baym Gleichungen. Diese sind exakte Bewegungsgleichungen für Korrelationsfunktionen von Quantenfeldern außerhalb des thermischen Gleichgewichts. Wir lösen die Bewegungsgleichungen für gaußsche Anfangsbedingungen mit beliebig großer Abweichung vom Gleichgewicht in voller Allgemeinheit. Die gefundenen Ausdrücke enthalten Integralkerne, die nicht-markowsche Effekte parameterisieren. Wenn die Zerfallsbreiten der Resonanzen im Plasma klein sind, können diese *Memory-Integrale* approximativ gelöst werden. Wir vergleichen die exakten Lösungen mit Ergebnissen, die mittels anderer Verfahren gefunden wurden. Wir beweisen, dass die häufig verwendete stochastische Beschreibung durch eine effektive Langevin Gleichung zu den Kadanoff-Baym Gleichungen äquivalent ist. Wir zeigen des weiteren, dass die klassischen Boltzmann Gleichungen den Grenzfall der Kadanoff-Baym Gleichungen in einem verdünnten Gas bilden, wenn Quantenkohärenzen vernachlässigbar sind, und diskutieren den Zusammenhang zu Quanten Boltzmann Gleichungen. Letztere sind effektive, von den Kadanoff-Baym Gleichungen abgeleitete Boltzmann Gleichungen, in denen nicht-markowsche und Quanteneffekte durch zeit- und temperaturabhängige Stoßterme parameterisiert sind. Bei der Formulierung effektiver Boltzmann Gleichungen, die deutlich einfacher zu lösen sind als die Kadanoff-Baym Gleichungen selbst, ist es von besonderem Interesse, unter welchen Umständen der Einfluss des Mediums auf die Kinematik von Streuprozessen und Zerfällen in einer Beschreibung durch Quasiteilchen parameterisiert werden kann. Dies ist der Fall, wenn die Zerfallsbreiten der Resonanzen im Plasma klein sind und Off-Shell Effekte vernachlässigt werden können. Die Dispersionsrelationen der Quasiteilchen und die Zustandsgleichung des Systems können jedoch selbst dann stark von dem in einem Gas aus freien Quasiteilchen zu erwartenden Verhalten abweichen. Wir illustrieren unsere Ergebnisse anhand eines skalaren und eines Yukawa Modells für die Zusammensetzung des Bads. Beide finden direkte Anwendung in der Kosmologie. Das skalare Modell kann zur Beschreibung der Reheating Phase am Ende der kosmischen Inflation verwendet werden. Mit den Ergebnissen aus dem Yukawa Modell stehen die Mittel für eine quantenmechanische Beschreibung der thermischen Leptogenese zur Verfügung.

Acknowledgements

I would like to express my gratitude to the various people who supported me in completing this work during the past three years. First of all, I would like to thank my supervisor Wilfried Buchmüller for his guidance and valuable advice. I have greatly benefited from sharing his expertise in the fields of particle physics and cosmology. I am also grateful to Alexey Anisimov and Sebastian Mendizabal, in collaboration with whom most of the results in this thesis were achieved. In a more indirect way, many other colleagues in the DESY theory group and the theory group at the Universität Hamburg have contributed to the completion of this work through many valuable discussions. To name just the most prominent, there are Laura Covi, Jonas Schmidt (thanks also for proof-reading), Istvan Montvay and Markus Diehl.

A special thanks goes to Susha Parameswaran and Clare Burrage for their regular advice on English language issues and Christian Hambrock for continuous IT support. I would also like to thank all the people from outside Hamburg whom I met on various occasions for helpful and inspiring scientific discussions, in particular Lev Kofman, Yu Lu, Owe Philipsen, Dietrich Bödeker and Jun'ichi Yokoyama.

Finally, I would like to thank my friends and family who made my life outside physics here in Hamburg a pleasant one. Most importantly there is my parents, to whom I owe so much during all the previous years. Yet another thanks goes to Sebastian and Chrischi, and for shorter periods Hao and Cecilie as well as our welcome visitor Chloé, for sharing an awesome time with me in the office... and of course to the rest of my family, in particular Oma Erika, Pascal, Verena and Nadine as well as Keule, Ferry, Frosch, Till, Camel, Tjark, Christin, Meikel, S-Bo, Dr.T. and all the other close friends who have been part of my life here in Hamburg for so many years.

My last thank is devoted to Nancy for her incredible patience and willingness to respect my decision to stay in the field of high energy physics, do a PhD here at DESY and accept a job offer in Europe. Thanks for waiting for me for all those years Nancy, and for your readiness to come a long way to be with me.

Contents

0.1	Acknowledgements	4
0.2	Introduction	7
0.3	Outline	9
1	Thermodynamics of Quantum Systems	10
1.1	Boltzmann Equations	10
1.2	Limitations of Boltzmann Equations	12
1.2.1	Breakdown of the Particle Concept	13
1.2.2	Oscillations and Decoherence Effects	17
1.3	Kadanoff-Baym Equations	17
1.3.1	Bosons	18
1.3.2	Fermions	27
1.3.3	Thermal Equilibrium	28
2	Weak Coupling to a thermal Bath	32
2.1	Langevin Equation	34
2.2	Solving the Kadanoff-Baym Equations	37
2.2.1	Solutions for Scalars	37
2.2.2	Solutions for Fermions	45
2.2.3	Approach to Thermal Equilibrium	48
2.3	Plasma Properties	50
2.3.1	Comparison to Boltzmann Equations	51
2.3.2	Quantum Boltzmann Equations	58
2.3.3	Kinematics of the Resonances	61
3	Simple Models for the Bath	71
3.1	A Scalar Field coupled to a Bath of Scalars	71
3.1.1	The trilinear Coupling g	72
3.1.2	The quartic Couplings h_i	76
3.1.3	Numerical Results	77
3.2	A Fermion with Yukawa Couplings	82

4 Applications in Cosmology	91
4.1 Inflaton Decay and Reheating	92
4.2 Thermal Leptogenesis	95
5 Conclusion	100
A Right Handed Neutrinos and the Seesaw Mechanism	103
B Some explicit Computations	105
B.1 Time Translation Invariance of Δ^-	105
B.2 The Fermion Self Energy	110
B.3 Analytic Properties of Propagators and Self Energies	117
B.4 S^+ in the narrow Width Limit and the use of Cauchy's Theorem	118

Introduction

Today, there exists overwhelming evidence suggesting that the observable universe is expanding and originates from a volume that was many orders of magnitude smaller than its current size (cf. [1, 2]). Consequently, the compressed matter was exposed to enormous density, pressure and temperature in the past. Many properties of the universe are the result of out-of-equilibrium processes during this very early, high-temperature phase (cf. [1, 3]). This includes cosmological phase transitions and the various freezeout processes that are crucial to give many cosmological parameters the values we observe today, in particular the creation of a matter-antimatter asymmetry, the production of dark matter, the formation of light elements and the decoupling of photons leading to the cosmic microwave background. Another example is the reheating after a possible inflationary phase.

The energy densities during the very early epochs of the history of the universe by far exceed those that can be realised in any human made experiment. Thus, the early universe is an excellent testing ground for predictions from theories beyond the standard model of particle physics. Hence, the study of nonequilibrium processes in the primordial plasma is interesting from a cosmology as well as particle physics point of view.

Freezeout processes in the early universe are usually described by means of Boltzmann equations. These are first order differential equations that describe the time evolution of particle number densities. They have proven an extremely useful tool in describing the creation of light elements and the decoupling of the cosmic microwave background from the primordial plasma in good agreement with observation [4]. However, Boltzmann equations are based on semiclassical approximations. They can be expected to hold in a weakly coupled, dilute plasma, but not in the presence of strong interactions or at high density. Given that the temperature of the primordial plasma increases as one goes backwards in time, it is questionable whether Boltzmann equations correctly describe processes that occurred earlier in the history of the universe. Furthermore, Boltzmann equations are unable to describe quantum phenomena like coherent oscillations, which may e.g. crucially influence the generation of a matter-antimatter asymmetry.

This makes a fully quantum mechanical treatment mandatory. Relativistic quantum mechanics generally enforces the abandonment of the concept of particle numbers, with correlation functions of quantum fields replacing them as the dynamical quantities. Unfortunately, the resulting equations of motion in most cases cannot be solved in a transparent way. One way to proceed is to employ numerical methods, generally at the loss of transparency. Though Boltzmann equations usually also have to be solved numerically to obtain quantitative results, they allow a better qualitative understanding of the

results and their parameter dependence, and often an approximate analytic solution can be obtained. In many cases numerical methods currently appear to be the only choice. Following another strategy, one can save some of the benefits of Boltzmann equations by modifying them to so called quantum Boltzmann equations. They can be derived from the full quantum theory as effective equations of motion when a number of simplifying assumptions is justified. Though being formulated in terms of particle numbers or classical phase space distribution functions, quantum Boltzmann equations include some of the quantum and non-Markovian effects left out by ordinary Boltzmann equations. This allows to treat complex problems without losing track of the relevant parameters.

In this work, we follow a third approach. Cosmological freezeout processes for different particle species are technically relatively simple problems if two conditions are fulfilled. First, it is assumed that only one or a few particle species freeze out simultaneously and the number of degrees of freedom out of equilibrium is much smaller than the total number of degrees of freedom in the plasma. Second, they should not coincide with other events such as cosmological phase transitions. We furthermore assume that self interactions of the field that is out of equilibrium are weak. However, we emphasise that we do not put any restrictions on the deviation from equilibrium. It can be arbitrarily large. In this case, there are three important simplifications:

- (1) The system is spatially homogeneous and isotropic.
- (2) In good approximation only one or a few degrees of freedom are out of equilibrium. The primordial plasma forms a large thermal bath to which these are weakly coupled. The many degrees of freedom in the bath make backreaction negligible, it approximately remains in thermal equilibrium on the timescale associated with particle reactions. The temperature changes only slowly due to Hubble expansion.
- (3) The quanta of the field which is out of equilibrium mainly scatter with quanta of the bath fields, not amongst themselves. The occupation numbers in the bath are determined by few parameters, the temperature T and chemical potentials μ_i , which considerably simplifies computations of the gain and loss rates. The same applies to decays and inverse decays.

This thesis is devoted to systems in which these conditions are fulfilled. In this case we can solve the equations of motion for the quantum mechanical correlation functions analytically up to an integral kernel that contains memory effects. The solutions allow to keep track of all parameters and give a deep conceptual insight into the behaviour of quantum fields out of thermal equilibrium. They can, if the above conditions are fulfilled, directly be applied to a number of cosmological situations including baryogenesis, dark matter production or the late phase of reheating. Furthermore, the improved conceptual understanding of quantum effects in a hot plasma can also provide a guideline when dealing with technically more complex problems.

Outline

In chapter 1, we introduce the standard techniques to treat quantum systems out of equilibrium. We briefly summarise the derivation of the standard Boltzmann equations in Sec. 1.1 and discuss the limitations of their applicability in the following section, 1.2. In Sec. 1.3, the Kadanoff-Baym equations are derived from first principles. They are the exact equations of motion for correlation functions of quantum fields out of equilibrium and can be viewed as quantum mechanical generalisation of the Boltzmann equations.

In chapter 2 we focus on systems in which the conditions we formulated in the introduction are fulfilled, namely fields that are weakly coupled to a large thermal bath. In Sec. 2.1 we prove that in such systems the Kadanoff-Baym equations are equivalent to a description in terms of a stochastic Langevin equation. Then, in Sec. 2.2, we solve the Kadanoff-Baym equations for scalars and fermions. The rest of the chapter is devoted to the discussion of the solutions. We first study the approach to equilibrium in Sec. 2.2.3. Then, in Sec. 2.3.1 and 2.3.2, we show that Boltzmann equations emerge from the Kadanoff-Baym equations in a dilute gas and briefly discuss quantum Boltzmann equations as an intermediate step. Finally, in Sec. 2.3, we study the plasma properties. We in particular investigate the validity of the quasiparticle approximation and the role effective masses in the plasma. A detailed discussion is devoted to kinematic aspects, in particular the role of off-shell and scattering processes in the plasma.

In chapter 3 we concretise the previous discussion by considering two specific models, a scalar coupled to a bath of two other scalars by a trilinear coupling and a fermion with Yukawa coupling. Analytic solutions for the imaginary parts of the self energy are provided for both cases.

In chapter 4 we apply the results to two cosmological problems. Sec. 4.1 uses the scalar model to study kinematic bounds on the reheating temperature after cosmic inflation. In Sec. 4.2 we use the results from the Yukawa model to formulate a framework that paves the way to a fully quantum mechanical treatment of leptogenesis.

Chapter 5 summarises and discusses our results. Many of the results presented in this work, in particular Sec.2.1, 2.2 and most of 3.1, have previously been published in [5].

Throughout this thesis we use natural units $\hbar = c = k_B = 1$, where k_B is the Boltzmann constant. For the metric in Minkowski space we chose the convention $g_{\mu\nu} = \text{diag}(1, -1, -1, -1)$.

Thermodynamics of Quantum Systems

In this chapter we review the standard methods used to describe nonequilibrium systems. In Sec. 1.1 we briefly sketch the derivation of the standard Boltzmann equations, following [3]. Then, in Sec. 1.2, we discuss when and why those can be expected to fail. In Sec. 1.3 we then introduce the Schwinger-Keldysh formalism and derive the Kadanoff-Baym equations which provide exact equations of motion for the correlation functions of quantum fields out of equilibrium.

1.1 Boltzmann Equations

Boltzmann equations are equations of motion for classical phase space distribution functions. In abstract form they read

$$\hat{L}[f_i] = \hat{C}[f_1, \dots, f_n]. \quad (1.1)$$

Here f_i are the distribution functions for n particle species and \hat{L} is the Liouville operator which in general relativity has the form

$$\hat{L} = p^\mu \partial_{x^\mu} - \Gamma_{\rho\sigma}^\mu p^\rho p^\sigma \partial_{p^\mu}. \quad (1.2)$$

Here p^μ is the conjugate momentum to the coordinate x^μ and $\Gamma_{\rho\sigma}^\mu$ are the Christoffel symbols or metric connection. \hat{L} describes the classical propagation of the system in phase space when there are no interactions. \hat{C} is the collision term that characterises the

interactions. It is computed from S -matrix elements that are imported into the classical framework from quantum field theory and allows for the creation and annihilation of particles in inelastic collisions. The two sides of (1.1) show the semiclassical nature of Boltzmann equations. The system is understood as an ensemble of classical particles with distribution functions f_i . They move freely according to \hat{L} between pointlike quantum mechanical interactions characterised by \hat{C} .

In a Friedmann-Robertson-Walker universe (1.2) reads

$$\hat{L} = \omega \partial_t - H \mathbf{p}^2 \partial_\omega, \quad (1.3)$$

where ω and \mathbf{p} are energy and momentum and H is the Hubble parameter. The number density can be defined as

$$n_i = g_i \int \frac{d^3 \mathbf{p}}{(2\pi)^3} f_i. \quad (1.4)$$

Then (1.1), divided by ω and integrated by parts, leads to

$$\dot{n}_i + 3Hn_i = \frac{g_i}{(2\pi)^3} \int \frac{d^3 \mathbf{p}}{\omega} \hat{C}[f_1, \dots, f_n]. \quad (1.5)$$

g_i counts the number of internal degrees of freedom of species i . Here we have neglected redshifting of ω because we assumed that the particles are massive and their energy $\omega = \omega_{\mathbf{p}} = \sqrt{\mathbf{p}^2 + m^2}$ is dominated by the mass. The momentum contribution gets redshifted, but can be neglected if the particles are heavy. For massless particles, the $3Hn$ term in (1.5) has to be replaced by $4Hn$. The collision term for a process with particles of species $i \dots k$ in the initial and $u \dots v$ in the final state can be written as

$$\begin{aligned} & \frac{g_i}{(2\pi)^3} \int \frac{d^3 \mathbf{p}_i}{\omega_i} \hat{C} = \\ & - \int \prod_{a=i}^k \left(\frac{g_a}{(2\pi)^3} \frac{d^3 \mathbf{p}_a}{\omega_a} \right) \prod_{b=u}^v \left(\frac{g_b}{(2\pi)^3} \frac{d^3 \mathbf{p}_b}{\omega_b} \right) \delta^{(4)}(p_i + \dots + p_k - p_u - \dots - p_v) \\ & (|\mathcal{M}|_{i\dots k \rightarrow u\dots v}^2 f_i \dots f_k (1 \pm f_u) \dots (1 \pm f_v) - |\mathcal{M}|_{u\dots v \rightarrow i\dots k}^2 f_u \dots f_v (1 \pm f_i) \dots (1 \pm f_k)). \end{aligned} \quad (1.6)$$

\mathcal{M} are the S -matrix elements for scatterings with particles of species $i \dots k$ in the initial and $u \dots v$ in the final state. The \pm are $+$ if the corresponding species is bosonic and $-$ if it is fermionic, in the former case enhancing the transition due to the induced effect and in the latter case suppressing it due to Pauli blocking. Quantum mechanical concepts as internal degrees of freedom or Bose-Einstein/Fermi-Dirac statistics have to be implemented by hand. The collision term couples the Boltzmann equations for the different species. This generally makes it difficult to solve them. Fortunately, for many cases of interest there are tremendous simplifications, though numerical computations may be done

without them. Due to phase space arguments, one usually has to consider only decays and $2 \rightarrow n$ scatterings. Unless many different species freeze out simultaneously, one can in good approximation assume that all species except for the one(s) freezing out are in equilibrium. The only change that Hubble expansion does to equilibrium distribution functions of relativistic particles can be parameterised in a time dependent temperature. In absence of Bose-Einstein condensation or Fermi degeneracy, the occupation numbers are small for all momenta. One can replace $1 \pm f \approx 1$ and use Maxwell-Boltzmann distributions for all species in equilibrium, regardless of their spin. On the side of the matrix elements, the symmetries of the interactions can often lead to simplifications. For instance, in transitions that only involve CP -invariant interactions, $|\mathcal{M}|^2$ is invariant under exchange of the initial and final state. If the background medium remains in equilibrium at any time, detailed balance implies that the sum of all gain rates $\gamma_i^>$ and the sum of all loss rates $\gamma_i^<$ fulfil the relation $\gamma_i^< = \pm e^{-\beta\omega} \gamma_i^>$ and the Boltzmann equation for the distribution function simplifies to

$$\dot{f}_i + 3Hf_i + \gamma_i(f_i - f_i^{eq}) = 0, \quad (1.7)$$

where $\gamma_i = \gamma_i^< - \gamma_i^>$ and f_i^{eq} is the distribution function in equilibrium. Since γ_i^{\gtrless} depend on the various distribution functions, they are functions of time. Hubble expansion can be viewed as an external force that acts on the system. As long as $\gamma \gg H$, the interactions continuously keep all species in thermal and chemical equilibrium. The state can then be characterised by the temperature and, potentially, a chemical potential for each conserved quantity. These few parameters uniquely dictate the abundance of particles for each species. When $\gamma \ll H$, γ can be neglected in (1.7). Then the only change that n_i undergoes is due to Hubble dilution and the number of particles in a comoving volume remains constant. Physically this means that the density of possible scattering partners becomes so low that the corresponding species effectively decouples. While the rest of the plasma keeps cooling, its comoving number density remains frozen roughly at the value it had when $\gamma \approx H$. The photons of the cosmic microwave background, the light elements in the intergalactic medium, dark matter and the excess of matter over antimatter in the universe are all relics that have been created this way.

1.2 Limitations of Boltzmann Equations

Despite their great success, Boltzmann equations have shortcomings. These affect both, the propagation as well as the interaction of particles.

The Boltzmann equations assume that classical particles move freely between scatterings. This neglects the fact that they feel the interaction with neighbouring particles at any time, not just during scatterings. It also neglects their quantum mechanical nature as wavepackets which becomes relevant once the average distance between two particles

is comparable to its de Broglie wavelength. It also neglects entanglement and the possibility of coherent oscillations of the quantum state during propagation, which cannot be described in the picture of classical particles.

The scattering amplitudes are computed from S -matrix elements in vacuum. They have no knowledge of the system's history and ignore possible non-Markovian effects. In addition, the computations are based on the particles' properties in vacuum and do not take into account possible changes due to their environment. It is a well known phenomenon that the properties of particles are changed if they move in a medium. Examples are the effective mass of electrons in a solid state or the Debye screening of a charged particle in a plasma. If those effects are not too strong, they can be parameterised by introducing a quasiparticle which resembles the properties of the screened particle seen from some distance. Then Boltzmann equations for those quasiparticles can correctly describe some properties of the system while ordinary Boltzmann equations give incorrect results. These effects can be expected to become increasingly important with increasing density.

1.2.1 Breakdown of the Particle Concept

The basic dynamical quantities in Boltzmann equations are particle numbers or phase space distributions. In an interacting quantum field theory, particle number is not a well defined quantity. In many situations, one can nevertheless refer to elementary excitations of fields as particles. This is very well motivated for if they exist as asymptotically free states. In the asymptotic limit, long before and long after a collision, the interaction can be neglected and the theory is effectively free. In this limit, the particle number is well defined, allowing to prepare and measure states of sharp particle number. The spectrum is discrete, with each state corresponding to freely moving on-shell particles. The notion of particles is still a very useful concept in an interacting theory if the spectrum, or density of quantum mechanical states, shows sharp peaks at some points in phase space. Those resonances can be interpreted as 'unstable particles'. If the coupling is weak, their properties are usually very close to what would be a stable particle in absence of the interaction.

The density of states with a given set of quantum numbers in phase space characterised by a spectral function or spectral density ρ . The analytic structure of a typical spectral function, in this case for simplicity of a scalar, is given by

$$\rho \propto \frac{\text{Im}\Pi_{\mathbf{q}}^R(\omega)}{|\omega^2 - \mathbf{q}^2 - m^2 - \Pi_{\mathbf{q}}^R(\omega)|^2}. \quad (1.8)$$

Here ω and \mathbf{q} are the energy and spatial momentum components of the four vector $q = (\omega, \mathbf{q})$. Π^R is the retarded self energy. In a free theory, Π^R is zero everywhere and ρ proportional to the sum of two δ functions at the poles $\pm\omega_{\mathbf{q}}$. With interaction, the poles

of (1.8) appear as the complex solutions to

$$\omega^2 - \mathbf{q}^2 - m^2 - \Pi_{\mathbf{q}}^R(\omega) = 0. \quad (1.9)$$

If those lie on the real ω -axis below the lowest multiparticle threshold, they give rise to δ -function shaped contributions to ρ that can be interpreted as stable states. When they lie close to the real axis, they still give rise to a sharp peak of ρ with a width given by their imaginary part and a height proportional to its inverse. Those can be interpreted as unstable states, or resonances. The poles and peaks in ρ apart from those corresponding to the one particle state can be interpreted as bound states. In addition, the spectrum receives continuous contributions above the lowest multiparticle threshold where Π shows a discontinuity across the real ω axis and the numerator of (1.8) becomes non-zero. However, in vacuum the one-particle state remains the excitation with the smallest energy, and $\text{Im}\Pi^R$ is zero below the lowest multiparticle threshold.

In a plasma the spectrum becomes more complicated¹. In the simplest case, when the background plasma is in equilibrium, Π^R becomes a function of a single temperature T and, in general, chemical potentials². The self energy then can always be written as the sum of its value in vacuum and a temperature dependent correction. The latter can give rise to additional solutions to (1.9) that correspond to collective excitations in the plasma, and the existing solutions are shifted by a temperature depended amount. Furthermore, in general Π^R is complex along the whole ω axis and all resonances, even those that are stable in vacuum, obtain a finite width due to the possibility of scatterings with virtual quanta in the plasma.

We now define $\omega = \hat{\Omega}_{\mathbf{q}}$ as the complex solution $\omega(\mathbf{q})$ to (1.9) that converges to $\omega_{\mathbf{q}}$ in the limit of vanishing coupling and³

$$\Omega_{\mathbf{q}} = \text{Re}\hat{\Omega}_{\mathbf{q}}, \quad (1.10)$$

$$\Gamma_{\mathbf{q}} = 2\text{Im}\hat{\Omega}_{\mathbf{q}}. \quad (1.11)$$

In a homogeneous and isotropic system, $\hat{\Omega}_{\mathbf{q}}$ can only depend on $|\mathbf{q}|$ and not on the direction. If the width of a resonance is small, namely

$$\Gamma_{\mathbf{q}} \ll \Omega_{\mathbf{q}}, \quad (1.12)$$

¹Throughout this work, we use the words 'spectrum' and 'spectral function' equivalently. Those are not to be confused with the spectrum of (eigenvalues of) the full Hamiltonian which is of course independent of the state in which the system is prepared, and therefore in particular independent of the temperature. The temperature dependence here arises from the statistical nature of thermodynamic systems. The resonances are not to be viewed as excitations above the ground state, but statistical averages over excitations above states of different energies contained in the grand canonical ensemble.

²In (1.9) we have written Π as a function of a single four vector q . In general, $\Pi(x_1, x_2)$ in coordinate space depends on two four vectors independently. However, in the following we focus on the case of a thermalised background plasma. Since thermal equilibrium is a translation- and rotation invariant state, Π only depends on the relative coordinate $x_1 - x_2$ and its Fourier transform $\Pi_{\mathbf{q}}(\omega)$ on a single vector q .

³Many authors use definitions that correspond to $\Gamma_{\mathbf{q}} = \text{Im}\hat{\Omega}_{\mathbf{q}}$. Here we chose the definition (1.11) because it relates Γ to the relaxation time of the system in real time by $\tau = 1/\Gamma$, see Sec.2.2

the spectral function shows sharp peaks at $\omega = \pm\Omega_{\mathbf{q}}$. Landau pointed out [6] that in this case the system can in good approximation be understood as a gas of screened particles with modified interactions, or quasiparticles. $\Omega_{\mathbf{q}}$ can be interpreted as a quasiparticle's energy. In this case one can formulate an approximate dispersion relation that puts the resonance quasi-on-shell, fixing its four vector to $(\Omega_{\mathbf{q}}, \mathbf{q})$. The dispersion relations are given by the real part of (1.9),

$$\omega^2 - \mathbf{q}^2 - m^2 - \text{Re}\Pi_{\mathbf{q}}^R(\omega) = 0. \quad (1.13)$$

Then one can approximate

$$\Gamma_{\mathbf{q}} \approx -\frac{\text{Im}\Pi_{\mathbf{q}}^R(\Omega_{\mathbf{q}})}{\Omega_{\mathbf{q}}}. \quad (1.14)$$

An effective mass M ⁴ can be defined as⁵

$$M(\mathbf{q}, T) = (\Omega_{\mathbf{q}}^2 - \mathbf{q}^2)^{\frac{1}{2}}. \quad (1.15)$$

We will in the following call $\Omega_{\mathbf{q}}$ and other possible solutions of (1.13) for which the dispersion relation $\omega(\mathbf{q})$ is similar to that of a free particle *free quasiparticles*. This applies if the momentum dependence of the correction due to $\text{Re}\Pi$ is small⁶, hence we will refer to the approximation in which this dependence is neglected as *free quasiparticle approximation*.

Obviously the real part of the self energy is responsible for the temperature- and generally momentum-dependent mass shift while its imaginary part gives rise to the finite width. One immediate feature of quasiparticles is that they are not stable and decay with a relaxation time of $\tau = 1/\Gamma$ [7]. In particular they do not exist as asymptotic (free) states because their properties are given by interactions. This in general makes the definition of a particle number ambiguous, though useful definitions have been suggested [8, 9].

To understand the properties of the plasma, one can distinguish between three qualitatively different regimes.

1. *particle regime*: If the corrections to $\text{Re}\Pi^R$ and $\text{Im}\Pi^R$ coming from interactions with the medium are both small with respect to the particle's on-shell energy $\omega_{\mathbf{q}}$ and all mass differences to particles with the same conserved quantum numbers,

⁴Throughout this thesis we generally use small letters for zero temperature masses and capital letters for thermal masses. The only exception are the masses of right handed neutrinos in Sec.4.2 which we, in accordance with the common notation in the literature, denote by capital letters.

⁵There are other possible definitions than (1.15), e.g. defining M as the momentum independent piece of $\text{Re}\Pi^R$ that comes from local diagrams, as the energy $\Omega_{\mathbf{q}=0}$ when the quasiparticle is at rest, as the minimal possible value of $\Omega_{\mathbf{q}}$ as a function of $|\mathbf{q}|$ or via the inverse curvature of $\Omega_{\mathbf{q}}$ at its minimum as a function of $|\mathbf{q}|$. For *free quasiparticles*, the meaning of all of those coincides.

⁶It is by no means clear that the dispersion relation has a parabolic form if one moves away from a minimum. The complicated band structures in condensed matter systems are an obvious counter-example.

the influence of the plasma on particle properties is negligible. Then conventional Boltzmann equations can be expected to describe the kinematics of the system with sufficient accuracy. However, even in this regime, they cannot account for effects related to the coherence of quantum states.

2. *quasiparticle regime*: If the correction to $\text{Re}\Pi^R$ due to the medium becomes non-negligible, it can qualitatively change the shape of the spectrum. The resonances that exist at $T = 0$ receive a temperature dependent mass shift, and new resonances which correspond to collective excitations can appear. However, if the width of all of them is still much smaller than their energy and their dispersion relations do not cross or get so closed together that the finite widths overlap, all plasma waves can be described as quasiparticles in the sense defined above. Their properties can differ significantly from those of the particles in vacuum, but kinematically they in good approximation behave like (generally unstable) particles. In the following we will always refer to resonances with these "particle-like" properties as quasiparticles, regardless of whether they originate from screened particles or have a collective origin⁷.
3. *broad resonance regime*: If the width of a resonance becomes comparable to its energy, it cannot be interpreted as a (quasi)particle with a well-defined energy any more. This is expected in a strongly coupled system. It can also happen for a small coupling constant if the temperature, and consequently density, become sufficiently high that interactions with the background plasma make the lifetime of a state short, hence its width large.

In a weakly coupled theory there is a simple classical argument which suggests that the quasiparticle picture should hold even in the high temperature regime $T \gg m$. One should certainly observe quasiparticle behaviour if the kinetic energy is much larger than the potential, or interaction energy. The interaction energy can be estimated by a Coulomb law $E_{\text{pot}} \sim g/r$ where g is the gauge coupling constant and r the distance between two particles. This distance in a hot plasma is $\sim T^{-1}$, thus $E_{\text{pot}} \sim gT$. Remarkably, this result coincides with a first order quantum field theoretical computation for the thermal Debye mass [10]. In contrast, the kinetic energy is $E_{\text{kin}} \sim T$, hence $g \ll 1$ implies $E_{\text{kin}} \gg E_{\text{pot}}$. However, this simple picture does not always hold, see 2.3.3.

⁷This deviates from the more common definition that restricts quasiparticles to those resonances that correspond to dressed particles, as opposed to collective phenomena. However, for our later discussion the origin of the plasma waves is of no relevance and we refer to them as quasiparticle whenever they have a definite dispersion relation.

1.2.2 Oscillations and Decoherence Effects

Boltzmann equations are formulated in terms of number densities for classical particles. By construction they cannot describe quantum phenomena like coherent oscillations, which can be of great importance in the early universe. In the standard model of particle physics the quark mass eigenstates are not identical to their flavour eigenstates, but rotated by the CKM matrix [11]. The reason is that the Yukawa couplings to the Higgs field that give the quarks masses do not couple to the same directions in flavour space as the SU(2) gauge coupling. A similar situation may be realised in the see-saw mechanism [12], see appendix A ⁸. There the Yukawa coupling matrix that connects heavy neutrinos to Higgs and leptons is generally not diagonalisable in the same basis as the charged lepton Yukawa couplings. This can have important consequences in leptogenesis [13], where the CP-violating decay of a heavy Majorana neutrinos into Higgs and leptons generates a matter-antimatter asymmetry⁹. The decay of a heavy Majorana neutrino produces leptons in a coherent superposition of flavours, leading to flavour oscillations. The generated lepton number is determined by the competition between decays and scatterings that produce leptons and their inverse, the washout processes. Between their production and possible absorption in a washout process, the leptons propagate through the plasma. During this time, flavour dependent interactions with the background plasma can destroy the coherence of the quantum state. This has an effect on the efficiency of washout processes. For example, if the interactions via the charged lepton Yukawa couplings happen fast, they effectively freeze the system in the corresponding flavour state. When leptogenesis is studied in terms of Boltzmann equations, there are two different ways to proceed. Either one sums over all flavours and does the computations for an overall lepton number or one computes the production rates for each flavour separately. Either way, classical Boltzmann equations cannot take proper account of coherent oscillations and decoherence effects.

We here chose the example of leptogenesis. These effects are of course not specific to this example. They can be relevant whenever couplings are involved that single out different directions in flavour or another space.

1.3 Kadanoff-Baym Equations

The previous considerations point out the need for a full quantum mechanical description of nonequilibrium systems.

⁸Here we refer to the type-I see-saw mechanism. Two alternative ideas to explain the smallness of neutrino masses are known as type-II and type-III see-saw mechanism: the addition of SU(2) triplet Higgses [14] and the addition of SU(2) triplet fermions [15] to the Standard Model.

⁹The importance of flavour in leptogenesis has been studied by a large number of authors, see [16] and references therein for a partial list.

Such a description is provided by the Kadanoff-Baym equations. In this approach, the n -point correlation functions replace the phase space distribution function as the dynamical quantities by which a system is described. Their equations of motion are given by the Kadanoff-Baym equations [17]. Those can be derived closed-time-path or Schwinger-Keldysh formalism [18, 19, 20, 21]. Here we briefly sketch the derivation of this technique, mainly following [22, 8].

A nonequilibrium system is not a pure quantum state and has to be described in terms of a density matrix ϱ . Expectation values of observables are computed as

$$\langle \mathcal{A} \rangle = \text{Tr}(\varrho \mathcal{A}) \quad (1.16)$$

The density matrix ϱ has a statistical interpretation as an ensemble of identical systems in different quantum states¹⁰. (1.16) involves an averaging over quantum fluctuations and statistical initial conditions. This will become more obvious later. Direct computation of the time evolution of ϱ is difficult¹¹, but it is equivalent to study the time evolution of all correlation functions of the theory. The infinitely many degrees of freedom of the initial density matrix are mapped onto their infinitely many initial conditions. Though a full characterisation of the system in principle involves all n -point functions, it is often sufficient to study the one- and two-point function. This in particular applies to all cases of interest in this work.

Time ordered correlation functions can, as in field theory at vanishing temperature, be computed from a generating functional. However, it turns out useful not to restrict the analysis to fields with real time arguments, but instead consider a time ordering along some general contour C in the complex time plane. We will first derive the relevant equations for real scalars and then for fermions. The generalisation to complex scalars and gauge fields is straightforward, though in the latter case the treatment of the unphysical gauge degrees of freedom can be technically challenging and the phenomenology is much richer. For instance, in covariant gauges at finite temperature, Faddeev-Popov ghosts are necessary to remove unphysical degrees of freedom even in abelian gauge theories, and in non-abelian gauge theories a new mass scale, the magnetic mass, appears, see [10].

1.3.1 Bosons

Consider a real scalar field ϕ with a Lagrangian $\mathcal{L} = \mathcal{L}_{\text{free}} - \mathcal{V}$ where $\mathcal{L}_{\text{free}}$ is the Lagrangian of the free field and \mathcal{V} some potential that provides a self interaction. We specify the

¹⁰Note that particle number in relativistic quantum field theory is not a conserved quantity. Therefore different states of the same system include the vacuum, pure states with an arbitrary number of quanta and possible superpositions of states with different particle numbers.

¹¹Generally, the von Neumann equation can only be solved perturbatively for a reduced density matrix with an effective Hamiltonian. In most practical applications to date, a number of additional assumptions is made that effectively makes this approach equivalent to what we refer to as quantum Boltzmann equations in Sec. 2.3.2. A powerful formalism of this kind has been developed in [23] and is widely used to treat neutrino oscillations.

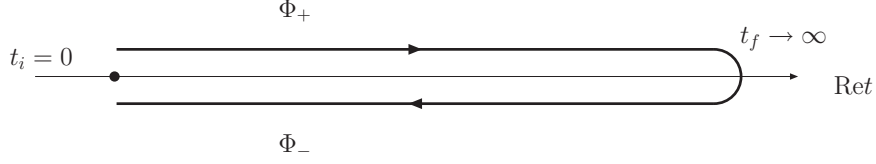


Figure 1.1: Path in the complex time plane for nonequilibrium correlation functions.

contour C as the Keldysh-contour \mathcal{C} (cf. Figure 1.1) that starts at some initial value $x^0 = t_i + i\epsilon$, runs parallel to the real x^0 axis until $t_f + i\epsilon$ where it follows a semicircle around $x^0 = t_f$ until $x^0 = t_f - i\epsilon$ and then runs back to $t_i - i\epsilon$. The parameter ϵ shall be thought of as infinitesimal. To include correlation functions for arbitrarily large times after t_i , we send $t_f \rightarrow \infty$. A generating functional for time ordered correlation functions can be written as¹²

$$Z_C[J] = \text{Tr} \left(\text{T}_C \exp \left(i \int_C d^4x J(x) \phi(x) \right) \varrho \right), \quad (1.17)$$

with time ordered n -point functions given by

$$\langle \phi(x_1) \dots \phi(x_n) \rangle = \frac{1}{Z[J]} \frac{\delta^n}{i\delta J(x_1) \dots i\delta J(x_n)} Z[J] \Big|_{J=0} \quad (1.18)$$

Here T_C is the time ordering along the contour \mathcal{C} in the complex time plane and $\int_C d^4x$ implies a time integration along that contour while the spatial integrations $d^3\mathbf{x}$ are performed over the whole three dimensional space in the usual manner. The generating functional has a path integral representation

$$Z_C[J] = \int \mathcal{D}\phi_i^{[1]} \mathcal{D}\phi_i^{[2]} \langle \phi_i^{[1]} | \varrho | \phi_i^{[2]} \rangle \langle \phi_i^{[2]} | \text{T}_C \exp \left(i \int_C d^4x (\mathcal{L}(x) + J(x)\phi(x)) \right) | \phi_i^{[1]} \rangle. \quad (1.19)$$

Here $\langle \phi_i^{[1]} |$ and $| \phi_i^{[2]} \rangle$ are eigenstates of the Heisenberg field operator $\phi(t_i \pm i\epsilon)$ at the beginning and end of \mathcal{C} . In the limit $\epsilon \rightarrow 0$ one can represent

$$\langle \phi_i^{[2]} | \text{T}_C \exp \left(i \int_C d^4x (\mathcal{L}(x) + J(x)\phi(x)) \right) | \phi_i^{[1]} \rangle = \int_{\phi_i^{[1]}}^{\phi_i^{[2]}} \mathcal{D}\phi \exp \left(i \int_C d^4x (\mathcal{L}(x) + J(x)\phi(x)) \right), \quad (1.20)$$

leading to

$$Z_C[J] = \int \mathcal{D}\phi_i^{[1]} \mathcal{D}\phi_i^{[2]} \langle \phi_i^{[1]} | \varrho | \phi_i^{[2]} \rangle \int_{\phi_i^{[1]}}^{\phi_i^{[2]}} \mathcal{D}\phi \exp \left(i \int_C d^4x (\mathcal{L}(x) + J(x)\phi(x)) \right). \quad (1.21)$$

¹²Here we chose the Heisenberg picture where ϱ is time independent.

(1.20) provides the motivation for choosing the closed time path \mathcal{C} . The integrations $\mathcal{D}\phi_i^{[1]}\mathcal{D}\phi_i^{[2]}$ correspond to an ensemble average over the initial conditions $\langle\phi_i^{[1]}|\varrho|\phi_i^{[2]}\rangle$ while the $\mathcal{D}\phi$ is the usual quantum mechanical path integral averaging. The initial density matrix can be represented as

$$\langle\phi_i^{[1]}|\varrho|\phi_i^{[2]}\rangle = \mathfrak{N}e^{i\mathfrak{f}[\phi]} \quad (1.22)$$

with

$$\mathfrak{f}[\phi] = \alpha_0 + \sum_{n=1}^{\infty} \frac{1}{n!} \int_{\mathcal{C}} \prod_{i=1}^n dx_i \alpha_n(x_0, \dots, x_i) \phi(x_1) \dots \phi(x_i). \quad (1.23)$$

The α_n contain the initial correlations and vanish for times $t \neq t_i$ while \mathfrak{N} is simply a normalisation factor. In this work we will only consider two types of initial conditions, equilibrium and a Gaussian density matrix. For both of these, \mathfrak{f} can be absorbed in an elegant way. Here we discuss Gaussian ϱ , the equilibrium case is treated in Sec. 1.3.3.

Gaussian initial conditions can be a good approximation for the physical reality in many cases¹³. They can be parameterised as

$$\mathfrak{f}[\phi] = \alpha_0 + \int_{\mathcal{C}} d^4x_1 \alpha_1(x_1) \phi(x_1) + \frac{1}{2} \int_{\mathcal{C}} d^4x_1 d^4x_2 \alpha_2(x_1, x_2) \phi(x_1) \phi(x_2), \quad (1.24)$$

giving the exponential in (1.21) the simple shape

$$\begin{aligned} & \exp\left(i \int_{\mathcal{C}} d^4x_1 d^4x_2 \left(\frac{1}{2} \alpha_2(x_1, x_2) + \delta_{\mathcal{C}}^{(4)}(x_1 - x_2) \frac{1}{2} (\partial_{x_1} \partial_{x_2} - m^2)\right) \phi(x_1) \phi(x_2)\right) \\ & \times \exp\left(i \int_{\mathcal{C}} d^4x (\alpha_1(x) + J(x)) \phi(x) - \mathcal{V}[\phi(x)]\right). \end{aligned} \quad (1.25)$$

α_1 can be absorbed into the source, $J(x) \rightarrow J(x) + \alpha_1(x)$, and α_2 into the mass, $\delta_{\mathcal{C}}^{(4)}(x_1 - x_2) m^2 \rightarrow \delta_{\mathcal{C}}^{(4)}(x_1 - x_2) m^2 - \alpha_2(x_1, x_2)$. This way the initial density matrix formally disappears from the computations and only re-enters via the initial conditions for the correlation functions. As in vacuum theory, in the absence of interactions, $\mathcal{V} = 0$, (1.25) is Gaussian and (1.21) can, after partial integration in x_2 be solved as

$$Z_{\mathcal{C}}^{\text{free}}[J] = \mathfrak{N}' \exp\left(-\frac{1}{2} \int_{\mathcal{C}} d^4x_1 d^4x_2 J(x_1) \Delta_{\mathcal{C}}^{\text{free}}(x_1, x_2) J(x_2)\right). \quad (1.26)$$

\mathfrak{N}' is again a normalisation factor and $\Delta_{\mathcal{C}}^{\text{free}}$ the free propagator on the contour with modified mass m for which, analogue to the vacuum case,

$$(\square_1 + m^2) \Delta_{\mathcal{C}}^{\text{free}}(x_1, x_2) = -i \delta_{\mathcal{C}}^{(4)}(x_1 - x_2). \quad (1.27)$$

¹³Note that, even if the initial density matrix is purely Gaussian, higher order correlation functions build up at later times.

Here $\square_1 = \partial_\mu \partial^\mu$ with all derivatives with respect to the components of x_1 . From (1.21) it is easy to see that

$$Z_C[J] = \exp\left(-i \int_C d^4\mathcal{V} \left[\frac{\delta}{i\delta J(x)}\right]\right) Z_C^{\text{free}}[J(x)]. \quad (1.28)$$

As in vacuum theory, one can now define the generating functional for the connected correlation functions by

$$W[J] = i \ln Z[J]. \quad (1.29)$$

As usual, functional derivatives of $W[J]$ with respect to J give connected time ordered n -point correlation functions,

$$\frac{\delta^n W[J]}{\delta J[x_1] \dots \delta J[x_n]} \Big|_{J=0} = (i)^{n+1} \langle \text{T}_C(\phi(x_1) \dots \phi(x_n)) \rangle_c. \quad (1.30)$$

The effective action is obtained by Legendre transform,

$$\Gamma[\phi_c] = -W[J] - \int_C d^4x J(x) \phi_c(x), \quad (1.31)$$

and fulfils the stationarity condition

$$\frac{\delta \Gamma[\phi_c]}{\delta \phi_c(x_1)} = -J(x_1) \quad (1.32)$$

where $\phi_c = \langle \phi \rangle$ is the expectation value of the classical field, computable from (1.30). It allows to define the n -point vertex functional, or one-particle irreducible n -point function

$$\Gamma_n(x_1 \dots x_n) = \frac{\delta^n \Gamma[\phi_c]}{\delta \phi_c(x_1) \dots \delta \phi_c(x_n)} = -i \langle \phi(x_1) \dots \phi(x_n) \rangle_{1PI}. \quad (1.33)$$

It follows

$$\begin{aligned} \frac{\delta}{\delta J(x_2)} \frac{\delta \Gamma[\phi_c]}{\delta \phi_c(x_1)} &= \int_C d^4x' \frac{\delta \phi_c(x')}{\delta J(x_2)} \frac{\delta^2 \Gamma[\phi_c]}{\delta \phi_c(x') \delta \phi_c(x_1)} \\ &= - \int_C d^4x' \frac{\delta^2 W[J]}{\delta J(x_2) \delta J(x')} \frac{\delta^2 \Gamma[\phi_c]}{\delta \phi_c(x') \delta \phi_c(x_1)} = - \frac{\delta J(x_1)}{\delta J(x_2)}. \end{aligned} \quad (1.34)$$

This, with (1.33) and (1.30), implies for the connected two point function on the contour

$$\int_C d^4x' (\Delta_C(x_1, x'))_c \Gamma_2(x', x_2) = -i \delta_C^{(4)}(x_1 - x_2). \quad (1.35)$$

Γ_2 can be written as a free part plus a self energy Π , defining the latter:

$$\Gamma_2(x_1, x_2) = \Gamma_2^{\text{free}}(x_1, x_2) + \Pi_C(x_1, x_2). \quad (1.36)$$

From (1.35) it is clear that Γ_2^{free} is the negative of the inverse free time ordered propagator on the contour, implying

$$\Gamma_2^{\text{free}}(x_1, x_2) = (\square_1 + m^2)\delta_{\mathcal{C}}^{(4)}(x_1 - x_2) \quad (1.37)$$

The Dyson-Schwinger equation (1.35) can now be written in the familiar form

$$(\square_1 + m^2)(\Delta_{\mathcal{C}}(x_1, x_2))_c + \int_{\mathcal{C}} d^4x' \Pi_{\mathcal{C}}(x_1, x')(\Delta_{\mathcal{C}}(x', x_2))_c = -i\delta_{\mathcal{C}}(x_1 - x_2) , \quad (1.38)$$

The propagator can be decomposed as

$$(\Delta_{\mathcal{C}}^c(x_1, x_2))_c = \theta_{\mathcal{C}}(x_1^0, x_2^0)\Delta^>(x_1, x_2) + \theta_{\mathcal{C}}(x_2^0, x_1^0)\Delta^<(x_1, x_2) . \quad (1.39)$$

The θ -functions enforce path ordering along the contour \mathcal{C} , and $\Delta^>$ and $\Delta^<$ are defined as

$$\Delta^>(x_1, x_2) = \langle \phi(x_1)\phi(x_2) \rangle_c \quad (1.40)$$

$$\Delta^<(x_1, x_2) = \langle \phi(x_2)\phi(x_1) \rangle_c . \quad (1.41)$$

The self-energy can be decomposed in the same way

$$\Pi_{\mathcal{C}}(x_1, x_2) = \theta_{\mathcal{C}}(x_1^0, x_2^0)\Pi^>(x_1, x_2) + \theta_{\mathcal{C}}(x_2^0, x_1^0)\Pi^<(x_1, x_2) . \quad (1.42)$$

In the Schwinger-Dyson equation the time coordinates of $\Delta_{\mathcal{C}}$ and $\Pi_{\mathcal{C}}$ can be on the upper or lower branch of the contour \mathcal{C} . To leave the contour and turn to correlation functions on the real axis, we have to pay the price of a doubling of degrees of freedom, treating fields on the upper and lower branch independently. We denote fields on the upper branch by the subscript '+' and those on the lower branch by '-'. This of course does not mean that the number of physical degrees of freedom changes, ϕ_- has to be viewed as an auxiliary quantity. Consistency obviously implies

$$\phi_+(t_f, \mathbf{x}) = \phi_-(t_f, \mathbf{x}) \quad (1.43)$$

Using the same notation for the correlators and self energies, one can write

$$\Delta_{-+}(x_1, x_2) = \Delta^>(x_1, x_2) , \quad \Delta_{+-}(x_1, x_2) = \Delta^<(x_1, x_2) , \quad (1.44)$$

$$\Pi_{-+}(x_1, x_2) = \Pi^>(x_1, x_2) , \quad \Pi_{+-}(x_1, x_2) = \Pi^<(x_1, x_2) , \quad (1.45)$$

Δ_{++} , Π_{++} are the time-ordered and Δ_{--} , Π_{--} the anti-time-ordered two-point functions and self energies. From the Schwinger-Dyson equation (1.38) one obtains for the correlation functions $\Delta^<$ and $\Delta^>$,

$$(\square_1 + m^2)\Delta^<(x_1, x_2) = \int d^4x' (-\Pi_{++}(x_1, x')\Delta^<(x', x_2) + \Pi^<(x_1, x')\Delta_{--}(x', x_2)) , \quad (1.46)$$

$$(\square_1 + m^2)\Delta^>(x_1, x_2) = \int d^4x' (-\Pi^>(x_1, x')\Delta_{++}(x', x_2) + \Pi_{--}(x_1, x')\Delta^>(x', x_2)) , \quad (1.47)$$

where the relative sign in the integrands is due to the anti-causal time ordering on the lower branch of \mathcal{C} .

It is convenient to introduce retarded and advanced propagators,

$$\begin{aligned}\Delta^R(x_1, x_2) &= \theta(t_1 - t_2)(\Delta^>(x_1, x_2) - \Delta^<(x_1, x_2)) \\ &= \theta(t_1 - t_2)\langle[\phi(x_1), \phi(x_2)]\rangle \\ &= \Delta_{++}(x_1, x_2) - \Delta_{+-}(x_1, x_2) \\ &= \Delta_{-+}(x_1, x_2) - \Delta_{--}(x_1, x_2) ,\end{aligned}\tag{1.48}$$

$$\begin{aligned}\Delta^A(x_1, x_2) &= -\theta(t_2 - t_1)(\Delta^>(x_1, x_2) - \Delta^<(x_1, x_2)) \\ &= -\theta(t_2 - t_1)\langle[\phi(x_1), \phi(x_2)]\rangle \\ &= \Delta_{++}(x_1, x_2) - \Delta_{-+}(x_1, x_2) \\ &= \Delta_{+-}(x_1, x_2) - \Delta_{--}(x_1, x_2) ,\end{aligned}\tag{1.49}$$

$$\begin{aligned}\Pi^R(x_1, x_2) &= \theta(t_1 - t_2)(\Pi^>(x_1, x_2) - \Pi^<(x_1, x_2)) \\ &= \Pi_{++}(x_1, x_2) - \Pi_{+-}(x_1, x_2) \\ &= \Pi_{-+}(x_1, x_2) - \Pi_{--}(x_1, x_2) ,\end{aligned}\tag{1.50}$$

$$\begin{aligned}\Pi^A(x_1, x_2) &= -\theta(t_2 - t_1)(\Pi^>(x_1, x_2) - \Pi^<(x_1, x_2)) \\ &= \Pi_{++}(x_1, x_2) - \Pi_{-+}(x_1, x_2) \\ &= \Pi_{+-}(x_1, x_2) - \Pi_{--}(x_1, x_2) .\end{aligned}\tag{1.51}$$

They allow, with Eqs. (1.46) and (1.47), to formulate the Kadanoff-Baym equations for the correlation functions $\Delta^>$ and $\Delta^<$,

$$(\square_1 + m^2)\Delta^>(x_1, x_2) = - \int d^4x' (\Pi^>(x_1, x')\Delta^A(x', x_2) + \Pi^R(x_1, x')\Delta^>(x', x_2)) ,\tag{1.52}$$

$$(\square_1 + m^2)\Delta^<(x_1, x_2) = - \int d^4x' (\Pi^<(x_1, x')\Delta^A(x', x_2) + \Pi^R(x_1, x')\Delta^<(x', x_2)) .\tag{1.53}$$

These can be rewritten conveniently in terms of the real symmetric and antisymmetric correlation functions

$$\Delta^+(x_1, x_2) = \frac{1}{2}\langle\{\phi(x_1), \phi(x_2)\}\rangle ,\tag{1.54}$$

$$\Delta^-(x_1, x_2) = i\langle[\phi(x_1), \phi(x_2)]\rangle ,\tag{1.55}$$

and self-energies

$$\Pi^+(x_1, x_2) = -\frac{i}{2}(\Pi^>(x_1, x_2) + \Pi^<(x_1, x_2)) ,\tag{1.56}$$

$$\Pi^-(x_1, x_2) = \Pi^>(x_1, x_2) - \Pi^<(x_1, x_2) ,\tag{1.57}$$

which can be related the retarded and advanced self-energies,

$$\Pi^R(x_1, x_2) = \theta(t_1 - t_2)\Pi^-(x_1, x_2) , \quad \Pi^A(x_1, x_2) = -\theta(t_2 - t_1)\Pi^-(x_1, x_2) . \quad (1.58)$$

One can obtain a homogeneous equation for Δ^- and an inhomogeneous equation for Δ^+ by adding and subtracting the Kadanoff-Baym equations (1.52) and (1.53) and using (1.48)-(1.51) and (1.54)-(1.57),

$$(\square_1 + m^2)\Delta^-(x_1, x_2) = - \int d^3\mathbf{x}' \int_{t_2}^{t_1} dt' \Pi^-(x_1, x')\Delta^-(x', x_2) , \quad (1.59)$$

$$\begin{aligned} (\square_1 + m^2)\Delta^+(x_1, x_2) &= - \int d^3\mathbf{x}' \int_{t_i}^{t_1} dt' \Pi^-(x_1, x')\Delta^+(x', x_2) \\ &+ \int d^3\mathbf{x}' \int_{t_i}^{t_2} dt' \Pi^+(x_1, x')\Delta^-(x', x_2) . \end{aligned} \quad (1.60)$$

Δ^- and Δ^+ are known as spectral function and statistical propagator (cf. [8]). The time ordered propagator on the contour can be expressed as

$$(\Delta_C(x_1, x_2))_c = \Delta^+(x_1, x_2) - \frac{i}{2}\text{sign}_C(x_1^0 - x_2^0)\Delta^-(x_1, x_2) . \quad (1.61)$$

Δ^- is, up to a factor i , the Fourier transform of the spectral function ρ and carries information about the spectrum of the system while Δ^+ is related to occupation numbers of different modes. From the definitions (1.54) and (1.55) it follows that

$$\Delta^-(x_2, x_1) = -\Delta^-(x_1, x_2) \quad (1.62)$$

$$\Delta^+(x_2, x_1) = \Delta^-(x_1, x_2) . \quad (1.63)$$

Using microcausality and the canonical quantisation condition for a real scalar field,

$$[\phi(x_1), \phi(x_2)]|_{t_1=t_2} = [\dot{\phi}(x_1), \dot{\phi}(x_2)]|_{t_1=t_2} = 0 , \quad (1.64)$$

$$[\phi(x_1), \dot{\phi}(x_2)]|_{t_1=t_2} = i\delta(\mathbf{x}_1 - \mathbf{x}_2) , \quad (1.65)$$

one can derive the initial conditions for Δ^- .

$$\Delta^-(x_1, x_2)|_{t_1=t_2} = 0 , \quad (1.66)$$

$$\partial_{t_1}\Delta^-(x_1, x_2)|_{t_1=t_2} = -\partial_{t_2}\Delta^-(x_1, x_2)|_{t_1=t_2} = \delta(\mathbf{x}_1 - \mathbf{x}_2) , \quad (1.67)$$

$$\partial_{t_1}\partial_{t_2}\Delta^-(x_1, x_2)|_{t_1=t_2} = 0 . \quad (1.68)$$

Note that they do not depend on the physical initial conditions of the system encoded in the initial density matrix. Those enter via the initial conditions of Δ^+ , the mean field $\langle\phi\rangle$

and their derivatives with respect to time. If the involved couplings are small, Π can be computed perturbatively from loop integrals that involve Δ^+ , Δ^- and $\langle\phi\rangle$,

$$\Pi = \Pi[\Delta^+, \Delta^-, \langle\phi\rangle].$$

Feynman rules can be derived from (1.28). There are two differences to the procedure in vacuum. First, the propagator depends on two arguments separately, not only their difference. Second, there is a doubling of degrees of freedom since ϕ_+ and ϕ_- have to be treated as two independent fields. ϕ_- is not physical and acts like a ghost field that only appears in the loops. Though ϕ_{\pm} cannot mix in vertices, they can propagate into each other via Δ_{+-} and Δ_{-+} . Since the couplings are local, only one type of field can appear at each vertex. Thus there are two types of vertices. The number of diagrams contributing to a certain process increases by a factor 2^n where n is the number of internal vertices because every vertex can be of each type. Fortunately, in practice only two of the four propagators $\Delta_{\pm\pm}$ are independent because with (1.61) all of them can be constructed from Δ^+ and Δ^- .

Since our interest is motivated by cosmological problems, where the cosmological principle applies, we can restrict the analysis to homogeneous and isotropic systems. In this case all quantities only depend on the difference of the three vectors \mathbf{x}_1 and \mathbf{x}_2 . The generalisation to inhomogeneous systems is straightforward though often computationally difficult. It is convenient to perform a Fourier transformation in the relative spatial coordinate. The correlation functions $\Delta_{\mathbf{q}}^{\pm}(t_1, t_2)$ satisfy the two Kadanoff-Baym equations

$$(\partial_{t_1}^2 + \omega_{\mathbf{q}}^2)\Delta_{\mathbf{q}}^-(t_1, t_2) + \int_{t_2}^{t_1} dt' \Pi_{\mathbf{q}}^-(t_1, t')\Delta_{\mathbf{q}}^-(t', t_2) = 0, \quad (1.69)$$

$$(\partial_{t_1}^2 + \omega_{\mathbf{q}}^2)\Delta_{\mathbf{q}}^+(t_1, t_2) + \int_{t_i}^{t_1} dt' \Pi_{\mathbf{q}}^-(t_1, t')\Delta_{\mathbf{q}}^+(t', t_2) = \int_{t_i}^{t_2} dt' \Pi_{\mathbf{q}}^+(t_1, t')\Delta_{\mathbf{q}}^-(t', t_2), \quad (1.70)$$

The initial conditions (1.66)-(1.68) for the spectral function become

$$\Delta_{\mathbf{q}}^-(t_1, t_2)|_{t_1=t_2} = 0, \quad (1.71)$$

$$\partial_{t_1}\Delta_{\mathbf{q}}^-(t_1, t_2)|_{t_1=t_2} = -\partial_{t_2}\Delta_{\mathbf{q}}^-(t_1, t_2)|_{t_1=t_2} = 1, \quad (1.72)$$

$$\partial_{t_1}\partial_{t_2}\Delta_{\mathbf{q}}^-(t_1, t_2)|_{t_1=t_2} = 0. \quad (1.73)$$

The physical initial conditions can in many cases be well approximated by a Gaussian density matrix ρ . The most general Gaussian density matrix contains only five indepen-

dent parameters for each mode (see [8]),

$$\begin{aligned}
\langle \phi_i^{[1]} | \varrho | \phi_i^{[2]} \rangle &= (2\pi \Delta_{\mathbf{q},\text{in}}^+)^{-1/2} \exp \left(i\phi_{\mathbf{q},\text{in}}(\phi_{\mathbf{q}}^{[1]} - \phi_{\mathbf{q}}^{[2]}) + \frac{i\dot{\Delta}_{\mathbf{q},\text{in}}^+}{2\Delta_{\mathbf{q},\text{in}}^+} ((\phi_{\mathbf{q}}^{[1]} - \phi_{\mathbf{q},\text{in}})^2 - (\phi_{\mathbf{q}}^{[2]} - \phi_{\mathbf{q},\text{in}})^2) \right. \\
&\quad - \frac{4 \left(\Delta_{\mathbf{q},\text{in}}^+ \ddot{\Delta}_{\mathbf{q},\text{in}}^+ - (\dot{\Delta}_{\mathbf{q},\text{in}}^+)^2 \right) + 1}{8\Delta_{\mathbf{q},\text{in}}^+} ((\phi_{\mathbf{q}}^{[1]} - \phi_{\mathbf{q},\text{in}})^2 + (\phi_{\mathbf{q}}^{[2]} - \phi_{\mathbf{q},\text{in}})^2) \\
&\quad \left. + \frac{4 \left(\Delta_{\mathbf{q},\text{in}}^+ \ddot{\Delta}_{\mathbf{q},\text{in}}^+ - (\dot{\Delta}_{\mathbf{q},\text{in}}^+)^2 \right) - 1}{4\Delta_{\mathbf{q},\text{in}}^+} (\phi_{\mathbf{q}}^{[1]} - \phi_{\mathbf{q},\text{in}})(\phi_{\mathbf{q}}^{[2]} - \phi_{\mathbf{q},\text{in}}) \right) \quad (1.74)
\end{aligned}$$

with

$$\phi_{\mathbf{q},\text{in}} = \langle \phi_{\mathbf{q}}(t_1) \rangle |_{t_1=0}, \quad (1.75)$$

$$\dot{\phi}_{\mathbf{q},\text{in}} = \partial_{t_1} \langle \phi_{\mathbf{q}}(t_1) \rangle |_{t_1=0}, \quad (1.76)$$

$$\Delta_{\mathbf{q},\text{in}}^+ = \Delta_{\mathbf{q}}^+(t_1, t_2) |_{t_1=t_2=0}, \quad (1.77)$$

$$\dot{\Delta}_{\mathbf{q},\text{in}}^+ = \partial_{t_1} \Delta_{\mathbf{q}}^+(t_1, t_2) |_{t_1=t_2=0} = \partial_{t_2} \Delta_{\mathbf{q}}^+(t_1, t_2) |_{t_1=t_2=0}, \quad (1.78)$$

$$\ddot{\Delta}_{\mathbf{q},\text{in}}^+ = \partial_{t_1} \partial_{t_2} \Delta_{\mathbf{q}}^+(t_1, t_2) |_{t_1=t_2=0}. \quad (1.79)$$

Eq. (1.74) establishes the connection between the initial density matrix ϱ and the initial conditions for Δ^+ and $\langle \phi \rangle$. This is the only point where ϱ enters, and the modified mass obtained by absorbing the initial correlation α_2 into m^2 does not affect the equations of motion at any other time than t_i since all α_i vanish for $t \neq t_i$. A pure quantum mechanical state with $\text{Tr} \varrho^2 = 1$ is realised for $\ddot{\Delta}_{\mathbf{q},\text{in}}^+ \Delta_{\mathbf{q},\text{in}}^+ - (\dot{\Delta}_{\mathbf{q},\text{in}}^+)^2 = \frac{1}{4}$ ¹⁴.

To derive the Kadanoff-Baym equations (1.59) and (1.60), we employed standard functional methods known from field theory in vacuum. We formulated a generating functional $Z[J]$ with one source term J from which we obtained the effective action $\Gamma[\phi_c]$ that generates one-particle irreducible correlation functions. There exist an alternative derivation (see [8]) that starts from a generating functional with n non-local sources and uses the n -particle effective actions $\Gamma^{(n)}$. Those are functionals of all connected m -point functions $\Delta(x_1, \dots, x_m)$ with $m \leq n$ and allow to derive equations of motion for them by first order functional derivation, using the stationarity condition

$$\frac{\delta \Gamma^{(n)}}{\delta \Delta(x_1, \dots, x_m)} = 0. \quad (1.80)$$

In particular, the two-particle irreducible effective action [24] has become a standard tool in nonequilibrium field theory. However, these methods are completely equivalent to the

¹⁴If ϕ is coupled to other fields, e.g. a thermal bath, entanglement with those will generally lead to decoherence even if the initial density matrix ϱ_ϕ of ϕ corresponds to a pure state.

approach presented here if the full perturbative series is taken into account. Differences are technical and related to the truncation of the series. The n -particle irreducible effective action provides a useful scheme to resum infinitely many Feynman diagrams. It also allows to understand in an intuitive way why the formalism is free of secular terms that appear in conventional perturbative approaches to time-dependent problems that involve more than one time scale [8].

The above description was formulated in Minkowski spacetime and neglects Hubble expansion. A straightforward generalisation to curved spacetimes and in particular the Friedmann-Robertson-Walker universe has been discussed in [25].

1.3.2 Fermions

The generalisation of the above to fermions is straightforward. Analogue to Eqs. (1.40) and (1.41) one can define

$$S_{\alpha\beta}^>(x_1, x_2) = \langle \Psi_\alpha(x_1) \bar{\Psi}_\beta(x_2) \rangle_c \quad (1.81)$$

$$S_{\alpha\beta}^<(x_1, x_2) = -\langle \bar{\Psi}_\beta(x_2) \Psi_\alpha(x_1) \rangle_c \quad (1.82)$$

$$(1.83)$$

as well as the spectral and statistical propagators

$$S_{\alpha\beta}^- = i\langle \{\Psi_\alpha(x_1), \bar{\Psi}_\beta(x_2)\} \rangle_c = i(S_{\alpha\beta}^>(x_1, x_2) - S_{\alpha\beta}^<(x_1, x_2)) \quad (1.84)$$

$$S_{\alpha\beta}^+ = \frac{1}{2}\langle [\Psi_\alpha(x_1), \bar{\Psi}_\beta(x_2)] \rangle_c = \frac{1}{2}(S_{\alpha\beta}^>(x_1, x_2) + S_{\alpha\beta}^<(x_1, x_2)) \quad (1.85)$$

Here Ψ is a Dirac spinor and α and β are spinor indices which we will always suppress in the following. The symmetry relations analogue to (1.62) and (1.63) are

$$S^-(x_2, x_1) = -\gamma^0 (S^-(x_1, x_2))^\dagger \gamma^0 \quad (1.86)$$

$$S^+(x_2, x_1) = \gamma^0 (S^+(x_1, x_2))^\dagger \gamma^0. \quad (1.87)$$

As for scalars, this allows to derive Kadanoff Baym equations for the spectral and statistical propagators,

$$(i\partial_1 - m)S^-(x_1, x_2) = \int d^3\mathbf{x}' \int_{t_2}^{t_1} dt' \Sigma^-(x_1, x') S^-(x', x_2), \quad (1.88)$$

$$\begin{aligned} (i\partial_1 - m)S^+(x_1, x_2) &= \int d^3\mathbf{x}' \int_{t_i}^{t_1} dt' \Sigma^-(x_1, x') S^+(x', x_2) \\ &\quad - \int d^3\mathbf{x}' \int_{t_i}^{t_2} dt' \Sigma^+(x_1, x') S^-(x', x_2). \end{aligned} \quad (1.89)$$

Here, as usual, $\partial = \gamma^\mu \partial_\mu$ and the subscript $_1$ indicates that derivatives are to be taken with respect to the components of the vector x_1 .

1.3.3 Thermal Equilibrium

Thermal equilibrium is a very special state. In the spirit of the ergodic hypothesis, any large closed system with components that are in touch with each other should approach equilibrium for late times and remain there on relevant time scales¹⁵. In Sec. 2.2.3 we show explicitly that our solutions asymptotically approach the equilibrium state on a characteristic time scale τ for arbitrary initial conditions. In equilibrium, the density matrix ϱ can without approximation be characterised by a small number of parameters which, in the system of rest of the plasma, have a physical interpretation as temperature and chemical potentials [27, 28]. Then ϱ can be written as

$$\varrho_{eq} = \frac{\exp(\beta(-\mathcal{H} + \mu_i \mathcal{Q}_i))}{\text{Tr} \exp(\beta(-\mathcal{H} + \mu_i \mathcal{Q}_i))} \quad (1.90)$$

where \mathcal{H} is the Hamiltonian of the system, β the inverse temperature, \mathcal{Q}_i some conserved charges and μ_i the corresponding chemical potentials. In the cases we will discuss, chemical potentials are negligible, leading to

$$\varrho_{eq} = \frac{\exp(-\beta\mathcal{H})}{\text{Tr} \exp(-\beta\mathcal{H})}. \quad (1.91)$$

There exist several formalisms to treat quantum fields in equilibrium (see e.g. [10] and [29] for a detailed list of references). They are generally based on the observation that (1.91) formally is a time evolution operator in imaginary time [30]. Here we will use the real-time formalism which directly connects to the discussion in the previous section. We again consider correlation functions in the complex time plane, for a moment without specification of a contour. Since equilibrium is a time- and space-translation invariant state, the correlators Δ^{\gtrless} only depend on relative coordinates

$$\Delta^{\gtrless}(x_1, x_2) \rightarrow \Delta^{\gtrless}(x_1 - x_2). \quad (1.92)$$

Using ϱ_{eq} as a time evolution operator and the cyclicity of the trace in (1.16), it is then easy to prove that

$$\Delta^<(t + i\beta) = \Delta^>(t) \quad (1.93)$$

where we have suppressed the spatial dependence. (1.93) is called the Kubo-Martin-Schwinger (KMS) relation. For it to have any meaning, the functions $\Delta^>$ and $\Delta^<$ should be defined in the strips $-\beta \leq \text{Im}x^0 \leq 0$ and $0 \leq \text{Im}x^0 \leq \beta$. In momentum space, the KMS condition reads

$$\Delta_{\mathbf{q}}^<(\omega) = \Delta_{\mathbf{q}}^>(-\omega) = e^{-\beta\omega} \Delta_{\mathbf{q}}^>(\omega). \quad (1.94)$$

¹⁵In practice, equilibration is a highly non-trivial issue. Many real systems, e.g. ferromagnets or glass, show *ergodicity breaking* on relevant time scales. Also in relativistic quantum field theories approximate non-thermal fixed points can appear, see e.g. [8, 26].

For Δ^\pm that implies

$$\Delta_{\mathbf{q}}^+(\omega) = -\frac{i}{2} \coth\left(\frac{\beta\omega}{2}\right) \Delta_{\mathbf{q}}^-(\omega). \quad (1.95)$$

The same relation can be derived for the self-energies,

$$\Pi_{\mathbf{q}}^+(\omega) = -\frac{i}{2} \coth\left(\frac{\beta\omega}{2}\right) \Pi_{\mathbf{q}}^-(\omega). \quad (1.96)$$

The KMS relation, which can be physically interpreted as a manifestation of detailed balance, is unique to equilibrium and can also be used to characterise the equilibrium state. It allows to write the time ordered propagator in a convenient form,

$$(\Delta_C(x_1 - x_2))_c = \int \frac{d^4q}{(2\pi)^4} e^{-iq(x_1 - x_2)} (\theta_C(x_1^0 - x_2^0) + f_B(\omega)) \rho_{\mathbf{q}}(\omega). \quad (1.97)$$

Here $\rho_{\mathbf{q}}(\omega) = -i\Delta_{\mathbf{q}}^-(\omega)$ is the spectral function and

$$f_B(\omega) = \frac{1}{e^{\beta\omega} - 1}. \quad (1.98)$$

Again using ϱ_{eq} as a time evolution operator, one can eliminate the initial density matrix from the generating functional (1.19),

$$Z_C[J] = \int \mathcal{D}\phi' \langle \phi'(\mathbf{x}; t_i + i\beta) | \text{T}_C \exp\left(i \int_C d^4x (\mathcal{L}(x) + J(x)\phi(x))\right) | \phi'(\mathbf{x}; t_i) \rangle, \quad (1.99)$$

leading to

$$Z_C[J] = \int \mathcal{D}\phi \exp\left(i \int_C d^4x (\mathcal{L}(x) + J(x)\phi(x))\right). \quad (1.100)$$

Here, the boundary conditions are $\phi(t, \mathbf{x}) = \phi(t - i\beta, \mathbf{x})$ and $t_f = t_i - i\beta$. Let us now specify the contour. It has to start at t_i and end at $t_i - i\beta$. Furthermore, it should include the real axis if we aim to calculate correlation functions for real time arguments and want to avoid analytic continuations¹⁶. There is a third condition that can be explained by looking at $\Delta^>$ and performing the trace in a set of eigenstates $|n\rangle$ of the Hamiltonian for energies E_n , here for simplicity assumed to be discrete,

$$\Delta^>(t_1 - t_2) = Z[0]^{-1} \sum_{n,m} e^{iE_n(t_1 - t_2 + i\beta)} e^{-iE_m(t_1 - t_2)} \langle n | \phi(t = 0, \mathbf{x}_1) | m \rangle \langle m | \phi(t = 0, \mathbf{x}_2) | n \rangle. \quad (1.101)$$

¹⁶The first consistent treatment of quantum fields in equilibrium was formulated by Matsubara for correlation functions with imaginary time arguments [31] and is widely used if all fields are in equilibrium. Here we chose a real time contour because it allows to treat in- and out-of-equilibrium fields in the same framework.

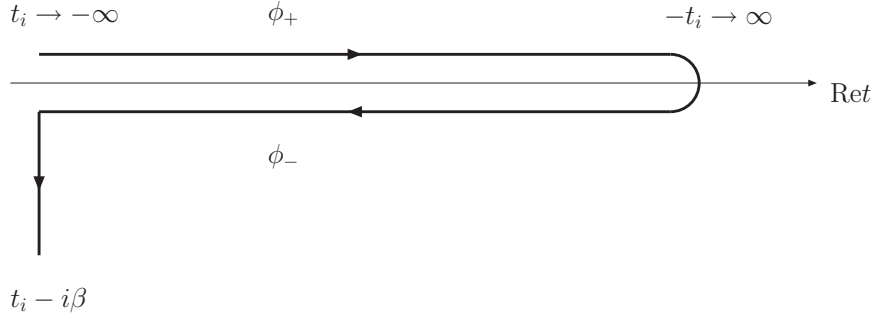


Figure 1.2: Path in the complex time plane for thermal correlation functions.

The convergence of the sums is assumed to be governed by the exponentials, which provides the conditions

$$\text{Im}(x_1^0 - x_2^0) \leq 0, \quad \text{Im}(x_1^0 - x_2^0) + \beta \geq 0 . \quad (1.102)$$

When constructing a time-ordered propagator on the contour as in (1.39), t_1 is later than t_2 . Finiteness of the time ordered propagator via (1.102) therefore enforces that the imaginary part of the later time is smaller, meaning that the contour can run only downward in $\text{Im}x^0$ while it is free to run forward and backward in $\text{Re}x^0$ direction. To make connection to the nonequilibrium discussion, we here chose the contour \mathcal{C}_β shown in Fig. 1.2. The generating functional (1.100) can be written in the same form as in the nonequilibrium case (1.28). \mathcal{C}_β consists of three parts: \mathcal{C}_1 runs along the real axis from t_i , assumed to be negative without loss of generality, to $-t_i$. \mathcal{C}_2 runs back to t_i and \mathcal{C}_3 then parallel to the imaginary axis down to $t_i - i\beta$. It can be shown that¹⁷ one can perform the limit $t_i \rightarrow -\infty$. Then the generating functional $Z_{\mathcal{C}_\beta}[J]$ factorises into a part that generates correlation functions on $\mathcal{C}_1 \cup \mathcal{C}_2$ and one for those on \mathcal{C}_3 , $Z_{\mathcal{C}_\beta} = Z_{\mathcal{C}_1 \cup \mathcal{C}_2} Z_{\mathcal{C}_3}$. Since we are not interested in imaginary time arguments, $Z_{\mathcal{C}_3}$ is an irrelevant normalisation factor that drops out. The derivation of Feynman rules, including the doubling of degrees of freedom by introducing fields ϕ_\pm on the forward and backward branch of the contour, is equivalent to that for out-of-equilibrium fields following (1.28). The computations in equilibrium are much simpler than out of equilibrium because even the dressed propagators only depend on relative coordinates. Feynman rules can be applied as in vacuum, with the difference that there are two types of internal vertices, '+' and '-', which couple fields of the corresponding kind. Practically, computations are done as follows: Draw all diagrams, assign '+' and '-' to each vertex, considering all combinatorial possibilities, connect two '+'-type vertices by Δ_{++} , two '-'-type vertices by Δ_{--} and so on. Then perform all loop integral as in vacuum. To do so, one requires the four thermal propagators. They can be found from (1.97) with the knowledge of the free spectral function. With

¹⁷There are some ambiguities related to this limit, see [10, 29] and references therein for a discussion.

$\rho_{\mathbf{q}}^{\text{free}}(\omega) = 2\pi\text{sign}(\omega)\delta(q^2 - m^2)$, see (2.46), one obtains

$$\begin{aligned}\Delta_{++}(q) &= \frac{i}{q^2 - m^2 + i\epsilon} + f_B(|\omega|)2\pi\delta(q^2 - m^2), & \Delta_{+-}(q) &= f_B(\omega)2\pi\text{sign}(\omega)\delta(q^2 - m^2), \\ \Delta_{-+}(q) &= (1 + f_B(\omega))2\pi\text{sign}(\omega)\delta(q^2 - m^2), & \Delta_{--}(q) &= \frac{-i}{q^2 - m^2 - i\epsilon} + f_B(|\omega|)2\pi\delta(q^2 - m^2).\end{aligned}\tag{1.103}$$

All the above expressions are computed in the rest frame of the thermal bath and not invariant under Lorentz transformations. The theory itself of course remains covariant, and the manifest covariance can be restored by the replacement $\beta\omega \rightarrow \beta q_\mu u^\mu$, where u^μ is the four-velocity of the thermal bath. The bath simply singles out a frame of reference in which computations are particularly simple and $T = 1/\beta$ has a physical interpretation as temperature. For fermions, the anti-commutativity of Grassmann fields enforces a different KMS relation

$$S_{\mathbf{q}}^<(\omega) = -e^{-\beta\omega}S_{\mathbf{q}}^>(\omega),\tag{1.104}$$

leading to

$$S_{\mathbf{q}}^+(\omega) = -\frac{i}{2}\tanh\left(\frac{\beta\omega}{2}\right)S_{\mathbf{q}}^-(\omega)..\tag{1.105}$$

It is very convenient to express the various correlators in terms of the spectral function and the distribution functions $f_{B,F}$

$$\begin{aligned}\Delta_{\mathbf{q}}^-(\omega) &= i\rho_{\mathbf{q}}(\omega), & \Delta_{\mathbf{q}}^+(\omega) &= \left(\frac{1}{2} + f_B(\omega)\right)\rho_{\mathbf{q}}(\omega) \\ S_{\mathbf{q}}^-(\omega) &= i\rho_{\mathbf{q}}(\omega), & S_{\mathbf{q}}^+(\omega) &= \left(\frac{1}{2} - f_F(\omega)\right)\rho_{\mathbf{q}}(\omega)\end{aligned}\tag{1.106}$$

where

$$f_F(\omega) = \frac{1}{e^{\beta\omega} + 1}.\tag{1.107}$$

The Bose-Einstein and Fermi-Dirac distributions that characterise equilibrium arise naturally from the boundary conditions of the correlation functions. Finally, we can establish the connection to usual thermodynamic quantities by noticing that the generating functional (1.100) for vanishing source can be identified with the partition function \mathcal{Z} of a grand canonical ensemble.

$$\mathcal{Z} = Z[J = 0]\tag{1.108}$$

This, in the infinite volume limit $V \rightarrow \infty$, allows to compute thermodynamic pressure as well as entropy-, energy- and charge-density from $Z[0]$

$$\begin{aligned}\mathcal{P} &= T\frac{\partial \ln \mathcal{Z}}{\partial V} = \frac{T}{V}\ln \mathcal{Z} & s &= \frac{\mathcal{S}}{V} = \frac{\partial \mathcal{P}}{\partial T} \\ \epsilon &= -\frac{1}{V}\frac{\partial \ln \mathcal{Z}}{\partial \beta} & q_i &= \frac{\partial \mathcal{P}}{\partial \mu_i}.\end{aligned}$$

The von Neumann-entropy can, as usual in the statistical quantum mechanics, be written in terms of the density matrix ϱ ,

$$\mathcal{S} = -\langle \ln \varrho \rangle.\tag{1.109}$$

Weak Coupling to a thermal Bath

The Kadanoff-Baym equations provide a tool to study the dynamics of arbitrary nonequilibrium systems. Unfortunately, in most cases they can only be solved numerically. For the case of interest in this work one can make a number of simplifications. These correspond to a scenario where one field that is out of equilibrium is in contact with a large thermal bath. They are well-motivated for various cosmological processes including leptogenesis, the freezeout of a weakly coupled dark matter particle, some models of warm inflation or the late phase of reheating. In this case, we can prove that the Kadanoff-Baym equations for the correlation functions are equivalent to a stochastic description in terms of a Langevin equation for the field itself. Furthermore, in this situation we can find the most general solution to the Kadanoff-Baym equations analytically up to an integral kernel that contains memory effects. In the quasiparticle regime we can even solve this integral and present a full analytic leading order result. We then use this to show how the Boltzmann equations emerge from the Kadanoff-Baym equations in the limit of weak coupling. Finally, we discuss the properties of the plasma. We find that even in the quasiparticle regime the equation of state can significantly deviate from the naive expectation. We also point out that at high temperature, in the quasiparticle regime the phase space becomes dynamical due to the temperature dependent plasma wave dispersion relation, which can in the simplest case be parameterised by temperature dependent effective masses. Those put kinematical restrictions on processes in the plasma. Beyond the quasiparticle regime these are not effective due to significant contributions from off-shell processes.

The assumption of weak coupling to a large thermal bath in the framework of Kadanoff-Baym equations implies that self energies are computed from equilibrium propagators of bath fields only. For couplings that are linear in the out-of-equilibrium field, this also corresponds to a leading order perturbative expansion in the coupling constant. Higher

order corrections are known cause uncertainties in perturbative solutions of Boltzmann equations at late times. The reason is that terms of higher order in the gain-and loss rates $\sim \gamma$ can give non-negligible contributions when $\gamma t \geq 1$. Our approach makes no approximation on the quantum side and consistently includes all memory effects at a given order, but in principle inherits the technical uncertainties related to a perturbative expansion in time dependent problems. However, no explicit secular terms appear, the equations remain consistent in the sense that they do not contain time dependent "source terms" involving the solutions of the equations of motion at different order in the expansion parameter. Furthermore, in the systems of consideration, possible contributions are not only suppressed by the coupling, but mainly by the number of degrees of freedom in the bath so that they may safely be neglected .

The assumption that the background medium equilibrates instantaneously on the time scale of consideration of course does not take account of the details of the equilibration process. In reality, there may be effects related to the finite equilibration time and the finite size of the quasiparticles. For example, if a particle with $M \gg T$ decays, the released energy will locally destroy the thermal equilibrium. If the separation of time scales is large enough, such effects should be small since the total percentage of the plasma affected by them is small at any time.

We first consider a real scalar field that is coupled to a bath of other fields \mathcal{X} . with a Lagrangian of the form

$$\mathcal{L} = \frac{1}{2} \partial_\mu \phi \partial^\mu \phi - \frac{1}{2} m_\phi^2 \phi^2 - g \phi \mathcal{O}[\mathcal{X}] + \mathcal{L}_\mathcal{X}. \quad (2.1)$$

$\mathcal{O}[\mathcal{X}]$ can stand for any operator of the bath fields \mathcal{X} ¹. The coupling g is assumed to be much smaller than the couplings that keep the fields \mathcal{X} in equilibrium. Then the time scale on which ϕ evolves is much longer than the scale $\tau_\mathcal{X}$ on which the \mathcal{X} thermalise so that the bath is in local equilibrium and can be characterised by a single temperature T at any time. No other assumptions are made about the nature of the \mathcal{X} and their interactions, they could in principle represent an arbitrary number of bosonic or fermionic fields with various types of couplings amongst each other, including gauge interactions. All of this is included in $\mathcal{L}_\mathcal{X}$. We now introduce relative and centre of mass time coordinates $y = t_1 - t_2$ and $t = \frac{1}{2}(t_1 + t_2)$ and write

$$\Delta_{\mathbf{q}}^-(t; y) := \Delta_{\mathbf{q}}^-(t_1 = t + y/2, t_2 = t - y/2) \quad (2.2)$$

and so on. Correlation functions of fields in thermal equilibrium are time translation invariant. The self energy Π^R is by assumption given by loop diagrams that only contain \mathcal{X} propagators. Therefore it inherits this property, $\partial_t \Pi^\pm = 0$. In appendix B.1 we prove that then also $\partial_t \Delta^- = 0$. Physically this is intuitive. Δ^- encodes the spectrum, if backreaction is neglected, the dressing of resonances will happen only by interaction with

¹We exclude the case that \mathcal{O} is just given by a single field operator, $\mathcal{O}[\mathcal{X}] = \mathcal{X}$.

a time translation invariant background. Hence the spectrum has to be time translation invariant. The Kadanoff-Baym equations (1.69) and (1.70) then simplify to

$$(\partial_{t_1}^2 + \omega_{\mathbf{q}}^2)\Delta_{\mathbf{q}}^-(t_1 - t_2) + \int_{t_2}^{t_1} dt' \Pi_{\mathbf{q}}^-(t_1 - t')\Delta_{\mathbf{q}}^-(t' - t_2) = 0 , \quad (2.3)$$

$$(\partial_{t_1}^2 + \omega_{\mathbf{q}}^2)\Delta_{\mathbf{q}}^+(t_1, t_2) + \int_{t_i}^{t_1} dt' \Pi_{\mathbf{q}}^-(t_1 - t')\Delta_{\mathbf{q}}^+(t', t_2) = \int_{t_i}^{t_2} dt' \Pi_{\mathbf{q}}^+(t_1 - t')\Delta_{\mathbf{q}}^-(t' - t_2) , \quad (2.4)$$

2.1 Langevin Equation

In classical physics, a system with a few degrees of freedom that is exposed to friction and dissipation by coupling to a large bath can be often described in terms of a Langevin equation. Such approach is generally applicable when the many degrees of freedom in the bath allow to neglect backreaction. This method can be generalised to quantum field theory and has been used by various authors (cf. [32, 33, 34, 9, 35, 36, 37, 38]). Some aspects of the connection to the Kadanoff-Baym equations has previously been discussed in [39]. In the following we will first sketch the derivation of an effective Langevin equation following [9] and then show its equivalence to the Kadanoff-Baym equations.

The starting point is the nonequilibrium generating functional (1.21) We assume that the initial density matrix factorises, $\varrho = \varrho_{\phi} \otimes \varrho_{\mathcal{X}}$, and the interaction is switched on when the system starts evolving in time. It is important to realise that ϕ and the \mathcal{X} have their time arguments on different contours. The \mathcal{X} are all in equilibrium, so their initial correlations can be absorbed by use of the integration contour \mathcal{C}_{β} . ϕ is defined on the Keldysh contour \mathcal{C} . We now split \mathcal{C} into a forward and a backward part, using the ϕ_{\pm} notation, and introduce sources J_{\pm} for fields of the different branches. Being interested in ϕ , we initially set the sources for all \mathcal{X} to zero.

$$Z[J_+, J_-] = \int \mathcal{D}\phi_i^+ \mathcal{D}\phi_i^- \langle \phi_{i+} | \varrho | \phi_{i+} \rangle \int \mathcal{D}\phi_{\pm} \mathcal{D}\mathcal{X}_{\beta} e^{iS[\phi_{\pm}, \mathcal{X}, J_{\pm}]} . \quad (2.5)$$

$\mathcal{D}\mathcal{X}_{\beta}$ indicates the choice of boundary conditions as described in Sec. 1.3.3. The action of the fields ϕ and \mathcal{X} is given by

$$S[\phi_{\pm}, \mathcal{X}, J_{\pm}] = \int_{t_i}^{\infty} d^4x (\mathcal{L}_{\phi}(\phi_+) + g\phi_+ \mathcal{O}[\mathcal{X}_+] + J_+ \phi_+ - \mathcal{L}_{\phi}(\phi_-) - g\phi_- \mathcal{O}[\mathcal{X}_-] - J_- \phi_-) + \int_{\mathcal{C}_{\beta}} d^4x \mathcal{L}_{\mathcal{X}}(\mathcal{X}) , \quad (2.6)$$

where \mathcal{L}_{ϕ} is the Lagrangian of a free massive field and $\phi_{i\pm}$ the fields ϕ_{\pm} at initial time. In the following we choose as initial time $t_i = 0$ without loss of generality. With regard to

the integrals over \mathcal{X} , ϕ_{\pm} simply act as sources. The term

$$\int \mathcal{D}\mathcal{X}_{\beta} e^{i \int_{\mathcal{C}_{\beta}} d^4x (\mathcal{L}_{\mathcal{X}} + g\phi_{+} \mathcal{O}[\mathcal{X}_{+}])} = \left\langle e^{i \int_{\mathcal{C}_{\beta}} d^4x g\phi_{+} \mathcal{O}[\mathcal{X}_{+}]} \right\rangle_{\mathcal{X}} \quad (2.7)$$

has the shape of a generating functional, where the averaging is performed only over bath fields. We now expand the exponential in (2.7) to second order in g , perform a spatial Fourier transform and change to new coordinates in field space,

$$\Phi(x) = \frac{1}{2} (\phi_{+}(x) + \phi_{-}(x)) , \quad (2.8)$$

$$R(x) = \phi_{+}(x) - \phi_{-}(x) . \quad (2.9)$$

The fields \mathcal{X} and R can be integrated out, a straightforward computation leaves [9]

$$\begin{aligned} \mathcal{Z}[J] = & \int \mathcal{D}\Phi_{\text{in}} \mathcal{D}\pi_{\text{in}} \mathcal{W}(\Phi_{\text{in}}; \pi_{\text{in}}) \int \mathcal{D}\Phi \mathcal{D}\xi \mathcal{P}[\xi] e^{i \int d^4x J(x)\Phi(x)} \\ & \times \delta \left[\ddot{\Phi}_{\mathbf{q}}(t) + \omega_{\mathbf{q}}^2 \Phi_{\mathbf{q}}(t) + \int_0^t dt' \Pi_{\mathbf{q}}^{-}(t-t') \Phi_{\mathbf{q}}(t') - \xi_{\mathbf{q}}(t) \right] . \end{aligned} \quad (2.10)$$

Here the measure $\mathcal{P}[\xi]$ is given by

$$\mathcal{P}[\xi] = \exp \left(\frac{1}{2} \int_0^{\infty} dt \int_0^{\infty} dt' \xi_{\mathbf{q}}(t) \Pi_{\mathbf{q}}^{+}(t-t')^{-1} \xi_{-\mathbf{q}}(t') \right) , \quad (2.11)$$

and $\xi_{\mathbf{q}}(t)$ is a *stochastic noise*. It mimics the effect of the bath degrees of freedom on Φ . Since the backreaction of the field Φ is neglected, the only relevant correlation functions are

$$\langle \xi_{\mathbf{q}}(t) \rangle = 0 , \quad (2.12)$$

$$\langle \xi_{\mathbf{q}}(t) \xi_{\mathbf{q}'}(t') \rangle = -\Pi_{\mathbf{q}}^{+}(t-t') \delta(\mathbf{q} + \mathbf{q}') . \quad (2.13)$$

$\Phi_{\mathbf{q}}(t)$ in (2.10) satisfies the initial conditions

$$\Phi_{\mathbf{q}}(0) = \Phi_{\mathbf{q},\text{in}} , \quad \dot{\Phi}_{\mathbf{q},\text{in}}(0) = \pi_{\mathbf{q},\text{in}} . \quad (2.14)$$

The function $\mathcal{W}(\Phi_{\text{in}}; \pi_{\text{in}})$ is a functional Wigner transform of the initial density matrix,

$$\mathcal{W}(\Phi_{\text{in}}; \pi_{\text{in}}) = \int \mathcal{D}R_{\text{in}} e^{-\int d^3x \pi_{\text{in}}(\mathbf{x}) R_{\text{in}}(\mathbf{x})} \varrho \left(\Phi_{\text{in}} + \frac{R_{\text{in}}}{2}; \Phi_{\text{in}} - \frac{R_{\text{in}}}{2} \right) \quad (2.15)$$

and encodes the initial conditions.

Correlation functions for Φ can be found from (2.10) by solving the classical *stochastic* Langevin equation,

$$(\partial_t^2 + \omega_{\mathbf{q}}^2) \Phi_{\mathbf{q}}(t) + \int_0^t dt' \Pi_{\mathbf{q}}^{-}(t-t') \Phi_{\mathbf{q}}(t') = \xi_{\mathbf{q}}(t) , \quad (2.16)$$

with the initial conditions (2.14).

The solution of the Langevin equation is conveniently expressed by an auxiliary function $f_{\mathbf{q}}(t)$ which is defined as solution of the homogeneous equation

$$(\partial_t^2 + \omega_{\mathbf{q}}^2) f_{\mathbf{q}}(t) + \int_0^t dt' \Pi_{\mathbf{q}}^-(t-t') f_{\mathbf{q}}(t') = 0 , \quad (2.17)$$

with the initial conditions

$$f_{\mathbf{q}}(0) = 0 , \quad \dot{f}_{\mathbf{q}}(0) = 1 . \quad (2.18)$$

In terms of $f_{\mathbf{q}}(t)$, the solution of the Langevin equation is

$$\Phi_{\mathbf{q}}(t) = \Phi_{\mathbf{q},\text{in}} \dot{f}_{\mathbf{q}}(t) + \pi_{\mathbf{q},\text{in}} f_{\mathbf{q}}(t) + \int_0^t dt' f_{\mathbf{q}}(t-t') \xi_{\mathbf{q}}(t') . \quad (2.19)$$

Correlation functions can now be obtained from (2.10) by calculating the expectation values

$$\langle \Phi_{\mathbf{q}_1}(t_1) \dots \Phi_{\mathbf{q}_n}(t_n) \rangle , \quad (2.20)$$

which involves averaging over the stochastic noise and the initial conditions. In a spatially homogeneous system the two-point function can be written as

$$\langle \Phi_{\mathbf{q}}(t_1) \Phi_{\mathbf{q}'}(t_2) \rangle \equiv g_{\mathbf{q}}(t_1, t_2) \delta(\mathbf{q} + \mathbf{q}') = g_{\mathbf{q}}(t_2, t_1) \delta(\mathbf{q} + \mathbf{q}') . \quad (2.21)$$

The Langevin equation (2.16) implies,

$$(\partial_t^2 + \omega_{\mathbf{q}}^2) \langle \Phi_{\mathbf{q}}(t_1) \Phi_{\mathbf{q}'}(t_2) \rangle + \int_0^{t_1} dt' \Pi_{\mathbf{q}}^-(t_1-t') \langle \Phi_{\mathbf{q}}(t') \Phi_{\mathbf{q}'}(t_2) \rangle \quad (2.22)$$

$$= \langle \xi_{\mathbf{q}}(t_1) \Phi_{\mathbf{q}'}(t_2) \rangle \quad (2.23)$$

$$= \delta(\mathbf{q} + \mathbf{q}') \int_0^{t_2} dt' \Pi_{\mathbf{q}}^+(t_1-t') f_{\mathbf{q}}(t' - t_2) , \quad (2.24)$$

and consequently

$$\begin{aligned} & (\partial_t^2 + \omega_{\mathbf{q}}^2) g_{\mathbf{q}}(t_1, t_2) + \int_0^{t_1} dt' \Pi_{\mathbf{q}}^-(t_1-t') g_{\mathbf{q}}(t', t_2) \\ & = \int_0^{t_2} dt' \Pi_{\mathbf{q}}^+(t_1-t') f_{\mathbf{q}}(t' - t_2) . \end{aligned} \quad (2.25)$$

(2.25) can be solved using the solution of the Langevin equation (2.16). When the initial field value and its time derivative vanish,

$$\langle \Phi_{\mathbf{q},\text{in}} \rangle = \langle \dot{\Phi}_{\mathbf{q},\text{in}} \rangle = 0 , \quad (2.26)$$

the relevant averages for the two-point function can be expressed

$$\langle \Phi_{\mathbf{q},\text{in}} \Phi_{\mathbf{q},\text{in}} \rangle = \delta(\mathbf{q} + \mathbf{q}') \alpha_{\mathbf{q}} , \quad (2.27)$$

$$\langle \dot{\Phi}_{\mathbf{q},\text{in}} \dot{\Phi}_{\mathbf{q}',\text{in}} \rangle = \delta(\mathbf{q} + \mathbf{q}') \beta_{\mathbf{q}} , \quad (2.28)$$

$$\langle \dot{\Phi}_{\mathbf{q},\text{in}} \dot{\Phi}_{\mathbf{q},\text{in}} \rangle = \delta(\mathbf{q} + \mathbf{q}') \gamma_{\mathbf{q}} . \quad (2.29)$$

Using the solution (2.19) and the correlations (2.13) one obtains

$$\begin{aligned} g_{\mathbf{q}}(t_1, t_2) &= \alpha_{\mathbf{q}} \dot{f}_{\mathbf{q}}(t_1) \dot{f}_{\mathbf{q}}(t_2) + \gamma_{\mathbf{q}} f(t_1) f(t_2) \\ &+ \beta_{\mathbf{q}} \left(f_{\mathbf{q}}(t_1) \dot{f}_{\mathbf{q}}(t_2) + \dot{f}_{\mathbf{q}}(t_1) f_{\mathbf{q}}(t_2) \right) \\ &+ \int_0^{t_1} dt' \int_0^{t_2} dt'' f_{\mathbf{q}}(t_1 - t') \Pi_{\mathbf{q}}^+(t' - t'') f_{\mathbf{q}}(t'' - t_2) . \end{aligned} \quad (2.30)$$

Comparison of Eqs. (2.17) and (2.25) to (2.3) and (2.4) shows that the equations of motion derived from the Langevin equation can be identified with the Kadanoff-Baym equations with the replacement $f_{\mathbf{q}}(t_1 - t_2) \equiv \Delta_{\mathbf{q}}^-(t_1 - t_2)$ and $g_{\mathbf{q}}(t_1, t_2) \equiv \Delta_{\mathbf{q}}^+(t_1, t_2)$, hence we have proven the equivalence of both approaches.

2.2 Solving the Kadanoff-Baym Equations

2.2.1 Solutions for Scalars

The equation for the Spectral Function

Let us now solve (2.3).

$$(\partial_y^2 + \omega_{\mathbf{q}}^2) \Delta_{\mathbf{q}}^-(y) + \int_0^y dy' \Pi_{\mathbf{q}}^-(y - y') \Delta_{\mathbf{q}}^-(y') = 0 . \quad (2.31)$$

The solution can be found elegantly by performing a Laplace transformation,

$$\tilde{\Delta}_{\mathbf{q}}^-(s) = \int_0^{\infty} dy e^{-sy} \Delta_{\mathbf{q}}^-(y) , \quad (2.32)$$

which yields

$$\tilde{\Delta}_{\mathbf{q}}^-(s) = \frac{\partial_y \Delta_{\mathbf{q}}^-(0) + s \Delta_{\mathbf{q}}^-(0)}{s^2 + \omega_{\mathbf{q}}^2 + \tilde{\Pi}_{\mathbf{q}}^-(s)} , \quad (2.33)$$

where the Laplace transform of Π^- is defined analogue to Δ^- . From (2.33), it is obvious that the general solution of (2.31) depends on two parameters, the boundary conditions of $\Delta_{\mathbf{q}}^-$ and $\partial_y \Delta_{\mathbf{q}}^-$ at $y = 0$. An inverse Laplace transform yields

$$\Delta_{\mathbf{q}}^-(y) = (\partial_y \Delta_{\mathbf{q}}^-(0) + \Delta_{\mathbf{q}}^-(0) \partial_y) \int_{C_B} \frac{ds}{2\pi i} \frac{e^{sy}}{s^2 + \omega_{\mathbf{q}}^2 + \tilde{\Pi}_{\mathbf{q}}^-(s)} . \quad (2.34)$$

Here \mathcal{C}_B is the Bromwich contour (see Figure 3): The part parallel to the imaginary axis is chosen such that all singularities of the integrand are to its left; the second part is the semicircle at infinity which closes the contour at $\text{Re}(s) < 0$. The boundary conditions for $\Delta_{\mathbf{q}}^-(y)$ are independent of the initial conditions and given by (1.71) and (1.72), leading to

$$\Delta_{\mathbf{q}}^-(y) = \int_{\mathcal{C}_B} \frac{ds}{2\pi i} \frac{e^{sy}}{s^2 + \omega_{\mathbf{q}}^2 + \tilde{\Pi}_{\mathbf{q}}^-(s)}. \quad (2.35)$$

From the definition of the Laplace transform one can see that $\tilde{\Pi}^-(s)$ is real on the real s axis because $\Pi^-(y)$ is real, but it has a discontinuity across the imaginary axis. The definitions (1.50) and (1.51) give rise to the spectral representations

$$\Pi^R(\omega) = i \int_{-\infty}^{\infty} \frac{dp_0}{2\pi} \frac{\Pi^-(p_0)}{\omega - p_0 + i\epsilon} \quad (2.36)$$

$$\Pi^A(\omega) = i \int_{-\infty}^{\infty} \frac{dp_0}{2\pi} \frac{\Pi^-(p_0)}{\omega - p_0 - i\epsilon} \quad (2.37)$$

$$\tilde{\Pi}^-(s) = i \int_{-\infty}^{\infty} \frac{dp_0}{2\pi} \frac{\Pi^-(p_0)}{is - p_0} \quad (2.38)$$

from which the relations summarised in Appendix B.3 can be derived. $\Pi_{\mathbf{q}}^{R,A}(\omega)$ and $\Pi_{\mathbf{q}}^-(\omega)$ all have discontinuities across the real ω axis. On the axis Π^R is defined as

$$\text{Re}\Pi_{\mathbf{q}}^R(\omega) = \frac{1}{2} (\Pi_{\mathbf{q}}^R(\omega + i\epsilon) + \Pi_{\mathbf{q}}^R(\omega - i\epsilon)) \quad (2.39)$$

$$\text{Im}\Pi_{\mathbf{q}}^R(\omega) = \frac{1}{2i} (\Pi_{\mathbf{q}}^R(\omega + i\epsilon) - \Pi_{\mathbf{q}}^R(\omega - i\epsilon)). \quad (2.40)$$

Eqs. (2.39) and (2.40) imply that

$$\text{Im}\Pi_{\mathbf{q}}^R(\omega) = \frac{1}{2i} (\tilde{\Pi}_{\mathbf{q}}^-(-i\omega + \epsilon) - \tilde{\Pi}_{\mathbf{q}}^-(-i\omega - \epsilon)) . \quad (2.41)$$

and

$$\text{Im}\Pi_{\mathbf{q}}^R(\omega) = \frac{1}{2i} \Pi_{\mathbf{q}}^-(\omega + i\epsilon). \quad (2.42)$$

These properties are analogue to the theory in vacuum. However, while in vacuum Π^R is analytic below the lowest multiparticle threshold, at finite temperature it has a discontinuity along the whole real ω axis, as we will show in Sec. 2.3.3. Since the integrand of (2.34) has singularities only on the imaginary axis, the second part can be deformed to run parallel to the imaginary axis as well: $\mathcal{C}_B \rightarrow \int_{-i\infty+\epsilon}^{i\infty+\epsilon} + \int_{i\infty-\epsilon}^{-i\infty-\epsilon}$. By change of integration variables and use of the relations in Appendix B.3 the expression (2.35) can be brought into the form

$$\Delta_{\mathbf{q}}^-(y) = i \int_{-\infty}^{\infty} \frac{d\omega}{2\pi} e^{-i\omega y} \rho_{\mathbf{q}}(\omega), \quad (2.43)$$

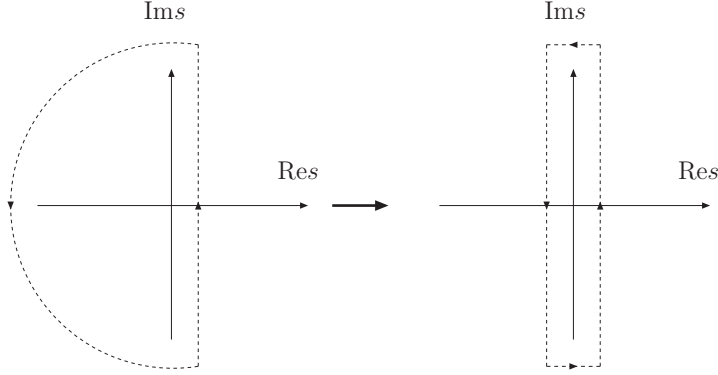


Figure 2.1: Bromwich contour

where the spectral function $\rho_{\mathbf{q}}(\omega)$ is given in terms of real and imaginary part of the self-energy $\Pi_{\mathbf{q}}^R(\omega)$,

$$\begin{aligned}
 \rho_{\mathbf{q}}(\omega) &= i\tilde{\Delta}_{\mathbf{q}}^-(i\omega) \\
 &= \left(\frac{i}{\omega^2 - \omega_{\mathbf{q}}^2 - \Pi_{\mathbf{q}}^A(\omega) - i\omega\epsilon} - \frac{i}{\omega^2 - \omega_{\mathbf{q}}^2 - \Pi_{\mathbf{q}}^R(\omega) + i\omega\epsilon} \right) \\
 &= \frac{-2\text{Im}\Pi_{\mathbf{q}}^R(\omega) + 2\omega\epsilon}{(\omega^2 - \omega_{\mathbf{q}}^2 - \text{Re}\Pi_{\mathbf{q}}^R(\omega))^2 + (\text{Im}\Pi_{\mathbf{q}}^R(\omega) + \omega\epsilon)^2}.
 \end{aligned} \tag{2.44}$$

The inversion in the last step is trivial because we assume that ϕ either carries no other index, such as flavour, or the self energy is diagonal with respect to such index. $\rho_{\mathbf{q}}(\omega)$ fulfils the well-known sum rule

$$\int d\omega \rho_{\mathbf{q}}(\omega) = 1. \tag{2.45}$$

The discussion following (1.8) can be directly applied to (2.44). In the limit of vanishing interaction, the spectral function reads

$$\rho_{\mathbf{q}}^{\text{free}}(\omega) = 2\pi \text{sign}(\omega) \delta(\omega^2 - \omega_{\mathbf{q}}^2) \tag{2.46}$$

As pointed out previously, the spectrum is time translation invariant because we neglected the backreaction of ϕ on the bath. In a cosmological context this is of course not exactly true. Even if backreaction is negligible, Hubble expansion still acts as an external force on the system. However, in many relevant cases the time scale associated with the dynamics of the field that is out of equilibrium is much shorter than that on which the expansion is relevant, but still much longer than the relaxation times of the stronger coupled bath fields. Though the spectrum changes with time and $\partial_t \Delta^- \neq 0$, the inequality

$$\partial_t \Delta_{\mathbf{q}}^-(t; y) \ll \partial_y \Delta_{\mathbf{q}}^-(t; y) \tag{2.47}$$

can still hold and justify to take

$$\Delta_{\mathbf{q}}^-(t_1, t_2) \rightarrow \Delta_{\mathbf{q}}^-(y; T(t)).$$

(2.47) allows to replace $\partial_{t_1}^2$ on the lhs of the first Kadanoff-Baym equation (2.3) by ∂_y^2 . Locally, if the separation y between t_1 and t_2 is small, $T(\frac{t_1+t'}{2})$ and $T(\frac{t'+t_2}{2})$ can both be replaced by the mean value $T(\frac{t_1-t_2}{2}) = T(t)$. Then (2.3) in relative and centre of mass coordinates reads

$$(\partial_y^2 + \omega_{\mathbf{q}}^2)\Delta_{\mathbf{q}}^-(t; y) = - \int_0^y dt' \Pi_{\mathbf{q}}^-(y - t', T(t))\Delta_{\mathbf{q}}^-(t'; T(t)) \quad (2.48)$$

The centre of mass time t is now just an external parameter and (2.48) can be solved by Laplace transform in y as in the t -independent case. The solution has the same shape as the spectral function at constant temperature (2.44), but implicitly depends on t via $T(t)^2$.

The self-energy $\Pi_{\mathbf{q}}^R(\omega)$, and consequently the spectral function $\rho_{\mathbf{q}}(\omega)$, are divergent and have to be renormalised. Physical particle properties shall be defined in vacuum. Hence, the renormalisation conditions are formulated at zero temperature. In the limit $T \rightarrow 0$ one then directly recovers the familiar interpretation of masses and couplings from vacuum theory. This is possible because medium effects are not relevant at very short distances and no UV divergences additional to those in vacuum appear in the theory. No temperature dependent counter-terms are needed and the usual mass and wave function renormalisation at zero temperature can be applied. In (2.44) $\omega_{\mathbf{q}}^2$ is replaced by $\omega_{\mathbf{q}(0)}^2 = m_0^2 + \mathbf{q}^2$, where m_0 is the bare mass of the field ϕ . We require that the spectral function has a pole at $\omega_{\mathbf{q}}^2 = m^2 + \mathbf{q}^2$ for $T = 0$,

$$\omega_{\mathbf{q}}^2 - \omega_{\mathbf{q}(0)}^2 - \text{Re}\Pi_{\mathbf{q}}^R(\omega_{\mathbf{q}})|_{T=0} = 0 . \quad (2.49)$$

The self energy is now expanded around $\omega_{\mathbf{q}}$ and renormalisation of the wave function allows to absorb another divergence,

$$\text{Re}\Pi_{\mathbf{q}}^R(\omega) = \text{Re}\Pi_{\mathbf{q}}^R(\omega_{\mathbf{q}})|_{T=0} + (1 - Z^{-1}) (\omega^2 - \omega_{\mathbf{q}}^2) + \text{Re}\hat{\Pi}_{\mathbf{q}}^R(\omega) , \quad (2.50)$$

where $\text{Re}\hat{\Pi}_{\mathbf{q}}^R(\omega)$ is the finite part and

$$Z^{-1} = 1 - \frac{1}{2\omega_{\mathbf{q}}} \left. \frac{\partial \text{Re}\Pi_{\mathbf{q}}^R(\omega)}{\partial \omega} \right|_{\omega=\omega_{\mathbf{q}}, T=0} . \quad (2.51)$$

²This procedure does of course not take proper account of memory effects. If T changes significantly over the time of consideration, a correct computation requires the use of a quantum Boltzmann equation with time dependent spectrum or even a full numerical solution of the Kadanoff-Baym equations.

The spectral function (2.44) now takes the form

$$\rho_{\mathbf{q}}(\omega) = Z \frac{-2Z\text{Im}\Pi_{\mathbf{q}}^R(\omega) + 2\omega\epsilon}{\left(\omega^2 - \omega_{\mathbf{q}}^2 - Z\text{Re}\hat{\Pi}_{\mathbf{q}}^R(\omega)\right)^2 + \left(Z\text{Im}\Pi_{\mathbf{q}}^R(\omega) + \omega\epsilon\right)^2} . \quad (2.52)$$

The renormalized spectral function $\rho_{\mathbf{q}}^r(\omega) = Z\rho_{\mathbf{q}}(\omega)$ takes same shape as (2.44) when expressed in terms of renormalised quantities, namely the renormalized field operator $\phi_r = \sqrt{Z}\phi$ and the renormalized self-energy $\Pi_{\mathbf{q}}^{R,r}(\omega) = Z\hat{\Pi}_{\mathbf{q}}^R(\omega)$,

$$\rho_{\mathbf{q}}^r(\omega) = \frac{-2\text{Im}\Pi_{\mathbf{q}}^{R,r}(\omega) + 2\omega\epsilon}{\left(\omega^2 - \omega_{\mathbf{q}}^2 - \text{Re}\Pi_{\mathbf{q}}^{R,r}(\omega)\right)^2 + \left(\text{Im}\Pi_{\mathbf{q}}^{R,r}(\omega) + \omega\epsilon\right)^2} . \quad (2.53)$$

The divergences of spectral function and statistical propagator can be removed in the same way by mass and wave function renormalisation at zero temperature. In the following we will drop the superscript ‘ r ’ to keep the notation simple.

Solution for the Statistical Propagator

We now turn to the Kadanoff-Baym equation (2.4) for the statistical propagator, which for initial time $t_i = 0$ is given by

$$(\partial_{t_1}^2 + \omega_{\mathbf{q}}^2)\Delta_{\mathbf{q}}^+(t_1, t_2) + \int_0^{t_1} dt' \Pi_{\mathbf{q}}^-(t_1 - t')\Delta_{\mathbf{q}}^+(t', t_2) = \zeta(t_1, t_2) , \quad (2.54)$$

with

$$\zeta(t_1, t_2) = \int_0^{t_2} dt' \Pi_{\mathbf{q}}^+(t_1 - t')\Delta_{\mathbf{q}}^-(t' - t_2) . \quad (2.55)$$

The solution can be written as a sum of the solution $\hat{\Delta}_{\mathbf{q}}^+(t_1, t_2)$ to the homogeneous equation

$$(\partial_{t_1}^2 + \omega_{\mathbf{q}}^2)\hat{\Delta}_{\mathbf{q}}^+(t_1, t_2) + \int_0^{t_1} dt' \Pi_{\mathbf{q}}^-(t_1 - t')\hat{\Delta}_{\mathbf{q}}^+(t', t_2) = 0 . \quad (2.56)$$

and an inhomogeneous piece. The full solution is given by

$$\Delta_{\mathbf{q}}^+(t_1, t_2) = \hat{\Delta}_{\mathbf{q}}^+(t_1, t_2) + \int_0^{t_1} dt' \Delta_{\mathbf{q}}^-(t_1 - t')\zeta(t', t_2) , \quad (2.57)$$

as one can easily verify. There is no derivative with respect to t_2 in the homogeneous equation. Thus, t_2 can be viewed as a parameter. Then (2.56) is identical to (2.31) with an additional parameter t_2 . That allows to read off the general solution from (2.34),

$$\hat{\Delta}_{\mathbf{q}}^+(t_1, t_2) = A_{\mathbf{q}}(t_2)\dot{\Delta}_{\mathbf{q}}^-(t_1) + B_{\mathbf{q}}(t_2)\Delta_{\mathbf{q}}^-(t_1) . \quad (2.58)$$

The definition of Δ^+ implies the symmetry $\hat{\Delta}_{\mathbf{q}}^+(t_1, t_2) = \hat{\Delta}_{\mathbf{q}}^+(t_2, t_1)$, which allows to write

$$A_{\mathbf{q}}(t_2)\dot{\Delta}_{\mathbf{q}}^-(t_1) + B_{\mathbf{q}}(t_2)\Delta_{\mathbf{q}}^-(t_1) = A_{\mathbf{q}}(t_1)\dot{\Delta}_{\mathbf{q}}^-(t_2) + B_{\mathbf{q}}(t_1)\Delta_{\mathbf{q}}^-(t_2) . \quad (2.59)$$

Use of the boundary conditions (1.71)-(1.73), $\Delta_{\mathbf{q}}^-(0) = \ddot{\Delta}_{\mathbf{q}}^-(0) = 0$ and $\dot{\Delta}_{\mathbf{q}}^-(0) = 1$, leads to the relations

$$A_{\mathbf{q}}(t) = A_{\mathbf{q}}(0)\dot{\Delta}_{\mathbf{q}}^-(t) + B_{\mathbf{q}}(0)\Delta_{\mathbf{q}}^-(t) , \quad B_{\mathbf{q}}(t) = \dot{A}_{\mathbf{q}}(0)\dot{\Delta}_{\mathbf{q}}^-(t) + \dot{B}_{\mathbf{q}}(0)\Delta_{\mathbf{q}}^-(t) . \quad (2.60)$$

$A_{\mathbf{q}}(t)$ and $B_{\mathbf{q}}(t)$ can be inserted into (2.59). The symmetry of $\hat{\Delta}_{\mathbf{q}}^+(t_1, t_2)$ then implies $B_{\mathbf{q}}(0) = \dot{A}_{\mathbf{q}}(0)$. The initial state of the system is therefore characterised by three constants, which can be identified with the initial correlations appearing in (1.74)

Eqs. (2.57), (2.58), (2.60) and the initial conditions (1.77)-(1.79) now provide the full solution for the statistical propagator,

$$\begin{aligned} \Delta_{\mathbf{q}}^+(t_1, t_2) &= \Delta_{\mathbf{q},\text{in}}^+\dot{\Delta}_{\mathbf{q}}^-(t_1)\dot{\Delta}_{\mathbf{q}}^-(t_2) + \ddot{\Delta}_{\mathbf{q},\text{in}}^+\Delta_{\mathbf{q}}^-(t_1)\Delta_{\mathbf{q}}^-(t_2) \\ &+ \dot{\Delta}_{\mathbf{q},\text{in}}^+ \left(\dot{\Delta}_{\mathbf{q}}^-(t_1)\Delta_{\mathbf{q}}^-(t_2) + \Delta_{\mathbf{q}}^-(t_1)\dot{\Delta}_{\mathbf{q}}^-(t_2) \right) \\ &+ \Delta_{\mathbf{q},\text{mem}}^+(t_1, t_2) , \end{aligned} \quad (2.61)$$

where

$$\Delta_{\mathbf{q},\text{mem}}^+(t_1, t_2) = \int_0^{t_1} dt' \int_0^{t_2} dt'' \Delta_{\mathbf{q}}^-(t_1 - t') \Pi_{\mathbf{q}}^+(t' - t'') \Delta_{\mathbf{q}}^-(t'' - t_2) . \quad (2.62)$$

This contribution to the statistical propagator, which is independent of the initial conditions, is often referred to as *memory integral*. It can be expressed in the form

$$\Delta_{\mathbf{q},\text{mem}}^+(t_1, t_2) = - \int_{-\infty}^{\infty} \frac{d\omega}{2\pi} e^{-i\omega(t_1-t_2)} \mathcal{H}_{\mathbf{q}}^*(t_1, \omega) \mathcal{H}_{\mathbf{q}}(t_2, \omega) \Pi_{\mathbf{q}}^+(\omega) , \quad (2.63)$$

where [9]

$$\mathcal{H}_{\mathbf{q}}(t, \omega) = \int_0^t dy e^{-i\omega y} \Delta_{\mathbf{q}}^-(y) . \quad (2.64)$$

In (2.61) three of the five parameters of the initial density matrix (1.74) reappear as initial conditions for the statistical propagator. The other two are recovered as initial conditions for the field expectation value, or one-point function. The field $\Phi(x)$ in (2.8) can be identified with the physical field expectation value [22] while $R(x)$ is a *response field*. With the knowledge of the previous section, we can write (2.19) as

$$\Phi_{\mathbf{q}}(t) = \Phi_{\mathbf{q},\text{in}}\dot{\Delta}_{\mathbf{q}}^-(t) + \dot{\Phi}_{\mathbf{q},\text{in}}\Delta_{\mathbf{q}}^-(t) + \int_0^t dt' \Delta_{\mathbf{q}}^-(t - t') \xi_{\mathbf{q}}(t') . \quad (2.65)$$

Performing the initial ensemble, stochastic noise and quantum mechanical averages as in (2.10) one obtains

$$\langle \phi_{\mathbf{q}}(t) \rangle = \dot{\phi}_{\mathbf{q},\text{in}} \Delta_{\mathbf{q}}^{-}(t) + \phi_{\mathbf{q},\text{in}} \dot{\Delta}_{\mathbf{q}}^{-}(t). \quad (2.66)$$

The solution (2.65) agrees with the expression found in [32, 40]. We have assumed that the system is in a symmetric phase and the minimum of the effective potential is at $\langle \phi \rangle = 0$. With Eqs. (2.61) and (2.66), all initial correlations in the Gaussian initial density matrix (1.74) are recovered.

At this point, we should note that the formalism we presented becomes more involved when considering non-Gaussian initial conditions other than thermal equilibrium. Then the Kadanoff-Baym equation for the statistical propagator (1.70) contains additional terms from the initial correlations [22]. In many physically relevant cases Gaussian initial conditions are a good approximation to the physical reality. However, they do not cover all potentially interesting states. An obvious example is thermal equilibrium. Therefore it is not possible by any choice of the parameters in (1.74) to produce a time translation invariant solution. These problems are addressed in some detail in [41, 42].

Let us now discuss the properties of the above solutions. $\Delta_{\mathbf{q},\text{mem}}^{+}(t_1, t_2)$ for late times determines the equilibrium configuration for the statistical propagator. Only the first two lines of (2.61) depend on the physical initial conditions. Since they are directly proportional to Δ^{-} and its derivatives, they are damped exponentially by $\text{Im}\Pi^R$ as one can see from (2.53). This becomes explicitly obvious in the quasiparticle regime. In Sec. 3.1 we present plots of the correlation functions for a particular model for the bath.

Quasiparticle Regime

For small width $\Gamma_{\mathbf{q}}$, ρ can be well approximated by a Breit-Wigner function

$$\rho_{\mathbf{q}}(\omega) \simeq \frac{Z_{\mathbf{q}}}{2\Omega_{\mathbf{q}}} \frac{\text{sign}(\omega)\Gamma_{\mathbf{q}}}{(|\omega| - \Omega_{\mathbf{q}})^2 + \frac{1}{4}\Gamma_{\mathbf{q}}^2}, \quad (2.67)$$

around the quasiparticle peaks. Here $\Gamma_{\mathbf{q}}$ is the quasi-particle width

$$\Gamma_{\mathbf{q}} = -Z_{\mathbf{q}} \frac{\text{Im}\Pi_{\mathbf{q}}^R(\Omega_{\mathbf{q}})}{\Omega_{\mathbf{q}}}, \quad (2.68)$$

and

$$Z_{\mathbf{q}} = \left(1 - \frac{1}{2\Omega_{\mathbf{q}}} \frac{\partial \text{Re}\Pi_{\mathbf{q}}^R(\omega)}{\partial \omega} \Big|_{\omega=\Omega_{\mathbf{q}}} \right)^{-1}. \quad (2.69)$$

Away from the quasiparticle peaks, $\rho_{\mathbf{q}}(\omega)$ is not well-approximated by (2.67), but any ω integration will be strongly dominated by the peak region. This allows to perform the

integral in (2.43). If $\pm\hat{\Omega}_{\mathbf{q}}$ are the only solutions to (1.9), one obtains

$$\Delta_{\mathbf{q}}^{-}(y) \simeq Z_{\mathbf{q}} \frac{\sin(\Omega_{\mathbf{q}} y)}{\Omega_{\mathbf{q}}} e^{-\Gamma_{\mathbf{q}} |y|/2} \approx \frac{\sin(\Omega_{\mathbf{q}} y)}{\Omega_{\mathbf{q}}} e^{-\Gamma_{\mathbf{q}} |y|/2}, \quad (2.70)$$

where the last step assumes that $\text{Re}\Pi^R$ is smooth around $\omega = \Omega_{\mathbf{q}}$. For the statistical propagator to leading order in $\Gamma_{\mathbf{q}}$ this yields

$$\begin{aligned} \Delta^{+}(t; y) &\approx \frac{\Delta_{\mathbf{q};\text{in}}^{+}}{2} (\cos(2\Omega_{\mathbf{q}} t) + \cos(\Omega_{\mathbf{q}} y)) e^{-\Gamma_{\mathbf{q}} t} \\ &\quad - \frac{\ddot{\Delta}_{\mathbf{q};\text{in}}^{+}}{2\Omega_{\mathbf{q}}^2} (\cos(2\Omega_{\mathbf{q}} t) - \cos(\Omega_{\mathbf{q}} y)) e^{-\Gamma_{\mathbf{q}} t} \\ &\quad + \frac{\dot{\Delta}_{\mathbf{q};\text{in}}^{+}}{\Omega_{\mathbf{q}}} \sin(2\Omega_{\mathbf{q}} t) e^{-\Gamma_{\mathbf{q}} t} \\ &\quad + \frac{\coth(\frac{\beta\Omega_{\mathbf{q}}}{2})}{2\Omega_{\mathbf{q}}} \cos(\Omega_{\mathbf{q}} y) (e^{-\Gamma_{\mathbf{q}} |y|/2} - e^{-\Gamma_{\mathbf{q}} t}). \end{aligned} \quad (2.71)$$

To obtain the last result, we have used Eqs. (1.95) and (2.42) to write

$$\Pi_{\mathbf{q}}^{+}(\omega) = (1 + 2f_B(\omega)) \text{Im}\Pi_{\mathbf{q}}^R(\omega) \quad (2.72)$$

and then applied Cauchy's theorem to perform the ω integration in (2.63). This in principle problematic because the factor $1 + 2f_B$ from the KMS relation has infinitely many poles along the imaginary axis. However, generally the integration in $\mathcal{H}_{\mathbf{q}}(t, \omega)$, see (2.64), produces quasi-poles at $\pm\Omega_{\mathbf{q}}$. One can, as previously, argue that the ω -integral is always dominated by the regions near the poles and therefore replace ω by $\Omega_{\mathbf{q}}$ before using Cauchy's theorem. This approximation is questionable for $t \ll 1/\Gamma$ but reasonable for all later times, when $\mathcal{H}_{\mathbf{q}}^{*}(t_1, \omega)\mathcal{H}_{\mathbf{q}}(t_2, \omega)$ develops narrow peaks around $\pm\Omega_{\mathbf{q}}$ and finally approaches a form that is proportional to $\rho_{\mathbf{q}}(\omega)$, an approximate δ -function, see Sec. 2.2.3³. We have also neglected $\Gamma_{\mathbf{q}}$ in the arguments of the distribution functions. Thus, it can be argued that the contributions from the poles on the imaginary axis are small except for early times⁴. This is confirmed by numerical comparison for the cases relevant for this work.

Note that the solution (2.71) for Δ^{+} does not become time translation invariant in the limit of vanishing interaction, $\Gamma_{\mathbf{q}} \rightarrow 0$ and $\Omega_{\mathbf{q}} \rightarrow \omega_{\mathbf{q}}$, unless one chooses $\dot{\Delta}_{\mathbf{q};\text{in}}^{+} = 0$ and $\Delta_{\mathbf{q};\text{in}}^{+} = \Omega_{\mathbf{q}}^2 \ddot{\Delta}_{\mathbf{q};\text{in}}^{+}$. Instead, it oscillates with twice the plasma frequency $\Omega_{\mathbf{q}} \rightarrow \omega_{\mathbf{q}}$.

³Note also that the common practice to use a narrow Breit-Wigner function like (2.67) as an approximate δ -function is only justified if the function that it is multiplied with under the integral does not change rapidly (e.g. oscillates) between $\Omega_{\mathbf{q}} - \Gamma_{\mathbf{q}} < \omega < \Omega_{\mathbf{q}} + \Gamma_{\mathbf{q}}$. This does not pose a problem here, but care has to be taken when inserting Δ^{\pm} into loop integrals.

⁴See corresponding discussion for fermions in B.4.

In this limit Δ^\pm can be understood as that of a *free nonequilibrium propagators*. They correspond the propagators in an ensemble of states that is characterised by some Gaussian density matrix in a free quantum field theory. However, the oscillations with t are not a consistency problem since Δ^+ itself is not an observable. As we will see in Sec. 2.3.1, e.g. the energy density $\epsilon_{\mathbf{q}}$ computed from (2.71) is time translation invariant in the free limit.

Eqs. (2.70) and (2.71) show explicitly that the system approaches equilibrium independent of the initial conditions after a characteristic time $\tau = 1/\Gamma$ which is sometimes referred to as the lifetime of a quasiparticle. This can be seen by taking the limit $t \rightarrow \infty$. Then Eqs. (2.70) and (2.71) fulfil the KMS relation (1.95). Here we prefer the term *relaxation time* for τ instead of *lifetime*. It is more precise because the abundance in the plasma is non-zero even in equilibrium. Furthermore, if one starts with an underpopulation of modes, equilibration actually means an overall production of quasiparticles. Examples are the thermal production of dark matter particles or that of the heavy neutrinos in thermal leptogenesis. Finally, the term lifetime can also be misleading because it suggests that one starts with a given number of particles that decay one by one. In fact, in a relativistic plasma a continuous creation and annihilation takes place with an overweight of either that leads to equilibration and τ should rather be seen as a relaxation time for the system as a whole.

If (1.9) has more solutions than $\pm\hat{\Omega}_{\mathbf{q}}$ and the narrow width condition (1.12) is fulfilled near all of them, all of those behave like quasiparticles even though they might have a collective origin. The integration can still be performed and the generalisation of Eqs. (2.70) and (2.71) is straightforward. Δ^\mp of course implicitly depend on T via Π^R .

2.2.2 Solutions for Fermions

Spectral Function The Kadanoff-Baym equations (1.88) and (1.89) for fermions can be solved in the same way as for bosons. With the assumptions made in the beginning of this chapter, the equation for the spectral propagator reads

$$(i\gamma^0\partial_y - \boldsymbol{q} - m)S_{\mathbf{q}}^-(y) = \int_0^y dy' \Sigma_{\mathbf{q}}^-(y - y')S_{\mathbf{q}}^-(y'), \quad (2.73)$$

where $\boldsymbol{q} = \mathbf{q}_i\gamma^i$. Again, we perform a Laplace transform

$$\tilde{S}_{\mathbf{q}}(s) = \int_0^\infty dy e^{-sy} S_{\mathbf{q}}(y), \quad (2.74)$$

and correspondingly for the self energy, to obtain

$$\tilde{S}_{\mathbf{q}}^-(s) = \left(-i\gamma^0 s + \boldsymbol{q} + m + \tilde{\Sigma}_{\mathbf{q}}^-(s)\right)^{-1} i\gamma^0 S_{\mathbf{q}}(0). \quad (2.75)$$

The equal-time anticommutation relations for fermions imply

$$S_{\mathbf{q}}^-(0) = i\gamma^0. \quad (2.76)$$

As for bosons, the initial conditions for the spectral propagator do not depend on the physical initial conditions. The back-transformation goes via the Bromwich contour, using the same deformation as in the scalar case.

$$S_{\mathbf{q}}^-(y) = i \int_{-\infty}^{\infty} \frac{d\omega}{2\pi} e^{-i\omega y} \rho_{\mathbf{q}}(\omega) \quad (2.77)$$

with

$$\rho_{\mathbf{q}}(\omega) = \left(\frac{i}{\not{q} - m - \Sigma_{\mathbf{q}}^R(\omega) + i\epsilon\gamma^0} - \frac{i}{\not{q} - m - \Sigma_{\mathbf{q}}^A(\omega) - i\epsilon\gamma^0} \right) \quad (2.78)$$

The integrand shall now be inverted. Σ carries two spinor indices and can be expanded in the basis

$$\Sigma = \Sigma_{(S)} \mathbb{1} + i\gamma_5 \Sigma_{(P)} + \gamma_{\mu} \Sigma_{(V)}^{\mu} + \gamma_{\mu} \gamma_5 \Sigma_{(A)}^{\mu} + \frac{1}{2} \sigma_{\mu\nu} \Sigma_{(T)}^{\mu\nu}. \quad (2.79)$$

In the simplest case, when there is no C and P violation, the pseudoscalar and axial vector part vanish. We assume that there is only one flavour or Σ is diagonal in flavour space. These simplifications have to be dropped when applying the result to leptogenesis, where CP violation and flavour mixing are essential. Finally we drop the tensor piece $\Sigma_{(T)}$ because it will not appear in the examples we discuss in the following chapter. Then the spectral function takes the shape

$$\rho_{\mathbf{q}}(\omega) = -2\text{Im} \left(\frac{1}{\mathcal{Q} - \mathcal{M}} \right) = -2\text{Im} \left(\frac{\mathcal{Q} + \mathcal{M}}{\mathcal{Q}^2 - \mathcal{M}^2} \right) \quad (2.80)$$

with the vector $\mathcal{Q} = \not{q} + i\epsilon u - \Sigma_{(V)}^R$ and the scalar $\mathcal{M} = m + \Sigma_{(S)}^R$. Here u is the four-velocity of the thermal bath. In the system of rest of the bath $u = (1, 0, 0, 0)$. The Lorentz components of Σ can conveniently be expressed by the three scalar functions $a_{\mathbf{q}}(\omega)$, $b_{\mathbf{q}}(\omega)$ and $c_{\mathbf{q}}(\omega)$,

$$\Sigma_{(V)}^R = a_{\mathbf{q}}(\omega) \not{q} + b_{\mathbf{q}}(\omega) \not{u}, \quad \Sigma_{(S)}^R = c_{\mathbf{q}}(\omega). \quad (2.81)$$

The functions $a_{\mathbf{q}}(\omega)$, $b_{\mathbf{q}}(\omega)$ and $c_{\mathbf{q}}(\omega)$ have to be computed from Feynman diagrams contributing to $\text{Im}\Sigma_{\mathbf{q}}^R(\omega)$. In the limit of vanishing interaction (2.80) simplifies to

$$\rho_{\mathbf{q}}^{\text{free}}(\omega) = 2\pi(\not{q} + m) \text{sign}(\omega) \delta(q^2 - m^2) \quad (2.82)$$

Statistical Propagator The equation for the statistical propagator can be written as

$$(i\gamma_0 \partial_{t_1} - \not{q} - m) S_{\mathbf{q}}^+(t_1, t_2) - \int_0^{t_1} dt' \Sigma_{\mathbf{q}}^-(t_1 - t') S_{\mathbf{q}}^+(t', t_2) = \zeta_{\mathbf{q}}(t_1, t_2) \quad (2.83)$$

with

$$\zeta_{\mathbf{q}}(t_1, t_2) = - \int_0^{t_2} dt' \Sigma_{\mathbf{q}}^+(t_1 - t') S_{\mathbf{q}}^-(t' - t_2). \quad (2.84)$$

We follow the same strategy as in the scalar case. The full solution can be written as the solution $\hat{S}_{\mathbf{q}}^+(t_1, t_2)$ to the homogeneous equation

$$(i\gamma_0\partial_{t_1} - \boldsymbol{q} - m)\hat{S}_{\mathbf{q}}^+(t_1, t_2) - \int_0^{t_1} dt' \Sigma_{\mathbf{q}}^-(t_1 - t')\hat{S}_{\mathbf{q}}^+(t', t_2) = 0 \quad (2.85)$$

and a memory integral $S_{\mathbf{q},\text{mem}}^+(t_1, t_2)$. Following the same steps as in the scalar case and using the symmetry relations (1.86) and (1.87), one can find

$$\hat{S}_{\mathbf{q}}^+(t_1, t_2) = -S_{\mathbf{q}}^-(t_1)\gamma^0 S_{\mathbf{q}}^+(0, 0)\gamma^0 S_{\mathbf{q}}^-(-t_2) \quad (2.86)$$

and

$$S_{\mathbf{q},\text{mem}}^+(t_1, t_2) = -\int_0^{t_1} dt' S_{\mathbf{q}}^-(t_1 - t')\zeta(t', t_2), \quad (2.87)$$

hence

$$S_{\mathbf{q}}^+(t_1, t_2) = -S_{\mathbf{q}}^-(t_1)\gamma^0 S_{\mathbf{q}}^+(0, 0)\gamma^0 S_{\mathbf{q}}^-(-t_2) + \int_0^{t_1} dt' S_{\mathbf{q}}^-(t_1 - t') \int_0^{t_2} dt'' \Sigma_{\mathbf{q}}^+(t' - t'') S_{\mathbf{q}}^-(t'' - t_2). \quad (2.88)$$

The solution for the nonequilibrium statistical propagator is, to the best of our knowledge, original and have not been known in the previous literature.

Weak Coupling We again consider the quasiparticle regime. This time we assume for simplicity that Ψ is sufficiently heavy and weakly coupled that one can neglect the thermal mass correction with respect to the intrinsic mass⁵. This is e.g. fulfilled for the heavy neutrinos in leptogenesis or a sufficiently weakly coupled dark matter candidate. The thermal width has to be kept because there is no large width at zero temperature compared to which it could be neglected. Finally, let us assume that the self energy is a pure Lorentz vector, $\Sigma_{(S)} = 0$ and $\Sigma = \Sigma_{(V)}^\mu \gamma_\mu$. We can then decompose

$$\begin{aligned} \Sigma_{\mathbf{q}}^+(\omega) &= -\frac{i}{2} (1 - 2f_F(\omega)) \Sigma_{\mathbf{q}}^-(\omega) = (1 - 2f_F(\omega)) \text{Im} \Sigma_{\mathbf{q}}^R(\omega) \\ &= (1 - 2f_F(\omega)) \text{Im} (a_{\mathbf{q}}(\omega)\boldsymbol{q} + b_{\mathbf{q}}(\omega)\not{\boldsymbol{q}}). \end{aligned} \quad (2.89)$$

Then the spectral propagator simplifies to

$$S^-(y) = e^{-\Gamma_{\mathbf{q}}|y|/2} \left(i\gamma^0 \cos(\omega_{\mathbf{q}}y) - \frac{\boldsymbol{\gamma}\mathbf{q} - m}{\omega_{\mathbf{q}}} \sin(\omega_{\mathbf{q}}y) \right), \quad (2.90)$$

⁵Here we use the term "intrinsic mass" to refer to the mass a particle has in vacuum, namely the pole of the two-point function after renormalisation. "Effective mass" or "thermal mass" then refers to the change of location of this pole due to the interaction with the medium.

from which also \hat{S}^+ can be found by insertion into (2.88). Here we have defined

$$\Gamma_{\mathbf{q}} = -2\text{Im} \frac{a_{\mathbf{q}}(\omega) + \omega b_{\mathbf{q}}(\omega)}{\omega} \Big|_{\omega=\omega_{\mathbf{q}}}. \quad (2.91)$$

The memory integral can be written in the form

$$\int \frac{d\omega}{2\pi} \left(\int_0^{t_1} dy_1 S^-(y_1) e^{i\omega y_1} \right) \Sigma^+(\omega) \left(\int_0^{t_2} dy_2 S^-(-y_2) e^{-i\omega y_2} \right) e^{-i\omega(t_1-t_2)}. \quad (2.92)$$

We again aim to find a simple expression in terms of the parameters m and $\Gamma_{\mathbf{q}}$. After inserting (2.90) and (2.89) into (2.92), the narrow width limit allows to perform the various integrations. As for the Bose-Einstein distribution in the scalar case, care has to be taken because $1 - 2f_F(\omega) = \tanh\left(\frac{\beta\omega}{2}\right)$ has an infinite number of poles along the imaginary axis. Fortunately, those do not contribute significantly except for early times, see Appendix B.4. To leading order in $\Gamma_{\mathbf{q}}$ the result is

$$\begin{aligned} S_{\mathbf{q},\text{mem}}^+(t_1, t_2) &\approx \frac{\tanh(\beta\omega_{\mathbf{q}}/2)}{2\omega_{\mathbf{q}}} \left(e^{-\Gamma/2|t_1-t_2|} - e^{-\Gamma/2(t_1+t_2)} \right) \\ &\times \left((m - \gamma_{\mathbf{q}}) \cos(\omega_{\mathbf{q}}(t_1 - t_2)) - i\gamma^0 \omega_{\mathbf{q}} \sin(\omega_{\mathbf{q}}(t_1 - t_2)) \right) \end{aligned} \quad (2.93)$$

or

$$\begin{aligned} S_{\mathbf{q},\text{mem}}^+(y; t) &\approx \frac{1}{2\omega_{\mathbf{q}}} (1 + 2f_F(\omega_{\mathbf{q}})) \\ &\times \left(e^{-\Gamma/2|y|} - e^{-\Gamma t} \right) \left((m - \gamma_{\mathbf{q}}) \cos(\omega_{\mathbf{q}} y) - i\gamma^0 \omega_{\mathbf{q}} \sin(\omega_{\mathbf{q}} y) \right). \end{aligned} \quad (2.94)$$

Again, one can explicitly see the approach to thermal equilibrium by verifying that the Fourier transforms of the propagators (2.90) and (2.94) fulfil the KMS relation (1.105) in the limit $t \rightarrow \infty$.

2.2.3 Approach to Thermal Equilibrium

In the previous chapter we showed explicitly that the system approaches thermal equilibrium on timescales $1/\Gamma$ in the quasiparticle regime. We now want to derive this result without use of the narrow width approximation. For simplicity, we will demonstrate the equilibration for scalars, the generalisation to fermions is straightforward. Equilibrium can be characterised by the condition that the integral

$$\Delta_{\mathbf{q}}^+(t, \omega) = \int_{-2t}^{2t} dy e^{i\omega y} \Delta_{\mathbf{q}}^+ \left(t + \frac{y}{2}, t - \frac{y}{2} \right), \quad (2.95)$$

which becomes a Fourier transform for $t \rightarrow \infty$, satisfies the KMS condition asymptotically,

$$\Delta_{\mathbf{q}}^+(\infty, \omega) = -\frac{i}{2} \coth\left(\frac{\beta\omega}{2}\right) \Delta_{\mathbf{q}}^-(\omega) \dots \quad (2.96)$$

Since $\Delta_{\mathbf{q}}^-(t)$ and $\dot{\Delta}_{\mathbf{q}}^-(t)$ fall off exponentially, at times $t \gg 1/\Gamma$ only the memory integral remains, and nothing else matters. One then obtains

$$\Delta_{\mathbf{q}}^+(\infty, \omega) = \Delta_{\mathbf{q}, \text{mem}}^+(\infty, \omega) = -|\mathcal{H}_{\mathbf{q}}(\infty, \omega)|^2 \Pi_{\mathbf{q}}^+(\omega) . \quad (2.97)$$

The quantity $\mathcal{H}_{\mathbf{q}}(\infty, \omega)$ at late times approaches the Laplace transform of the spectral function,

$$\begin{aligned} \mathcal{H}_{\mathbf{q}}(\infty, \omega) &= \int_0^\infty d\tau e^{-i(\omega - i\epsilon)\tau} \Delta_{\mathbf{q}}^-(\tau) \\ &= \tilde{\Delta}_{\mathbf{q}}^-(i\omega + \epsilon) \\ &= \frac{1}{s^2 + \omega_{\mathbf{q}}^2 + \tilde{\Pi}_{\mathbf{q}}(s)} \Big|_{s=i\omega+\epsilon} \\ &= -\frac{1}{\omega^2 - \omega_{\mathbf{q}}^2 - \text{Re}\Pi_{\mathbf{q}}^R(\omega) - i\text{Im}\Pi_{\mathbf{q}}^R(\omega)} , \end{aligned} \quad (2.98)$$

leading to

$$\begin{aligned} |\mathcal{H}_{\mathbf{q}}(\infty, \omega)|^2 &= \frac{1}{(\omega^2 - \omega_{\mathbf{q}}^2 - \text{Re}\Pi_{\mathbf{q}}^R(\omega))^2 + (\text{Im}\Pi_{\mathbf{q}}^R(\omega))^2} \\ &= -\frac{\rho_{\mathbf{q}}(\omega)}{2\text{Im}\Pi_{\mathbf{q}}^R(\omega)} . \end{aligned} \quad (2.99)$$

Insertion of this expression into (2.97) and use of the KMS condition for the self-energy as well as (2.42),

$$\Pi_{\mathbf{q}}^-(\omega) = 2i\text{Im}\Pi_{\mathbf{q}}^R(\omega) ,$$

yields (cf. (2.43),(2.44)),

$$\begin{aligned} \Delta_{\mathbf{q}}^+(\infty, \omega) &= -\coth\left(\frac{\beta\omega}{2}\right) \frac{\text{Im}\Pi_{\mathbf{q}}^R(\omega)}{(\omega^2 - \omega_{\mathbf{q}}^2 - \text{Re}\Pi_{\mathbf{q}}^R(\omega))^2 + (\text{Im}\Pi_{\mathbf{q}}^R(\omega))^2} \\ &= -\frac{i}{2} \coth\left(\frac{\beta\omega}{2}\right) \Delta_{\mathbf{q}}^-(\omega) . \end{aligned} \quad (2.100)$$

Hence, we can confirm that the system reaches microscopical equilibrium, characterised by the KMS condition (1.95), at late times.

In more complex systems, in particular when many degrees of freedom are out of equilibrium, thermalisation can be a highly nontrivial aspect. In general, there is more than one timescale involved. Subsystems can reach equilibrium before thermalising with each other. In other cases, macroscopic characteristics of the system can reach their equilibrium values well before microstate does, see e.g. [43, 44].

2.3 Plasma Properties

In the previous sections we have studied thermodynamical systems in terms of correlation functions. We now turn to physical observables that characterise the plasma properties. In some cases, the connection between correlation functions and observables is rather direct. For instance, the spectral function ρ of resonances in a medium can be measured for mesons propagating in nuclear matter, see Fig. 2.4. Such mesons can be generated in target nuclei by injection of high energetic photons. ω - and ϕ -mesons are short lived enough that they do not leave the nucleus before decaying. If the decay happens into two leptons, those can be detected and reveal information about the resonance's energy and momentum. The nucleus provides a medium in a close-to-equilibrium state with low temperature and high baryon chemical potential. To explore higher temperatures, in particular those near the QCD phase transitions, one can study similar signals in relativistic heavy ion collisions. Inconveniently, the collision initially leaves the system in a far-from-equilibrium state. It then undergoes phases of thermalisation and, at high energies, hadronisation. Measured data generally involves some integration over time, making it difficult to extract properties for a particular temperature. Another often studied observable that can be related to the spectral function is the shear viscosity η , which can be computed from ρ by $\eta = \pi \frac{\partial \rho}{\partial \omega} \Big|_{\omega=0}$. Here we will focus on the energy momentum tensor, which can be computed from the statistical propagator.

Unfortunately, none of the current laboratory experiments allows to study the conditions in the early universe directly, not even for those phenomena that happen at energies which are accessible to particle accelerators. The reason is that, due to the lack of anti-nuclei, laboratory experiments always involve a high baryon chemical potential while in the early universe the chemical potential was extremely tiny. It is therefore impossible to directly obtain information about the primordial plasma. However, the relic densities of various particles do provide us with some data. In case of the big bang nucleosynthesis, there is a good agreement between theoretical predictions based on Boltzmann equations and observational data [4].

In the following we study how the Boltzmann equations emerge from the Kadanoff-Baym equations when the plasma properties are that of a dilute gas and which modifications are necessary when going beyond that regime. Thereby we will focus on kinematic aspects as discussed in Sec. 1.2.1. These are equal for bosons and fermions. For simplicity we will study them for scalars, with straightforward generalisation to fermions. We base our analysis on energy densities to avoid the problems related to the definition of a particle number in an interacting quantum field theory. Since we neglect backreaction, the energy-momentum tensor $T_{\mu\nu}$ of the whole system, as a Noether current resulting from time and space translations, is not conserved in our setup. We focus on the quantity

$$T_{\mu\nu}^{\phi} = \partial_{\mu}\phi\partial_{\nu}\phi - \eta_{\mu\nu}\mathcal{L}, \quad (2.101)$$

the contribution of ϕ to $T_{\mu\nu}$. This allows to define the contribution of a mode with

momentum \mathbf{q} to energy density and pressure,

$$\epsilon_{\mathbf{q}}^{\phi} = \langle T_{00}^{\phi} - g\phi\mathcal{O}[\mathcal{X}] \rangle|_{\mathbf{q}} = \frac{1}{2} \langle \dot{\phi}^2 + (\nabla\phi)^2 + m^2\phi^2 \rangle|_{\mathbf{q}}, \quad (2.102)$$

$$p_{\mathbf{q}}^{\phi} = \langle T_{ii} - g\phi\mathcal{O}[\mathcal{X}] \rangle|_{\mathbf{q}} = \langle \frac{1}{3}(\nabla\phi)^2 + \frac{1}{2}(\dot{\phi}^2 - (\nabla\phi)^2 - m^2\phi^2) \rangle|_{\mathbf{q}}. \quad (2.103)$$

In terms of correlation functions, this yields

$$\epsilon_{\mathbf{q}}^{\phi}(t) = \frac{1}{2} (\partial_{t_1}\partial_{t_2} + \omega_{\mathbf{q}}^2) (\Delta_{\mathbf{q}}^+(t_1, t_2) + \langle \phi_{\mathbf{q}}(t_1) \rangle \langle \phi_{\mathbf{q}}(t_2) \rangle) \Big|_{t_1=t_2=t} \quad (2.104)$$

and

$$p_{\mathbf{q}}^{\phi}(t) = \left(\frac{1}{3}\mathbf{q}^2 + \frac{1}{2} (\partial_{t_1}\partial_{t_2} - \omega_{\mathbf{q}}^2) \right) (\Delta_{\mathbf{q}}^+(t_1, t_2) + \langle \phi_{\mathbf{q}}(t_1) \rangle \langle \phi_{\mathbf{q}}(t_2) \rangle) \Big|_{t_1=t_2=t} \quad (2.105)$$

for energy and momentum.

2.3.1 Comparison to Boltzmann Equations

In Sec. 1.2 we discussed the limitations of Boltzmann equations. We concluded that they can give a good physical description of weakly coupled systems when the density is low and coherence effects are not important. Therefore the solutions of Boltzmann equations should emerge as a low density limit of our solutions for the Kadanoff-Baym equations. Since the former are formulated in terms of particle numbers, it is intuitive to look for a correspondence in the regimes where this concept is meaningful, namely the particle and quasiparticle regime. We first confirm on general grounds that in this regime, the time evolution of a small deviation from equilibrium is governed by a Boltzmann equation [49]. The computation also shows the breakdown of this description beyond the quasiparticle regime. We then move on to a detailed comparison based on our explicit solutions for the spectral and statistical propagators before discussing quantum corrected Boltzmann equations in Sec. 2.3.2.

Breakdown beyond the Narrow Width Limit

We start from the Kadanoff-Baym equation for the statistical propagator (2.4),

$$(\partial_{t_1}^2 + \omega_{\mathbf{q}}^2)\Delta_{\mathbf{q}}^+(t_1, t_2) + \int_0^{t_1} dt' \Pi_{\mathbf{q}}^-(t_1 - t')\Delta_{\mathbf{q}}^+(t', t_2) = \int_0^{t_2} dt' \Pi_{\mathbf{q}}^+(t_1 - t')\Delta_{\mathbf{q}}^-(t' - t_2). \quad (2.106)$$

At times $t \gg \tau = 1/\Gamma$, the system is already close to equilibrium. It is known that then the deviation from thermal equilibrium fulfils a Boltzmann type equation [49]. We reproduce this result from first principles, without making an ansatz for the shape of Δ^+ . At late

times, the dependence on the initial values at $t_i = 0$ is negligible and one can extend the lower integration limit to $-\infty$,

$$(\partial_{t_1}^2 + \omega_{\mathbf{q}}^2)\Delta_{\mathbf{q}}^+(t_1, t_2) + \int_{-\infty}^{\infty} dt' (\Pi_{\mathbf{q}}^R(t_1 - t')\Delta_{\mathbf{q}}^+(t', t_2) + i\Pi_{\mathbf{q}}^+(t_1 - t')\Delta_{\mathbf{q}}^A(t' - t_2)) = 0 . \quad (2.107)$$

We change to relative and centre of mass time variables,

$$t = \frac{t_1 + t_2}{2} , \quad y = t_1 - t_2 , \quad \Delta_{\mathbf{q}}^+(t; y) \equiv \Delta_{\mathbf{q}}^+(t_1, t_2) , \quad (2.108)$$

and perform a derivative expansion,

$$\Delta_{\mathbf{q}}^+\left(\frac{t' + t_2}{2}; t' - t_2\right) = \Delta_{\mathbf{q}}^+(t; t' - t_2) + \frac{t' - t_1}{2}\partial_t\Delta_{\mathbf{q}}^+(t; t' - t_2) + \dots . \quad (2.109)$$

The expansion is justified because for $t \gg \tau$ the deviation from equilibrium is small and changes only slowly. Then one finds for the Fourier transforms with respect to the relative time,

$$\begin{aligned} & \left(\frac{1}{4}\partial_t^2 - i\omega\partial_t - \omega^2 + \omega_{\mathbf{q}}^2\right) \Delta_{\mathbf{q}}^+(t; \omega) \\ &= -\Pi_{\mathbf{q}}^R(\omega)\Delta_{\mathbf{q}}^+(t; \omega) - i\Pi_{\mathbf{q}}^+(\omega)\Delta_{\mathbf{q}}^A(t; \omega) - \frac{i}{2}\frac{\partial\Pi_{\mathbf{q}}^R(\omega)}{\partial\omega}\frac{\partial\Delta_{\mathbf{q}}^+(t; \omega)}{\partial t} . \end{aligned} \quad (2.110)$$

This is a complex equation. Its real and imaginary part have to be fulfilled separately. With the relations given in Appendix B.3, one can derive the two real equations,

$$\begin{aligned} \left(\frac{1}{4}\partial_t^2 - \omega^2 + \omega_{\mathbf{q}}^2\right) \Delta_{\mathbf{q}}^+(t, \omega) &= -\text{Re}\Pi_{\mathbf{q}}^R(\omega)\Delta_{\mathbf{q}}^+(t, \omega) + \Pi_{\mathbf{q}}^+(\omega)\text{Im}\Delta_{\mathbf{q}}^A(t, \omega) \\ &+ \frac{1}{2}\frac{\partial\text{Im}\Pi_{\mathbf{q}}^R(\omega)}{\partial\omega}\frac{\partial\Delta_{\mathbf{q}}^+(t, \omega)}{\partial t} + \dots , \end{aligned} \quad (2.111)$$

$$\begin{aligned} \omega\frac{\partial}{\partial t}\Delta_{\mathbf{q}}^+(t, \omega) &= \text{Im}\Pi_{\mathbf{q}}^R(\omega)\Delta_{\mathbf{q}}^+(t, \omega) + \Pi_{\mathbf{q}}^+(\omega)\text{Re}\Delta_{\mathbf{q}}^A(t, \omega) \\ &+ \frac{1}{2}\frac{\partial\text{Re}\Pi_{\mathbf{q}}^R(\omega)}{\partial\omega}\frac{\partial\Delta_{\mathbf{q}}^+(t, \omega)}{\partial t} + \dots , \end{aligned} \quad (2.112)$$

from the real and imaginary part of (2.110). One can always write $\Delta_{\mathbf{q}}^+(t, \omega)$ as the sum of its equilibrium value $\Delta_{\mathbf{q}}^+(\omega)$ and a deviation $\delta\Delta_{\mathbf{q}}^+(t, \omega)$,

$$\Delta_{\mathbf{q}}^+(t, \omega) = \Delta_{\mathbf{q}}^+(\omega) + \delta\Delta_{\mathbf{q}}^+(t, \omega) . \quad (2.113)$$

Equation (2.112) implies

$$\text{Im}\Pi_{\mathbf{q}}^R(\omega)\Delta_{\mathbf{q}}^+(\omega) + \Pi_{\mathbf{q}}^+(\omega)\text{Re}\Delta_{\mathbf{q}}^A(\omega) = 0 , \quad (2.114)$$

which is known to be satisfied because the relations of (B.99), (B.92) and the KMS conditions (1.95) and (1.96).

The first equation, (2.111), poses a condition on the equilibrium solution,

$$(\omega^2 - \omega_{\mathbf{q}}^2 - \text{Re}\Pi_{\mathbf{q}}^R(\omega)) \Delta_{\mathbf{q}}^+(\omega) = -\Pi_{\mathbf{q}}^+(\omega) \text{Im}\Delta_{\mathbf{q}}^A(\omega) . \quad (2.115)$$

For vanishing width, the condition is fulfilled when

$$\omega = \Omega_{\mathbf{q}} = \sqrt{\omega_{\mathbf{q}}^2 + \text{Re}\Pi_{\mathbf{q}}^R(\Omega_{\mathbf{q}})} , \quad (2.116)$$

where it is important to realise that the right hand side vanishes due to Eqs. (1.96) and (2.42) and the definition of $\Gamma_{\mathbf{q}}$. The finite width leads to a correction,

$$\omega = \Omega_{\mathbf{q}} + \delta\Omega_{\mathbf{q}} . \quad (2.117)$$

To leading order in $\delta\Omega_{\mathbf{q}}$, one obtains for (2.115),

$$2\Omega_{\mathbf{q}}\delta\Omega_{\mathbf{q}}\Delta_{\mathbf{q}}^+(\Omega_{\mathbf{q}}) + \Pi^+(\Omega_{\mathbf{q}})\text{Im}\Delta_{\mathbf{q}}^A(\Omega_{\mathbf{q}}) = 0 , \quad (2.118)$$

which implies

$$\delta\Omega_{\mathbf{q}} = -\frac{\Gamma_{\mathbf{q}} \text{Im}\Delta_{\mathbf{q}}^A(\Omega_{\mathbf{q}})}{2 \text{Re}\Delta_{\mathbf{q}}^A(\Omega_{\mathbf{q}})} . \quad (2.119)$$

With (B.92), we can use the free spectral function,

$$\Delta_{\mathbf{q}}^-(\omega) = 2\pi i \text{sign}(\omega) \delta(\omega^2 - \Omega_{\mathbf{q}}^2) , \quad (2.120)$$

to find an expression for $\text{Im}\Delta_{\mathbf{q}}^A(\Omega_{\mathbf{q}})$ to leading order in $\Gamma_{\mathbf{q}}$,

$$\text{Im}\Delta^A(\Omega_{\mathbf{q}}) = -\frac{1}{2\pi} \mathcal{P} \int \frac{\rho(\omega')}{\omega' - \Omega_{\mathbf{q}}} d\omega' = \frac{1}{4\Omega_{\mathbf{q}}^2} . \quad (2.121)$$

With Eqs. (2.119), (B.91), (2.44) and (2.68) we finally obtain

$$\delta\Omega_{\mathbf{q}} = \frac{1}{8} \frac{\Gamma_{\mathbf{q}}^2}{\Omega_{\mathbf{q}}} . \quad (2.122)$$

This shows that for $\Gamma_{\mathbf{q}} \ll \Omega_{\mathbf{q}}$, the leading term in the derivative expansion enforces $\omega = \Omega_{\mathbf{q}}$. This is self-consistent because we used the free spectral function in the derivation. If finite width effects are not negligible, however, off-shell effects become important and the derivative expansion becomes unreliable.

An equation of motion for the departure from equilibrium of the statistical propagator can be obtained by inserting $\omega = \Omega_{\mathbf{q}}$ into (2.112),

$$\left(\left(1 - \frac{1}{2\Omega_{\mathbf{q}}} \frac{\partial}{\partial \omega} \text{Re}\Pi_{\mathbf{q}}^R(\omega) \Big|_{\Omega_{\mathbf{q}}} \right) \frac{\partial}{\partial t} - \frac{1}{\Omega_{\mathbf{q}}} \text{Im}\Pi_{\mathbf{q}}^R(\Omega_{\mathbf{q}}) \right) \delta\Delta_{\mathbf{q}}^+(t; \Omega_{\mathbf{q}}) = 0 . \quad (2.123)$$

We can now compute the energy density

$$\begin{aligned}\epsilon_{\mathbf{q}}^{\phi}(t) &= \frac{1}{2} (\partial_{t_1} \partial_{t_2} + \omega_{\mathbf{q}}^2) \Delta_{\mathbf{q}}^+(t_1, t_2) \Big|_{t_1=t_2=t} \\ &= \frac{1}{2\omega_{\mathbf{q}}} \int_{-\infty}^{\infty} d\omega \left(\frac{1}{4} \partial_t^2 + \omega^2 + \omega_{\mathbf{q}}^2 \right) \Delta_{\mathbf{q}}^+(t; \omega),\end{aligned}\tag{2.124}$$

which approaches the equilibrium value

$$\epsilon_{\mathbf{q}}^{\phi}(\infty) = \int_{-\infty}^{\infty} \frac{\omega^2 + \omega_{\mathbf{q}}^2}{2\omega} \left(\frac{1}{2} + f_{\text{B}}(\Omega_{\mathbf{q}}) \right) \rho_{\mathbf{q}}(\omega),\tag{2.125}$$

cf. (1.106). This asymptotic equilibrium state is not that of a gas of free quasiparticles, as will be discussed in greater detail in the following. From Eqs. (2.123), (2.68) and (2.69) one can see that the deviation from equilibrium is described by a Boltzmann equation for quasiparticles,

$$(\partial_t + \Gamma_{\mathbf{q}}) \epsilon_{\mathbf{q}}^{\phi}(t) = 0.\tag{2.126}$$

The above derivation shows that $\partial_t \delta \Delta_{\mathbf{q}}^+(t; \Omega_{\mathbf{q}}) \sim \Gamma_{\mathbf{q}}$ to leading order, which implies the Boltzmann equation (2.126). However, this result was found by inserting $\omega = \Omega_{\mathbf{q}}$ into (2.112) to obtain (2.123). Considering (2.122), or a simple look at (2.44), show that the exact position of the pole is not at $\Omega_{\mathbf{q}}$. When $\Gamma_{\mathbf{q}}$ is not small, $\hat{\Omega}_{\mathbf{q}}$ shifts away from the real ω -axis and the quasiparticle peaks become less sharp. The narrow width approximation, namely replacing $\Pi_{\mathbf{q}}^R(\omega) \rightarrow \Pi_{\mathbf{q}}^R(\Omega_{\mathbf{q}})$ in (2.44) when integrating over ω , becomes increasingly bad because $\rho_{\mathbf{q}}(\omega)$ deviates significantly from zero away from $\pm\Omega_{\mathbf{q}}$. Physically this means that off-shell contributions become increasingly important - the quasiparticle picture breaks down.

Quasiparticle Regime

From Eqs. (2.71) and (2.104) one finds to leading order in $\Gamma_{\mathbf{q}}$,

$$\begin{aligned}
\epsilon_{\mathbf{q}}^{\phi}(t) &\simeq \frac{\dot{\phi}_{\mathbf{q},\text{in}}^2}{2\Omega_{\mathbf{q}}^2} (\omega_{\mathbf{q}}^2 \sin^2(\Omega_{\mathbf{q}}t) + \Omega_{\mathbf{q}}^2 \cos^2(\Omega_{\mathbf{q}}t)) e^{-\Gamma_{\mathbf{q}}t} \\
&+ \frac{\dot{\phi}_{\mathbf{q},\text{in}}\phi_{\mathbf{q},\text{in}}}{\Omega_{\mathbf{q}}} \sin(\Omega_{\mathbf{q}}t) \cos(\Omega_{\mathbf{q}}t) (\omega_{\mathbf{q}}^2 - \Omega_{\mathbf{q}}^2) e^{-\Gamma_{\mathbf{q}}t} \\
&+ \frac{\phi_{\mathbf{q},\text{in}}^2}{2} (\omega_{\mathbf{q}}^2 \cos^2(\Omega_{\mathbf{q}}t) + \Omega_{\mathbf{q}}^2 \sin^2(\Omega_{\mathbf{q}}t)) e^{-\Gamma_{\mathbf{q}}t} \\
&+ \frac{\Delta_{\mathbf{q},\text{in}}^+}{2} \left(\frac{\omega_{\mathbf{q}}^2 - \Omega_{\mathbf{q}}^2}{2} \cos(2\Omega_{\mathbf{q}}t) + \frac{\omega_{\mathbf{q}}^2 + \Omega_{\mathbf{q}}^2}{2} \right) e^{-\Gamma_{\mathbf{q}}t} \\
&- \frac{\ddot{\Delta}_{\mathbf{q},\text{in}}^+}{2\Omega_{\mathbf{q}}^2} \left(\frac{\omega_{\mathbf{q}}^2 - \Omega_{\mathbf{q}}^2}{2} \cos(2\Omega_{\mathbf{q}}t) - \frac{\omega_{\mathbf{q}}^2 + \Omega_{\mathbf{q}}^2}{2} \right) e^{-\Gamma_{\mathbf{q}}t} \\
&+ \frac{\dot{\Delta}_{\mathbf{q},\text{in}}^+}{\Omega_{\mathbf{q}}} \frac{\omega_{\mathbf{q}}^2 - \Omega_{\mathbf{q}}^2}{2} \sin(2\Omega_{\mathbf{q}}t) e^{-\Gamma_{\mathbf{q}}t} \\
&+ \left(\frac{1}{2} + f_B(\Omega_{\mathbf{q}}) \right) \frac{\omega_{\mathbf{q}}^2 + \Omega_{\mathbf{q}}^2}{2\Omega_{\mathbf{q}}} (1 - e^{-\Gamma_{\mathbf{q}}t}). \tag{2.127}
\end{aligned}$$

The first three lines in (2.127) correspond to the energy that is stored in the field value $\langle \phi \rangle$ while the remaining four lines represent the energy of its fluctuations, to be interpreted as (quasi)particles.

In the semiclassical description in terms of Boltzmann equations this system corresponds to a dilute gas of particles that move in a background field. To leading order g^2 there is no coupling of the gas to the field in our model. We can therefore treat them independently and concentrate on the particle contribution to the energy density. Let us consider the Boltzmann equation for particles of momentum \mathbf{q} and energy $E_{\mathbf{q}}$, where $E_{\mathbf{q}}$ is some function of \mathbf{q} that we expect to identify with $\omega_{\mathbf{q}}$ at low density. The competition between a gain and a loss term determines the change of the particle number density

$$\partial_t n_{\mathbf{q}}(t) = (1 + n_{\mathbf{q}}(t))\gamma_{\mathbf{q}}^< - n_{\mathbf{q}}(t)\gamma_{\mathbf{q}}^>, \tag{2.128}$$

When the medium is in equilibrium, production and decay rates satisfy the KMS relation as the self-energy of the field ϕ ,

$$\gamma_{\mathbf{q}}^> = e^{-\beta E_{\mathbf{q}}}\gamma_{\mathbf{q}}^< \equiv f_B(E_{\mathbf{q}})\gamma_{\mathbf{q}}. \tag{2.129}$$

$\gamma_{\mathbf{q}}$ is to be computed from scattering cross sections or, via the optical theorem, the imaginary part of the self energy,

$$\gamma_{\mathbf{q}} = -\frac{\text{Im}\Pi_{\mathbf{q}}^R(E_{\mathbf{q}})}{E_{\mathbf{q}}}. \tag{2.130}$$

Here $E_{\mathbf{q}}$ is the energy of a particle which might be identified with $\omega_{\mathbf{q}}$ or $\Omega_{\mathbf{q}}$, the latter corresponding to the use of thermal masses in Boltzmann equations. Using these relations, the Boltzmann equation (2.128) can be written in the form

$$\partial_t n_{\mathbf{q}}(t) = -\gamma_{\mathbf{q}}(n_{\mathbf{q}}(t) - f_B(E_{\mathbf{q}})) , \quad (2.131)$$

with the obvious solution

$$n_{\mathbf{q}}(t) = f_B(E_{\mathbf{q}}) + (n_{\mathbf{q}}(0) - f_B(E_{\mathbf{q}})) e^{-\gamma_{\mathbf{q}} t} . \quad (2.132)$$

The energy density of the gas is obtained by multiplying (2.132) with $E_{\mathbf{q}}$

$$\epsilon_{\mathbf{q}}^{\phi}(t) = E_{\mathbf{q}} f_B(E_{\mathbf{q}}) + E_{\mathbf{q}} (n_{\mathbf{q}}(0) - f_B(E_{\mathbf{q}})) e^{-\gamma_{\mathbf{q}} t} \quad (2.133)$$

and has to be compared to (2.127) for $\dot{\phi}_{\mathbf{q},\text{in}} = \phi_{\mathbf{q},\text{in}} = 0$. Obviously neither identifying $E_{\mathbf{q}}$ with $\omega_{\mathbf{q}}$ nor with $\Omega_{\mathbf{q}}$ generally leads to equivalence. In particular, (2.127) is the solution to a 2nd order differential equation and shows oscillations with the plasma frequency $\Omega_{\mathbf{q}}$ which even remain present in the limit $\Omega_{\mathbf{q}} \rightarrow \omega_{\mathbf{q}}$.

However, a consistent comparison between a quantum mechanical and a classical observable can only be done if the quantum system is set up with a initial state has a counterpart in the classical theory, namely one of definite initial (quasi)particle number. The construction of such a state is not trivial. Even for $T = 0$ the definition of a particle number is ambiguous in an interacting quantum field theory. One can define a useful quantity by $N_{\mathbf{q}}(t) = \epsilon_{\mathbf{q}}(t)/\omega_{\mathbf{q}}$. For vanishing coupling this coincides with the expectation value of the number operator $\langle a_{\mathbf{q}}^{\dagger} a_{\mathbf{q}} \rangle$ in a free theory [9]. With the initial conditions

$$\phi_{\mathbf{q},\text{in}} = 0, \quad \dot{\phi}_{\mathbf{q},\text{in}} = 0, \quad \Delta_{\mathbf{q},\text{in}}^+ = \frac{1}{\omega_{\mathbf{q}}} \left(\frac{1}{2} + \mathcal{N}_{\mathbf{q}} \right), \quad \dot{\Delta}_{\mathbf{q},\text{in}}^+ = 0, \quad \ddot{\Delta}_{\mathbf{q},\text{in}}^+ = \omega_{\mathbf{q}} \left(\frac{1}{2} + \mathcal{N}_{\mathbf{q}} \right)$$

one can indeed construct a state with a particle number $\mathcal{N}_{\mathbf{q}}$ in the sense of that definition, namely $N_{\mathbf{q}}(0) = \mathcal{N}_{\mathbf{q}}$. Unfortunately this choice of initial conditions cannot lead to a Boltzmann type solution since a cosine term remains present. Being in the quasiparticle regime, we chose the initial conditions

$$\phi_{\mathbf{q},\text{in}} = 0 \quad \dot{\phi}_{\mathbf{q},\text{in}} = 0 \quad \Delta_{\mathbf{q},\text{in}}^+ = \frac{1}{\Omega_{\mathbf{q}}} \left(\frac{1}{2} + \mathcal{N}_{\mathbf{q}} \right) \quad \dot{\Delta}_{\mathbf{q},\text{in}}^+ = 0 \quad \ddot{\Delta}_{\mathbf{q},\text{in}}^+ = \Omega_{\mathbf{q}} \left(\frac{1}{2} + \mathcal{N}_{\mathbf{q}} \right) \quad (2.134)$$

which seem to be the natural extrapolation to a state with well defined quasiparticle number $\mathcal{N}_{\mathbf{q}}$. This is a convenient choice despite our technical assumption that the interaction is switched on once the system starts evolving⁶. Then (2.127) reduces to

$$\epsilon_{\mathbf{q}}^{\phi}(t) = \left((\mathcal{N}_{\mathbf{q}} - f_B(\Omega_{\mathbf{q}})) e^{-\Gamma_{\mathbf{q}} t} + \left(\frac{1}{2} + f_B(\Omega_{\mathbf{q}}) \right) \right) \frac{\omega_{\mathbf{q}}^2 + \Omega_{\mathbf{q}}^2}{2\Omega_{\mathbf{q}}} \quad (2.135)$$

⁶A strict comparison between (2.127) and (2.133) would involve a renormalisation of (2.127). A consistent renormalisation of states with Gaussian initial conditions involves some technical difficulties, see [42].

The term in the brackets looks like the solution (2.132) to a Boltzmann equation for quasiparticles with $E_{\mathbf{q}} = \Omega_{\mathbf{q}}$, $\gamma_{\mathbf{q}} = \Gamma_{\mathbf{q}}$ and $n_{\mathbf{q}} = \mathcal{N}_{\mathbf{q}}$. However, the energy density is not computed by multiplying this term by the quasiparticle energy $\Omega_{\mathbf{q}}$ as suggested by (2.133). When attempting to define a particle number, neither $N_{\mathbf{q}}$ nor its intuitive generalisation $\epsilon_{\mathbf{q}}/\Omega_{\mathbf{q}}$ take the value $\mathcal{N}_{\mathbf{q}}$ at $t = 0$. One could be tempted to define a number operator for quasiparticles by $\epsilon_{\mathbf{q}} \frac{2\Omega_{\mathbf{q}}}{\omega_{\mathbf{q}}^2 + \Omega_{\mathbf{q}}^2}$, but it is questionable how useful this quantity is, so we prefer to keep the discussion on a level of energy densities and simply refer to (2.134) as the initial condition that lead to a Boltzmann type solution. (2.135) shows that the total energy density of a ϕ mode is not that of a gas of quasiparticles. It can be rewritten as

$$\begin{aligned} \epsilon_{\mathbf{q}}^{\phi}(t) &= \Omega_{\mathbf{q}} f_B(\Omega_{\mathbf{q}}) + \Omega_{\mathbf{q}} (\mathcal{N}_{\mathbf{q}} - f_B(\Omega_{\mathbf{q}})) e^{-\Gamma_{\mathbf{q}} t} \\ &+ \frac{\omega_{\mathbf{q}}^2 - \Omega_{\mathbf{q}}^2}{2\Omega_{\mathbf{q}}} f_B(\Omega_{\mathbf{q}}) + \frac{\omega_{\mathbf{q}}^2 - \Omega_{\mathbf{q}}^2}{2\Omega_{\mathbf{q}}} (\mathcal{N}_{\mathbf{q}} - f_B(\Omega_{\mathbf{q}})) e^{-\Gamma_{\mathbf{q}} t} + \frac{1}{2} \frac{\omega_{\mathbf{q}}^2 + \Omega_{\mathbf{q}}^2}{2\Omega_{\mathbf{q}}} \end{aligned} \quad (2.136)$$

The first line in (2.136) is, by comparison with (2.133), clearly the solution to a Boltzmann equation for quasiparticles. The second line can be interpreted as a vacuum term. In the particle regime, $\Omega_{\mathbf{q}} \rightarrow \omega_{\mathbf{q}}$, it converges to $\frac{1}{2}\omega_{\mathbf{q}}$, the quantum mechanical vacuum energy in the mode \mathbf{q} . For $\Omega_{\mathbf{q}} \neq \omega_{\mathbf{q}}$, the term depends on time and temperature and cannot be ignored as usually done at zero temperature. Such terms have previously been found for the case of equilibrium in [5]. (2.136) is the nonequilibrium generalisation of the result given there. The additional terms imply that the equilibrium configuration of an interacting quantum field theory is not simply a Bose-Einstein distribution, neither of particles nor of quasiparticles. Instead, one finds that the energy momentum tensor in thermal equilibrium can be decomposed in the following way,

$$\langle T_{\mu\nu}^{\phi} - g\phi\mathcal{O}[\mathcal{X}] \rangle|_{\mathbf{q}} = u_{\mu}u_{\nu} (\epsilon_{\mathbf{q}}^{\text{QP}} + p_{\mathbf{q}}^{\text{QP}}) - \eta_{\mu\nu} p_{\mathbf{q}}^{\text{QP}} + \eta_{\mu\nu} \kappa_{\mathbf{q}}^{\text{VAC}} . \quad (2.137)$$

Here

$$\epsilon_{\mathbf{q}}^{\text{QP}} = \Omega_{\mathbf{q}} \left(\frac{1}{2} + n_B(\Omega_{\mathbf{q}}) \right) , \quad (2.138)$$

$$p_{\mathbf{q}}^{\text{QP}} = \frac{1}{3} \frac{\mathbf{q}^2}{\Omega_{\mathbf{q}}} \left(\frac{1}{2} + n_B(\Omega_{\mathbf{q}}) \right) , \quad (2.139)$$

$$\kappa_{\mathbf{q}}^{\text{VAC}} = \frac{\omega_{\mathbf{q}}^2 - \Omega_{\mathbf{q}}^2}{2\Omega_{\mathbf{q}}} \left(\frac{1}{2} + n_B(\Omega_{\mathbf{q}}) \right) . \quad (2.140)$$

$\epsilon_{\mathbf{q}}^{\text{QP}}$ and $p_{\mathbf{q}}^{\text{QP}}$ agree with the corresponding expressions for a free gas, with the energy $\omega_{\mathbf{q}}$ of a free particle replaced by the quasi-particle energy $\Omega_{\mathbf{q}}$. This suggests to interpret them as energy and pressure of a quasiparticle gas. The ‘vacuum contribution’ $\kappa_{\mathbf{q}}^{\text{VAC}}$ vanishes for $\Omega_{\mathbf{q}} = \omega_{\mathbf{q}}$, namely at vanishing temperature. For large thermal effects, i.e. $\Omega_{\mathbf{q}} \gg \omega_{\mathbf{q}}$ or $\Omega_{\mathbf{q}} \ll \omega_{\mathbf{q}}$, the equation of state deviates significantly from that of a free gas. However, it

should be noted that practically also $\epsilon_{\mathbf{q}}^{\text{QP}}$ and $p_{\mathbf{q}}^{\text{QP}}$ contain a "ground state contribution". Consider

$$\epsilon_{\mathbf{q}}^{\text{QP}} = \frac{\Omega_{\mathbf{q}}}{2} + \Omega_{\mathbf{q}} n_{\text{B}}(\Omega_{\mathbf{q}}). \quad (2.141)$$

The second term looks like the classical energy of a free gas of quasiparticles with energy $\Omega_{\mathbf{q}}$. The first term at zero temperature becomes $\frac{\omega_{\mathbf{q}}}{2}$, the vacuum energy for the mode \mathbf{q} , and can be subtracted as an irrelevant constant. At finite temperature, $\frac{\Omega_{\mathbf{q}}}{2}$ has a temperature dependent piece that is not removed by the condition that the energy of the vacuum shall be zero. This is precisely the reason why we wrote this term into the second line in (2.136). It should also be kept in mind that in the definition of $\epsilon_{\mathbf{q}}^{\phi}$ we left out the $\langle g\phi\mathcal{O}[\mathcal{X}] \rangle$ contribution because it cannot uniquely be assigned to any of the fields. An analysis of the energy density of the whole system requires a proper treatment of this term and backreaction. $\epsilon_{\mathbf{q}}^{\phi}$ does not behave like the energy a quasiparticle gas. One remarkable feature of (2.140) is that for $\Omega_{\mathbf{q}}^2 < \omega_{\mathbf{q}}^2$, ϕ can actually give a negative contribution to the total pressure!

In this example, the emergence of classical Boltzmann equations is expected because the dissipation is driven by tree level processes. If the leading order contribution to the relevant processes occurs at quantum level, it is not obvious that they can be obtained as a consistent limit of the Kadanoff-Baym equations [47].

2.3.2 Quantum Boltzmann Equations

Eq. (2.135) is, as (2.70) and (2.71), Markovian in the sense that the state of the system at any time t allows to determine its state at time $t + \delta t$. There is no memory integral to be performed and the gain and loss terms encoded in $\Gamma_{\mathbf{q}}$ are the same at any time, independent of the history of the system and the initial conditions. Furthermore, it shows no oscillations. To understand how this simple behaviour arises from the non-Markovian second order differential equations (1.59) and (1.60), we revise the assumptions under which it has been obtained. Afterwards, we discuss approaches that allow to lift some of these restrictions within the quasiparticle regime and formulate quantum corrected Boltzmann equations, often referred to as *quantum Boltzmann equations*⁷.

First, the temperature has been kept constant. This is of course not strictly consistent. When the ϕ modes exchange energy with the bath, it is brought out of equilibrium. Even if the bath is strongly coupled and thermalises so fast that it can be assumed to be in equilibrium and characterised by a single temperature T , this temperature changes with time. For many cosmological applications our assumption of negligible backreaction can be a good approximation since the bath has many more degrees of freedom than ϕ , but

⁷There exists vast literature on quantum corrected kinetic equations. The assumptions and approximations made by different authors are generally similar, but not exactly identical. Here we focus on the approach used in [50] to formulate quantum Boltzmann equations for leptogenesis and refer the interested reader to [22, 29, 45] and references therein.

the temperature will also change due to Hubble expansion. If T changes with time, also $\Gamma_{\mathbf{q}}$ and the effective masses in $\Omega_{\mathbf{q}}$ depend on time. Then the first Kadanoff-Baym equation (2.3) can in general not be solved by Laplace transformation as done to obtain (2.44). If the change of T with time is much slower than any other timescale in the problem one might argue that (2.44) can still be an approximate solution to (2.3), with Π^R depending on time via $T(t)$. Even then non-Markovian behaviour will enter through the memory integral in (2.61).

Second, we restricted the discussion to systems with an initial state that corresponds to a well-defined particle number. Systems that e.g. are prepared as a superposition of states with different particle numbers cannot be well-described by Boltzmann equations.

Third, being in the quasiparticle regime, we neglected corrections of order $\Gamma_{\mathbf{q}}$ to $\epsilon_{\mathbf{q}}^{\phi}$. They correspond to off-shell processes that can affect the dynamics significantly as soon as one leaves the quasiparticle regime (see Sec. 2.3.3)⁸. Their negligence also leads to a divergence in Δ^+ in (2.71) for $\beta\Omega_{\mathbf{q}} \ll 1$ since

$$f_{\text{B}}(\Omega_{\mathbf{q}}) \simeq \frac{1}{\beta\Omega_{\mathbf{q}}} \gg 1. \quad (2.142)$$

The divergence also appears in the energy densities $\epsilon_{\mathbf{q}}^{\phi}$ in (2.127), (2.135) and (2.136) computed from Δ^+ . It disappears when including $\mathcal{O}(\Gamma)$ corrections. Starting from the KMS relation (1.106) and (2.44), one can see that in equilibrium

$$\Delta_{\mathbf{q}}^+|_{y=0} = \text{Re} \left(\frac{1}{\hat{\Omega}_{\mathbf{q}}} \left(\frac{1}{2} + f_{\text{B}}(\hat{\Omega}_{\mathbf{q}}) \right) \right). \quad (2.143)$$

Here we have assumed that Cauchy's theorem can be applied to perform the Fourier transform in ω and $\pm\hat{\Omega}_{\mathbf{q}}$ are the only poles. The imaginary part of $\hat{\Omega}_{\mathbf{q}}$ removes the divergence even if the real part vanishes,

$$|f_{\text{B}}(\hat{\Omega}_{\mathbf{q}})| \simeq \frac{1}{|\beta(\Omega_{\mathbf{q}} + \frac{i}{2}\Gamma_{\mathbf{q}})|} \leq \frac{2}{\beta\Gamma_{\mathbf{q}}}. \quad (2.144)$$

Furthermore, we considered only a single scalar field, hence no coherent oscillations, e.g. in flavour space, could occur. Such purely quantum mechanical phenomena have no correspondence in the Boltzmann approach. Finally, in the above discussion we have assumed that $\pm\hat{\Omega}_{\mathbf{q}}$ are the only two poles of $\rho_{\mathbf{q}}(\omega)$. The generalisation to cases where there are additional poles is straightforward as long as all of those have small imaginary parts, leading to resonances with quasiparticle character.

The use of quantum Boltzmann equations allows to relax the restrictions from the previous section while still dealing with first order differential equations for particle numbers. In thermal equilibrium the correlation functions (1.106) are uniquely characterised

⁸Recent studies suggest that off-shell contributions, together with quantum interference in the thermal bath, can have important effects even in the quasiparticle regime [47].

by two real valued, time independent functions ⁹: $\rho_{\mathbf{q}}(\omega)$ and $f_{B,F}(\omega)$. $\rho_{\mathbf{q}}(\omega)$ determines the spectrum of states and $f_{B,F}(\omega)$ their occupation numbers. It is intuitive to try a similar parameterisation for out-of-equilibrium states. Δ^- and Δ^+ play precisely this role, but in general they depend on two time variables t_1 and t_2 as well as two spatial positions \mathbf{x}_1 and \mathbf{x}_2 and have to be found as the solutions to coupled second order integro-differential equations.

It is very tempting to simply replace $f_{B,F}$ in Eqs. (1.103) by some general, time dependent distribution function $f(\omega, t)$ to obtain nonequilibrium propagators. Based on this ansatz, one can then formulate a perturbation theory analogue to the equilibrium case (see Sec. 1.3.3). This approach suffers from two problems. First, one encounters apparent singularities due to the δ -functions in (1.103) [46]. Second, the particular shape of Eqs. (1.103) relies on the KMS condition via (1.97). For a general nonequilibrium state, there is no such condition. The first problem can be solved by a resummation, effectively replacing the free spectral function in (1.97) by the dressed one. The finite width then regularises the singularity. Unfortunately, this requires knowledge of the dressed nonequilibrium spectral function, which has to be found as a solution to the first Kadanoff-Baym equation (1.59). The second problem can also be solved by leaving the restriction that the distribution function shall depend on ω and t only. Effectively, then one is back to Δ^+ , Δ^- and the Kadanoff-Baym equations and has not achieved a simplification.

However, there are two situations in which a simple parameterisation by a single distribution function is possible. One is a free theory. Then the spectrum is, independently of the physical state in which the system was prepared, given by the free spectral function (2.46) or (2.82). In this case, the particle number in each mode is well defined and has a sharp, time independent value. Furthermore, all particles are on-shell, hence the system can be described by a single distribution function $f(\omega) = f(\omega_{\mathbf{q}})$ for each degree of freedom. The other case is, due to the KMS relation, thermal equilibrium. Continuity arguments suggests that such parameterisation should provide a good description in situations either close to thermal equilibrium or in the quasiparticle regime [48, 49, 22]. As discussed in Sec. 2.3.1, in the former case the deviation from equilibrium obeys a Boltzmann equation [49]¹⁰.

Let us consider a system in which the above conditions are fulfilled and all involved fields are either close to equilibrium or very weakly coupled. If furthermore the system is in good approximation spatially homogeneous, it seems promising from the above arguments that an ansatz based on (1.97) with full spectral functions can be made in which the

⁹Our discussion focuses on the scalar propagators. For fermions or gauge fields, which have internal degrees of freedom, $\rho_{\mathbf{q}}(\omega)$ of course has a non-trivial Lorentz (and possibly flavour, colour...) structure. However, the following arguments regarding the parameterisation by distribution functions remain valid.

¹⁰See also [52] for a discussion.

distribution function only depends on ω and t .

$$(\Delta_C(x_1, x_2))_c \rightarrow \int \frac{d^4q}{(2\pi)^4} e^{-iq(x_1-x_2)} (\theta_C(x_1^0 - x_2^0) + f(\omega, (t_1+t_2)/2)) \rho_{\mathbf{q}}(\omega). \quad (2.145)$$

The situation simplifies further if the time dependence of ρ can be neglected. Differential equations for $f(\omega, t)$ can then be obtained by inserting the ansatz (2.145) into the Kadanoff-Baym equations. These are the quantum Boltzmann equations. Practical computations involve a number of simplifying assumptions, including a reasonable guess for the spectral functions. Self-consistently, these have to be thermal or quasiparticle spectra. For the fields in equilibrium one usually assumes free spectral functions or resummed one-loop results which lead to thermal quasiparticle spectra. At high temperature, this can be problematic since the precise spectrum of the Standard Model is unknown due to the poor convergence of the perturbative series, see Sec. 2.3.3.

The quantum Boltzmann equations are coupled first order differential equations for the distribution functions f_i of the various involved fields in which the damping terms are given by integral kernels. They correspond to Boltzmann equations for quasiparticles that include the time dependence of $\Gamma_{\mathbf{q}}$. Coherent oscillations in flavour space can be incorporated by parameterising correlations between different flavours in the same way. The quantum Boltzmann equations then form a set of coupled differential equations for the elements of a matrix in flavour space which can be related to the reduced density matrix used in [23]. The diagonal elements of this matrix can be identified with occupation numbers while the off-diagonal elements describe the coherences between different flavours. They account for non-Markovian effects via the integral kernels and allow to describe coherent oscillations as well as decays and scatterings in a common framework. When applicable, they provide a powerful formalism to treat nonequilibrium systems. However, in the form they have been used (see e.g. [49, 50, 53, 54, 51]), they rely on the assumption that all involved fields are in the quasiparticle regime and collective resonances play no role. Furthermore, the deviations from equilibrium are assumed to be small so that an expansion to linear order in that deviation is justified. This, though it can be well-motivated in many cases, is generally not true ¹¹.

2.3.3 Kinematics of the Resonances

In Boltzmann equations, the collision term is the quantity that characterises the interaction. In the Kadanoff-Baym equations, this role is taken by the self energy. It can be related to the total cross section by the optical theorem. As in vacuum, this connection holds at a level of single Feynman diagrams ¹². The self energy therefore naturally includes

¹¹By the time of printing, qualitative differences from the results given in [50] have been found in a full quantum mechanical computation based on Kadanoff-Baym equations [47].

¹²A generalisation of the Cutkosky rules [56] to systems with finite temperature and density was first found in [57].

all possible processes at a given order, and this is how they enter the Kadanoff-Baym equations. A leading order computation of $\text{Im}\Pi^R$ corresponds to a tree level computation of cross sections at order g . Higher order contributions to Π^R correspond to quantum corrections and higher order tree graphs. Via (2.44), Π^R governs the properties of resonances in the plasma. Since the breakdown of Boltzmann equations is related to the breakdown of the particle concept, we study how this shows up microscopically in single reactions.

For weak couplings cross sections and self energies in a plasma can be computed from Feynman rules. Those are described in Sec. 1.3. In equilibrium the only differences to the vacuum are the appearance of the auxiliary fields ϕ_- and the thermal propagators given in Eqs. (1.103),

$$\begin{aligned}\Delta_{++}(q) &= \frac{i}{q^2 - m^2 + i\epsilon} + f_B(|\omega|)2\pi\delta(q^2 - m^2), & \Delta_{+-}(q) &= f_B(\omega)2\pi\text{sign}(\omega)\delta(q^2 - m^2), \\ \Delta_{-+}(q) &= (1 + f_B(\omega))2\pi\text{sign}(\omega)\delta(q^2 - m^2), & \Delta_{--}(q) &= \frac{-i}{q^2 - m^2 - i\epsilon} + f_B(|\omega|)2\pi\delta(q^2 - m^2).\end{aligned}$$

The four thermal propagators share two important properties,

- They can be written as the sum of a zero temperature contribution, which vanishes for Δ_{+-} , and a temperature dependent correction.
- The thermal correction is always forced on-shell by a δ -function.

These properties are not specific to scalar propagators, but also apply to fermions, see (1.106), and gauge field propagators, see [10].

Since Feynman diagrams are computed from integrals over products of propagators, all quantities in perturbative computations share the first property. The usual Feynman propagator can be identified with the temperature independent part of Δ_{++} , the propagator of the physical field ϕ_+ . Regarding the second property, the δ -functions ensure energy and momentum conservation at vertices.

Leading Order: A Bath of Particles

To leading order the above means that the kinematic restrictions implied by energy and momentum conservation in vacuum also hold at vertices that connect fields in thermal equilibrium. However, one important difference to the vacuum lies in the possibility of scatterings with quanta from the medium. In vacuum, a single stable particle simply moves freely. This manifests in the fact that it corresponds to a singular pole, or δ -function, in the spectral function because $\text{Im}\Pi^R$ strictly vanishes at $\omega_{\mathbf{q}}$, $\text{Im}\Pi_{\mathbf{q}}^R(\omega_{\mathbf{q}}) = 0$. $\text{Im}\Pi^R$ is only non-zero above the lowest multiparticle threshold, $q^2 > \omega_{th1}^2$. The resulting analytic structure of $\rho_{\mathbf{q}}(\omega)$ is sketched in Fig. 2.2.

At finite temperature there can be scatterings with particles from the plasma. This implies that a particle can, even if it is the lightest particle in the theory, disappear

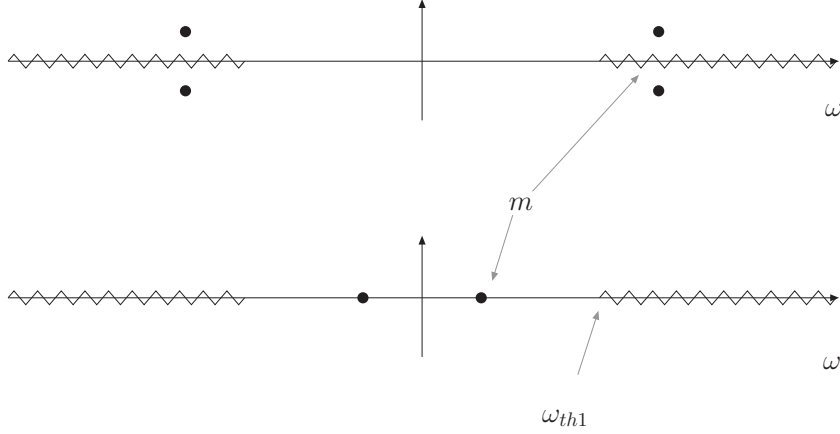


Figure 2.2: Poles and cuts of the spectral function $\rho(\omega)$ for unstable (upper plot) and stable (lower plot) particles with $\mathbf{q} = 0$ at $T = 0$

by Landau damping, engaging into a reaction with some particle from the plasma. At tree level, these scatterings are only possible with real quanta from the plasma due to the δ -functions in the thermal propagators. Hence, the energies and wave vectors of the particles have to be such that initial and final state are in accordance with energy momentum conservation.

To demonstrate the consequences for the fate of ϕ , we first consider a trilinear coupling $g\phi\mathcal{X}_1\mathcal{X}_2$ without further specification of the \mathcal{X}_i . This includes trilinear scalar couplings, Yukawa couplings and the Higgs coupling to gauge bosons. Since the kinematic properties are the same for higher spin fields, the discussion also covers gauge couplings to fermions and the three-vertices between gauge bosons¹³. The presence of the background medium changes the analytic structure of the ϕ -self-energy. The possibility of scatterings with bath particles implies a discontinuity, hence imaginary part, below a new threshold $q^2 < \omega_{th2}^2$. This property is carried over to the spectral function, see Fig. 2.3. If ϕ is in the quasiparticle regime and the only poles of the spectral function (2.44) are at $\omega = \pm\Omega_{\mathbf{q}}$, corresponding to dressed particles, one can set $\omega^2 = \Omega_{\mathbf{q}}^2$. The stability of ϕ quanta depends on the position of $\hat{\Omega}_{\mathbf{q}}$ in the complex ω plane. There are three different cases, see Fig. 2.3,

- (a) $q^2 > \omega_{th1}^2$
- (b) $q^2 < \omega_{th2}^2$
- (c) $\omega_{th2}^2 < q^2 < \omega_{th1}^2$.

The quasiparticles are stable in case (c). The stability in this region is a consequence of

¹³The Lagrangian (2.1) limits our analysis to couplings that are linear in ϕ . However, if some ϕ modes have reached equilibrium before others, they can form a “thermal bath” for the nonequilibrium modes.

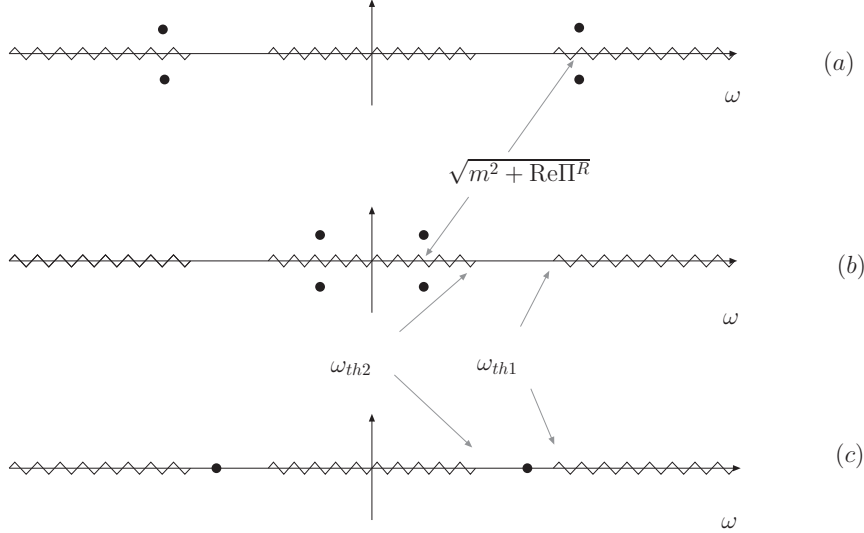


Figure 2.3: Poles and cuts of the spectral function $\rho(\omega)$ at leading order in the three cases (a), (b) and (c) for $\mathbf{q} = 0$ at $T \neq 0$.

the energy conserving δ -functions in the propagators that only allow on-shell processes: Computation of $\text{Im}\Pi^R$ involves integrating over a product of propagators. The leading order diagram for a trilinear coupling has the shape as shown in Fig. 3.1(a), (k) and (l). The zero temperature piece of $\text{Im}\Pi^R$ is known to vanish below ω_{th1} . The temperature dependent pieces of the propagators are proportional to on-shell δ -functions,

$$\text{Im}\Pi_{\mathbf{q}}^R(\omega) \sim \int \frac{d^4p}{(2\pi)^4} \delta(p_0^2 - \omega_{\mathbf{p}}^2) \delta((\omega - p_0)^2 - \omega_{\mathbf{q}-\mathbf{p}}^2) \dots, \quad (2.146)$$

and the integral vanishes unless there are points in the integration volume at which the arguments of all δ -functions vanish simultaneously. The supports of each δ functions form submanifolds in the integration volume, and the condition that those intersect leads to the thresholds. We study this effect in a particular model in Sec. 3.1. There the system with increasing temperature undergoes transitions including all three different cases (a), (b) and (c), cf. Fig. 3.2 and 3.3.

In scalar theories and non-abelian gauge theories one finds vertices that connect four lines. Such couplings generally do not allow stable particles at finite temperature. The reason is that couplings $\phi\mathcal{X}_i\mathcal{X}_j\mathcal{X}_k$ allow $2 \rightarrow 2$ scatterings at leading order which are always possible for appropriately chosen momenta. However, the available phase space can still be enlarged or reduced by thermal effects. This physically intuitive result is also demonstrated for a particular model in Sec. 3.1.

If (2.44) has more poles than $\pm\Omega_{\mathbf{q}}$, those correspond to plasma waves that have no correspondence in vacuum. If the poles are close to the real axis, these have a well-defined

dispersion relation and can be understood as quasiparticles. It is important to point out that the dispersion relations, even those given by $\omega = \pm\Omega_{\mathbf{q}}$ can be qualitatively very different from free particles. Unless the *free quasiparticle approximation* holds, it can be highly non-trivial to determine the range of allowed processes. The fact that the properties of the poles of (2.44) depend on temperature makes the phase space dynamical. If the temperature changes, the system can move from one regime into the other. Indeed, if backreaction is not negligible, the dissipation of ϕ into the plasma or thermal production of ϕ particles from the plasma can change the temperature. If ϕ is not in the quasiparticle regime, kinematic restrictions do not apply since off-shell ω can always give a contribution to (2.146).

A Bath of Quasiparticles

The analytic structure of the leading order expression for ρ in equilibrium is well-known [7]. In the following we investigate qualitative changes once one proceeds to higher order corrections. A leading order self energy computation is based on the use of the free propagators (1.103). The use of free propagators for the bath fields \mathcal{X} neglects their interaction with each other and effectively corresponds to the assumption that all \mathcal{X} are in the *particle regime*. In the light of our initial assumptions, this is not realistic since the bath is coupled more strongly than the particle that freezes out. The problem can be solved consistently by using dressed \mathcal{X} propagators and vertices when computing the ϕ -self-energy. Resummed propagators can be obtained from (1.97) by replacing the free spectral function (2.46) by its interacting counterpart (2.44) and (2.82) by (2.80) for fermions. If the bath fields \mathcal{X} are in the *quasiparticle regime* one can neglect $\text{Im}\Pi_{\mathcal{X}}^R$ in (2.44) in first approximation, leading to

$$\rho_{\mathbf{q}}(\omega) = 2\pi\text{sign}(\omega)\delta(\omega^2 - \omega_{\mathbf{q}}^2 - \text{Re}\Pi_{\mathbf{q}}^R(\omega)). \quad (2.147)$$

The spectral function remains proportional to a sum of δ -functions. These discrete contributions to the spectrum correspond to plasma waves that kinematically exactly behave like particles, though their dispersion relations can be very complicated. They are given by the solutions of

$$\omega^2 - \omega_{\mathbf{q}}^2 - \text{Re}\Pi_{\mathbf{q}}^R(\omega) = 0$$

and depend on the temperature. The previous arguments remain unchanged, but the fact that also the modified dispersion relations for bath fields have to be taken into account makes it practically much more difficult to take account of all possible processes. When there are no additional poles from collective excitations, the spectral function for a scalar reads

$$\rho_{\mathbf{q}}(\omega) = 2\pi\text{sign}(\omega)\delta(\omega^2 - \Omega_{\mathbf{q}}^2) = \frac{\pi}{\Omega_{\mathbf{q}}}(\delta(\omega - \Omega_{\mathbf{q}}) - \delta(\omega + \Omega_{\mathbf{q}})). \quad (2.148)$$

In the following we focus on the simplest case, when the medium-induced corrections to the dispersion relations depend only mildly on the wave vector and the *free quasiparticle approximation* holds. Then the medium effects can be parameterised by replacing all masses m_i by temperature dependent thermal masses $M_i(T)$. For trilinear couplings, one can define a critical temperature $T_c^{i \leftrightarrow j+k}$ by

$$M_i(T_c) = M_j(T_c) + M_k(T_c). \quad (2.149)$$

At $T = T_c$, decays and inverse decays of species i into species j and k become kinematically forbidden at leading order. If no thermal mass is larger than the sum of the two others, the interaction is effectively switched off.

Realistic quasiparticles always have a small finite width, but this does not have a significant effect unless the mass spectrum is quasi-degenerate. Loop integrals are performed over products of propagators, hence involve products of spectral functions. When $\rho_{\mathbf{q}}(\omega)$ is exactly a sum of δ -functions, the support of each spectral function forms lower-dimensional submanifolds in the integration volume on which the dispersion relation is fulfilled. As discussed previously, the integral is only non-zero if there are regions where the supports of all of them intersect. This condition gives rise to the threshold. When there is a finite width, the support of $\rho_{\mathbf{q}}(\omega)$ in principle can cover the whole integration volume. However, if the width is small, the region where ρ is significantly different from zero compared to its on-shell value only extends a distance of order Γ away from the hypersurfaces on which the dispersion relations are fulfilled. The result of the integral will still be very small unless those on-shell regions intersect or come very close to each other¹⁴. For the trilinear coupling, $\text{Im}\Pi_{\mathbf{q}}^R(\Omega_{\mathbf{q}})$ becomes non-zero in the region $\omega_{th2}^2 < M_\phi^2 < \omega_{th1}^2$ corresponding to case (c), but is suppressed by the smallness of $\Gamma_{\mathbf{q}}$ with respect to the regions $M_\phi^2 > \omega_{th1}^2$ and $M_\phi^2 < \omega_{th2}^2$. The processes that were strictly forbidden at leading order remain effectively forbidden (see Fig. 3.4). Of course, this suppression is a relative one in comparison to the result obtained by neglecting thermal masses. The reaction rate can still be relevant when it is significant compared to other processes in the plasma.

The above arguments explicitly use the spectral function for scalars (2.147), but it remains valid for fermions and gauge bosons. In the limit of vanishing width, their spectral functions are also proportional to sums of δ -functions. For instance, in the case of Dirac fermions the effective masses are given by the solutions of

$$Q^2 - \mathcal{M}^2 = 0 \quad (2.150)$$

and their complex conjugates, see (2.80).

Thus, we can understand the previous observation that in the quasiparticle regime the approach to equilibrium can be understood in terms of Boltzmann equations for quasiparticles from a microscopic point of view. The use of Boltzmann equations, however,

¹⁴Note that the commonly used rule that loop integrals are dominated by the $|\mathbf{p}| \sim T$ region does not apply if (almost) on-shell processes can contribute. For narrow spectral functions, the integral is always dominated by the overlap of the on-shell regions.

has to be treated with care since $\Omega_{\mathbf{q}}$ and $\Gamma_{\mathbf{q}}$ generally depend on time and collective resonances can appear as new particles. A simple replacement of vacuum masses by thermal masses in the usual Boltzmann can generally not account for all medium effects, though it can be a good approximation if all excitations are known to behave like free quasiparticles. *Quantum Boltzmann equations* allow to include these effects if all resonances can be treated as quasiparticles and their dispersion relations are known.

Beyond the Quasiparticle Regime

In the particle and quasiparticle regime, a sharp energy can be assigned to a resonance and energy and momentum of the resonances are conserved in scatterings and decays. When the width is large, one can formally still define $\Omega_{\mathbf{q}}$, but it has no meaning as a particle's energy because $\rho_{\mathbf{q}}(\omega)$ becomes a rather smooth function that has a large off-shell contribution away from $\omega = \Omega_{\mathbf{q}}$. When computing loop integrals, the region in which the spectral functions give significant contributions can cover large parts of the integration volume and extend far away from $\Omega_{\mathbf{q}}$. The result of the integration is proportional to the weighted overlap of the spectral functions. Contributions from the off-shell regions can be of comparable size as those from on-shell processes. Hence, smoothing out the δ -function in (1.97) results in erosion of kinematic restrictions.

The apparent non-conservation of energy and momentum in scatterings can be understood easily even in classical terminology. A dilute, weakly coupled gas is well-described by particles that move freely with energies $\omega_{\mathbf{q}}$ between scatterings. When the density becomes high, the average distance between them is so small that they always feel the presence of the neighbouring particles. Thus, their energy receives a contribution from potential energies, taking them "off-shell", $\omega \neq \omega_{\mathbf{q}}$. Due to this coupling to the environment, a scattering is never simply a two-body problem. The same applies to decays. Energy and momentum are only conserved for the system as a whole, not for the subsystem of the scattering particles. Exchange of energy and momentum with the environment can make processes possible that are strictly forbidden in vacuum. This effect is known in condensed matter and nuclear physics, where e.g. it is responsible for the β^+ -decay, but has long been ignored in cosmology.

Broad Resonances and the full Spectrum

The validity of Boltzmann or quantum Boltzmann equations crucially relies on the description of the spectrum in terms of quasiparticles. It is instructive to estimate under which circumstances this is a good approximation.

The quasiparticle picture is a useful tool whenever the width of a resonance is much smaller than its thermal on-shell energy and the difference to the on-shell energy of all other resonances with the same conserved quantum numbers. This is certainly true for a weakly coupled plasma with a non-degenerate mass spectrum at low T . For a strong

coupling, the spectrum is modified significantly by the interaction. The resonances in some cases might still behave like quasiparticles, even if they show little resemblance with the particles in vacuum, but in general, this is not the case. As a result, the quasiparticle picture and any type of Boltzmann equations fail to describe the system. One then is usually forced to solve the Kadanoff-Baym equations with nonperturbative methods.

Here we concentrate on weak couplings. In some cases there are interactions that give rise to local diagrams, or tadpoles, as those in Fig. 3.1 *e)* and *f)*. Then $\text{Re}\Pi^R$ is parametrically larger than $\text{Im}\Pi^R$ because such diagrams are purely real. They contribute to linear order in the coupling while the leading order contribution to the imaginary part is quadratic. When there are no local diagrams, real and imaginary part of the self energy appear at the same order and one has to study them in detail. At the end of Sec. 1.2.1 we presented a simple classical argument why the quasiparticle picture should hold in weakly coupled systems even at high temperatures. This is true for a Coulomb potential since $E_{\text{kin}} \sim T \gg E_{\text{pot}} \sim gT$. The interaction energy in non-abelian gauge theories is not well-described by a Coulomb potential. The argument already breaks down for a simple Yukawa coupling since it increases the interaction strength at short distances, so E_{pot} at high densities increases faster than linear in T . Even for a pure Coulomb interaction, the argument relies on the fact that average distance and average kinetic energy of particles are related by a single parameter T . This is only true in thermal equilibrium. With a general distribution function it is possible to combine a high density with a low average momentum. This is, for example, realised after inflation, see Sec. 4.1.

In general, it can be very difficult to determine the real and imaginary part of Π^R at high temperature. The main problem is that even in weakly coupled theories the convergence of the perturbative series is poor. With increasing order in the coupling, hence number of vertices in corresponding Feynman diagrams, also the number of temperature dependent propagators connecting them increases. A large T can compensate for a small coupling so that higher order contributions can be of comparable size as leading order terms. In addition, leading order results in gauge theories by themselves are generally not gauge invariant. In some cases the running of the coupling can be such that it improves the convergence. This happens in a quark gluon plasma due to asymptotic freedom. However, in our scalar model in Sec. 3.1 we observe a significant increase in the width while the mass shift is small if the dissipation is caused by decay, see Fig. 3.7. This phenomenon is known as *melting* of a peak and can be experimentally observed for mesons in nuclear matter, see Fig. 2.4. Resummed perturbation theory allows to compute gauge invariant results and improves the convergence of the perturbative series. The results suggest that at high temperature $\text{Re}\Pi^R \sim g^2T^2$, leading to thermal mass corrections of order gT while $\Gamma \sim g^2T$ [10]. This would imply that the quasiparticle picture holds even at high temperatures if g is small. These estimates are obtained by reorganising the perturbative series and resumming infinite sets of diagrams. Such resummations are possible when it is justified to single out classes of relevant higher order diagrams which can be computed from the knowledge of terms at lower order. For soft external momenta $\sim gT$, a *hard*

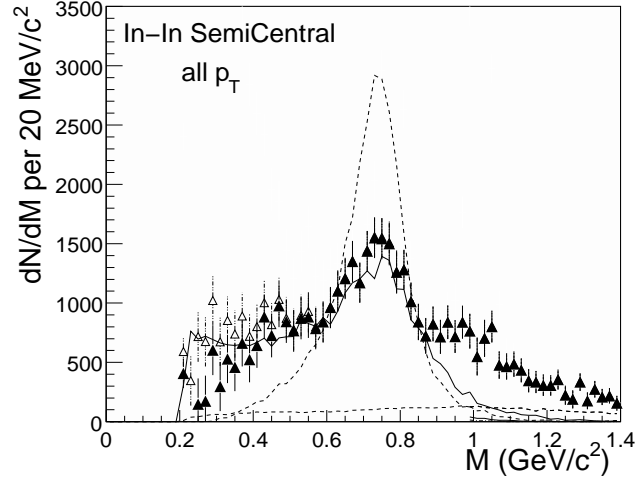


Figure 2.4: An example for the *melting* of a peak: The spectral function of a ρ -meson propagating in hot nuclear matter produced in a high energetic In-In-collision, plotted as a function of energy. The experimental data is compared to the spectral function in vacuum (dashed line) and theoretical prediction (solid line). The width of the resonance increases drastically without a significant mass shift. The plot is borrowed from [62].

thermal loop resummation can be employed [58]. It has been found that for very hard momenta $|\mathbf{q}| \gg T$, resonances behave like free on-shell particles at $\omega = \Omega_{\mathbf{q}}$ with a slightly modified effective mass [10]. The result confirms the intuition that the energy of a particle injected into a plasma with large momentum is dominated by the kinetic energy and only minimally modified by plasma interactions. Lorentz dilation furthermore enhances an unstable particle's lifetime in the bath's frame of rest. On the other hand, the realistic quantitative computation of the energy loss in a medium has proven very difficult in the context of heavy ion collisions, where the issue has been studied in detail [59]. For very soft momenta it has been found that $\Gamma \sim g^2 T$ [60], indicating quasiparticle behaviour. In the off-shell regime $\mathbf{q} > \omega$ Landau damping can give a large imaginary part of order of the Debye mass $\Gamma \sim gT$ (see [61]), but this can by definition not affect the width of the resonance. For high T and small chemical potential, a dimensional reduction can simplify computations in the Matsubara formalism [31] because the length β of the path in imaginary time becomes so small that field values do not change much along imaginary time direction.

Resummation techniques indicate that the quasiparticle nature in a weakly coupled theory is preserved at high temperature. However, as mentioned above, the validity of these results is limited. For momenta below the so called magnetic scale $g^2 T$ even the resummed perturbative series is known to break down and nonperturbative corrections are of the same order as the leading order results, see [61]. Furthermore, in order to fully

exploit the advantages of the quasiparticle approximation, knowledge of all dispersion relations is required.

The most common way to access the nonperturbative regime is provided by lattice calculations (see e.g. [63]). Unfortunately, lattice computations generally have to be performed in euclidean space. The mass of a resonance can be re-extracted from those relatively easily as the coefficient for the exponential fall-off of the euclidean correlation functions at large separation of arguments. Extraction of the width is significantly more difficult. It requires an analytic continuation. On numerical data this can only be performed by making a guess for the shape of the function in Minkowski space and fitting that guess to the data. Furthermore, the precision of lattice computations is limited by the available computation power.

In bosonic systems at high T one can simplify the computations by a classical approximation. This is justified because bosonic fields at large occupation numbers have a classical limit, see e.g. [64].

Recently, a new method treat nonperturbative systems has received a lot of attention, the so called AdS/CFT correspondence [65]. The method is based on the conjecture that a strongly coupled conformal field theory has a dual in string theory. The low energy limit of this dual appears as a higher dimensional theory of gravity. Strong coupling on one side of the duality corresponds to perturbative behaviour on the other. This allows to calculate quantities in the nonperturbative regime of the field theory via a perturbative calculation on the gravity side that is then translated into the field theory via the duality. Unfortunately non of the known interactions in nature is described by a conformal field theory. Nevertheless, there is some hope that properties can be found in conformal systems that are universal enough to be generalised to physical systems. A very popular candidate to resemble QCD is provided by a $N = 4$ supersymmetric non-abelian gauge theory. The method has been used to compute Keldysh propagators [66] and the meson spectrum [67]. The results of course inherently suffer from uncertainties due to the transfer from a conformal field theory to the Standard Model. At low temperatures, one can estimate the resulting error by comparison to experimental data.

To summarise this paragraph, we conclude that it is currently not possible to make a general quantitative statement about the behaviour of quasiparticle widths at very high temperature, not even in a weakly coupled theory. A well-known example for qualitative changes at high temperature are phase transitions. In the case of QCD it is theoretically predicted and experimentally established that meson resonances broaden and *melt* as one approaches the critical temperature of the QCD phase transition, see Fig. 2.4. In this example the melting is of course well understood since mesons are composite particles and described by an effective theory. However, the distinction between effective and fundamental theories is merely a question of the energy scale of consideration, and the physics at high energies cannot be completely predicted from knowledge of the low energy behaviour.

Simple Models for the Bath

Throughout the previous chapter, we have not specified the composition of the thermal bath. The discussion of medium effects on the spectral functions does not put restrictions on the type of interactions that generate them. In principle, the bath could consist of an arbitrary number of fermionic and bosonic fields with various interactions amongst each other, including gauge couplings.

In this chapter we demonstrate the results in two particular models. Both of them are applied to cosmological problems in the following chapter.

3.1 A Scalar Field coupled to a Bath of Scalars

We consider a scalar field ϕ that is coupled to a bath consisting of two other scalars χ_1 and χ_2 by trilinear and quartic couplings. The Lagrangian (2.1) then takes the shape

$$\mathcal{L} = \frac{1}{2}\partial_\mu\phi\partial^\mu\phi - \frac{1}{2}m_\phi^2\phi^2 + \sum_{i=1}^2 \left(\frac{1}{2}\partial_\mu\chi_i\partial^\mu\chi_i - \frac{1}{2}m_i^2\chi_i^2 - \frac{h_i}{4!}\phi\chi_i^3 \right) - g\phi\chi_1\chi_2 + \mathcal{L}_{\chi_{\text{int}}} . \quad (3.1)$$

The coupling g has mass dimension one and the h_i are dimensionless. All of them shall be small in the sense of perturbation theory. The couplings $\mathcal{L}_{\chi_{\text{int}}}$ need not be specified at this point except that it is sufficiently strong to keep the \mathcal{X} in equilibrium. As in the previous chapter, we neglect backreaction and take the χ_i in equilibrium at all times. One could e.g. imagine that the χ_i have strong couplings to very many degrees of freedom in equilibrium that immediately compensate for any exchange of energy with ϕ . We assume that the χ_i are in the symmetric phase, i.e. $\langle\chi_i\rangle = 0$, so that there are no contributions of

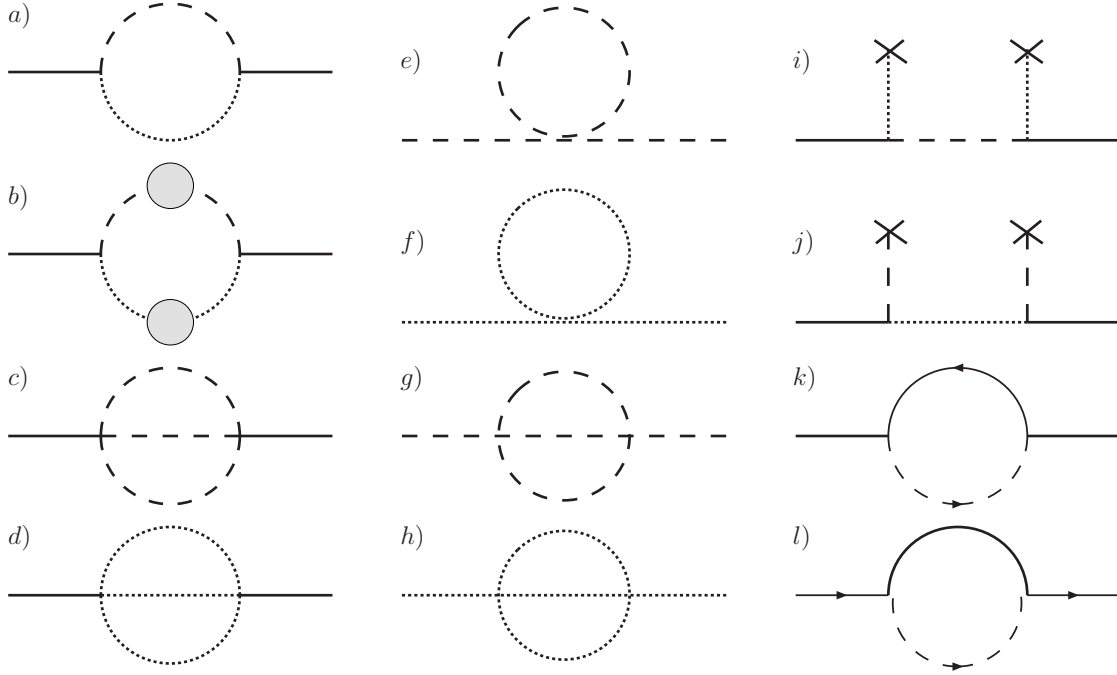


Figure 3.1: Relevant Feynman diagrams, lines represent ϕ (solid), χ_1 (dotted), χ_2 (dashed), Ψ_1 (solid with arrow) and Ψ_2 (dashed with arrow) propagators. The gray blobs represent resummed self-energy insertions and the crosses couplings to mean fields.

the type shown in Fig. 3.1 *i)* and *j)* to the self-energy of ϕ from couplings to mean fields.

3.1.1 The trilinear Coupling g

The ϕ -self-energy to leading order is given by the diagram shown in Fig. 3.1*a)*. We are interested in the imaginary part that determines the gain- and loss rates. With (2.42) and the KMS condition (1.96), $\text{Im}\Pi^R$ can be computed from $\Pi^<$ via

$$\text{Im}\Pi_{\mathbf{q}}^R(\omega) = \frac{1}{2i}\Pi_{\mathbf{q}}^<(\omega) (e^{\beta\omega} - 1). \quad (3.2)$$

For $\Pi^< = \Pi_{-+}$ the left vertex in Fig. 3.1*a)* is of the '-'-type and the right of the '+'-type. With the thermal Feynman rules (see Sec. 1.3.3) one finds

$$\Pi_{\mathbf{q}}^<(\omega) = -ig^2 \int \frac{d^4p}{(2\pi)^4} \Delta_{1\mathbf{p}}^<(p_0) \Delta_{2\mathbf{p}-\mathbf{q}}^<(\omega - p_0), \quad (3.3)$$

with

$$\Delta_1^<(p_0) = f_B(p_0)\rho_1(p_0). \quad (3.4)$$

Here, and in the following, quantities that carry an index 'i' such as $\Delta_i^<$, Π_i^R or $\omega_{(i)\mathbf{q}}$ refer to χ_i propagators, self energies, frequencies, et cetera, while those lacking such an index belong to ϕ . To further simplify notation, we will from now on suppress the spatial momentum whenever possible in this subsection. It shall be understood that '1'-quantities always have momentum \mathbf{p} while '2'-quantities have $\mathbf{q}-\mathbf{p}$. For example, $\omega_{\mathbf{q}} = (\mathbf{q}^2 + m_\phi^2)^{\frac{1}{2}}$, $\omega_1 = (\mathbf{p}^2 + m_1^2)^{\frac{1}{2}}$ and $\omega_2 = ((\mathbf{q}-\mathbf{p})^2 + m_2^2)^{\frac{1}{2}}$. To leading order $\text{Im}\Pi^R$ is then given by

$$\text{Im}\Pi_{\mathbf{q}}^R(\omega) = -\frac{g^2}{2} \int \frac{d^4p}{(2\pi)^2} \frac{f_B(p_0)f_B(\omega-p_0)}{f_B(\omega)} \text{sign}(p_0)\text{sign}(\omega-p_0)\delta(p_0^2-\omega_1^2)\delta((\omega-p_0)^2-\omega_2^2). \quad (3.5)$$

Using one of the δ -functions, this integral can be rewritten as

$$\begin{aligned} \text{Im}\Pi_{\phi}^R(q) &= -\frac{g^2}{2} \int \frac{d^3p}{(2\pi)^2} \frac{1}{4\omega_2\omega_1} \\ &\times \left(\left((f_1+1)(f_2+1) - f_2f_1 \right) \left(\delta(\omega - \omega_1 - \omega_2) - \delta(\omega + \omega_1 + \omega_2) \right) \right. \\ &\left. + \left((f_1+1)f_2 - (f_2+1)f_1 \right) \left(\delta(\omega - \omega_1 + \omega_2) - \delta(\omega + \omega_1 - \omega_2) \right) \right). \quad (3.6) \end{aligned}$$

Here $f_1 = f_B(\omega_1)$ and so on. The well known result (3.6) has a clear physical interpretation: The first line represents decays $\phi \rightarrow \chi\chi$ and their inverse $\chi\chi \rightarrow \phi$. The combinations of f_B make sure that the detailed balance ratio is fulfilled while the δ -functions guarantee energy conservation in particle reactions as discussed in Sec. 2.3.3. The second line represents $\chi\phi \rightarrow \chi$ and $\chi \rightarrow \phi\chi$ scatterings with quanta from the plasma. This channel corresponds to Landau damping and does not exist in vacuum. As expected, the second line vanishes if $T \rightarrow 0$. The integral (3.6) can be solved analytically [40, 9].

At this level, the quanta in the bath have been treated as free particles. Since their self interactions are by assumption stronger than the coupling to ϕ , this is inconsistent. Higher order corrections to the one loop integral (3.6) can consistently be incorporated by inserting resummed χ_i propagators in the loop, see Fig. 3.1 b). This can be done by replacing the free spectral function in (3.5) by its interacting counterpart. In the quasiparticle regime, one can neglect $\text{Im}\Pi^R$ and use (2.148) as a first approximation. Here we consider the simplest case and assume that the dressed one-particle states are the only resonances and corrections to their dispersion relations due to medium effects are in good approximation independent of the wave vectors. Then the free quasiparticle approximation can be applied and the analytic result found in [40, 9] remains valid, but with intrinsic masses replaced by thermal masses $m_i \rightarrow M_i(T)$. The result of (3.6) then reads

$$\text{Im}\Pi_{\mathbf{q}}^R(\omega) = \sigma_0(q) + \sigma_a(q, T) + \sigma_b(q, T). \quad (3.7)$$

Here σ_0 is the contribution due to the decay process $\phi \rightarrow \chi_1 \chi_2$,

$$\begin{aligned} \sigma_0(q) &= \frac{g^2}{16\pi q^2} \text{sign}(\omega) \theta(q^2 - (M_1 + M_2)^2) \\ &\quad \times \left((q^2)^2 - 2q^2(M_1^2 + M_2^2) + (M_1^2 - M_2^2)^2 \right)^{\frac{1}{2}}, \end{aligned} \quad (3.8)$$

$\sigma_\beta^{(a)}(q)$ is an additional temperature dependent contribution from such processes,

$$\begin{aligned} \sigma_a(q) &= \frac{g^2}{16\pi|\mathbf{q}|\beta} \text{sign}(\omega) \theta(q^2 - (M_1 + M_2)^2) \\ &\quad \times \left(\ln \left(\frac{1 - e^{-\beta\omega_+}}{1 - e^{-\beta\omega_-}} \right) + (M_1 \leftrightarrow M_2) \right), \end{aligned} \quad (3.9)$$

and $\sigma_b(q)$ the contribution from Landau damping

$$\begin{aligned} \sigma_b^{(b)}(q) &= \frac{g^2}{16\pi|\mathbf{q}|\beta} \text{sign}(\omega) \theta((M_1 - M_2)^2 - q^2) \\ &\quad \times \left(\ln \left(\frac{1 - e^{-\beta|\omega_-|}}{1 - e^{-\beta|\omega_+|}} \right) + (M_1 \leftrightarrow M_2) \right). \end{aligned} \quad (3.10)$$

We have used the abbreviations

$$\omega_\pm = \frac{|\omega|}{2q^2} (q^2 + M_1^2 - M_2^2) \pm \frac{|\mathbf{q}|}{2|q^2|} \left((q^2 + M_1^2 - M_2^2)^2 - 4q^2 M_1^2 \right)^{\frac{1}{2}}. \quad (3.11)$$

The real part of the self energy can be computed from this using the spectral representation

$$\text{Re}\Pi_{\mathbf{q}}(\omega) = \frac{1}{\pi} \mathcal{P} \int dq_0 \frac{\text{Im}\Pi_{\mathbf{q}}(q_0)}{q_0 - \omega}, \quad (3.12)$$

which follows from the Kramers-Kronig relations. It can give a positive or negative correction to the mass, see Fig. 3.9. For equal χ masses, $m_1 = m_2 = m_\chi$ and self couplings, the result for vanishing external momentum $\mathbf{q} = 0$ is particularly simple,

$$\Gamma_0(\omega) = \frac{g^2}{8\pi\omega} \left(1 - \left(\frac{2m_\chi}{m} \right)^2 \right)^{\frac{1}{2}} (1 + 2f_B(\omega)) \theta(\omega - m_\chi/2). \quad (3.13)$$

The temperature dependent part leads to an amplification due to induced transitions. The θ -functions in Eqs. (3.8)-(3.10) and (3.13) appear because the spectral function (2.148) puts the bath particles χ_i on-shell, allowing only on-shell processes to contribute to $\Gamma_{\mathbf{q}}$. We are interested in the fate of the *thermal on-shell* ϕ resonance, hence we replace

$$\omega \rightarrow \Omega_{\mathbf{q}}. \quad (3.14)$$

Without loss of generality, we assume $M_2 > M_1$. Then the three regimes defined in Sec. 2.3.3 correspond to (a) $M_\phi > M_1 + M_2$, (b) $M_2 > M_\phi + M_1$ and (c) $M_\phi < M_1 + M_2$ and $M_2 < M + M_1$.

In the first case, energy between ϕ and the bath is exchanged via decays and inverse decays $\phi \leftrightarrow \chi_1\chi_2$. In second one, χ_2 decays and inverse decays, $\chi_2 \leftrightarrow \phi\chi_1$ play that role. In the third case none of these processes is kinematically allowed. ϕ effectively decouples from the plasma and moves free of dissipation. The remarkable feature is that the phase space volume becomes dynamical due to the temperature dependence of the masses. A temperature change can bring the system from one situation into the other. Even within the regimes where (a) or (b) are realised, temperature changes can massively increase and decrease gain- and loss rates by changing the available phase space. In a realistic system, such changes will of course have a backreaction on the temperature. In Fig. 3.2 we plot $\Gamma_{\mathbf{q}}$ as a function of T and \mathbf{q} . Along the T axis one can clearly see how the system moves from regime (a) to (c) and finally to (b). A qualitative change along the \mathbf{q} axis occurs around $\mathbf{q} \approx m_\phi$ when the particles become relativistic. Fig. 3.3 compares the result to the would-be value when neglecting thermal masses. It shows that $\Gamma_{\mathbf{q}}$ is strongly overestimated when doing so.

As discussed in Sec. 2.3.3 the possibility of dissipationless movement in case (c) is caused by forcing the bath particles on-shell. It disappears when one takes the width of the χ_i into account because then energy exchange between ϕ and the bath can happen via off-shell processes. With non-vanishing widths the integral (3.3) generally has to be solved numerically. When all fields are in the quasiparticle regime, the contribution from off-shell processes is suppressed by the smallness of the widths. We illustrate this in Fig. 3.4 where we have used a quartic self-coupling $\frac{\lambda_i}{4!}\chi_i^4$ for the bath fields.

3.1.2 The quartic Couplings h_i

To leading order the contribution from the couplings $\frac{h_i}{4!}\phi\chi_i^3$ to the ϕ -width $\Gamma_{\mathbf{q}}$ comes from the diagrams shown in Fig. 3.1c) and d). Each is, analogously to (3.6), given by

$$\begin{aligned}
\text{Im}\Pi_{\mathbf{q}}^R(\omega) = & \pi \frac{h_i^2}{12} \int \frac{d^9\mathbf{p}_1\mathbf{p}_2\mathbf{p}_3}{(2\pi)^9} (2\pi)^3 \delta^{(3)}(\mathbf{p}_1 + \mathbf{p}_2 + \mathbf{p}_3 - \mathbf{q}) \frac{1}{8\omega_1\omega_2\omega_3} \\
& \times \left(\left((1+f_1)(1+f_2)(1+f_3) - f_1f_2f_3 \right) \right. \\
& \quad \left(\delta(\omega - \omega_1 - \omega_2 - \omega_3) - \delta(\omega + \omega_1 + \omega_2 + \omega_3) \right) \\
& + (f_1(1+f_2)(1+f_3) - (1+f_1)f_2f_3) \\
& \quad \left(\delta(\omega + \omega_1 - \omega_2 - \omega_3) - \delta(\omega - \omega_1 + \omega_2 + \omega_3) \right) \\
& + ((1+f_1)f_2(1+f_3) - f_1(1+f_2)f_3) \\
& \quad \left(\delta(\omega - \omega_1 + \omega_2 - \omega_3) - \delta(\omega + \omega_1 - \omega_2 + \omega_3) \right) \\
& + (f_1f_2(1+f_3) - (1+f_1)(1+f_2)f_3) \\
& \quad \left. \left(\delta(\omega + \omega_1 + \omega_2 - \omega_3) - \delta(\omega - \omega_1 - \omega_2 + \omega_3) \right) \right), \tag{3.15}
\end{aligned}$$

where all ω_i are to be taken with χ_i masses, $\omega_1 = \sqrt{\mathbf{p}_1^2 + m_{\chi_1}^2}$ etc., and $f_1 = f_B(\omega_1)$ etc. The first line describes the decay of ϕ into three χ and its inverse while the other lines include all possible scatterings $\phi\chi \rightarrow \chi\chi$. They are kinematically allowed for any choice of masses. The quartic interactions always couple ϕ to the bath via scatterings. Nevertheless, phase space arguments will influence the magnitude of $\Gamma_{\mathbf{q}}$ when thermal masses are taken into account.

Though some approximate analytic formulae have been computed [68, 69, 70, 71], the integral (3.15) can in general only be integrated numerically. For high T and $\mathbf{q} = 0$ it can be approximated by [68]

$$\Gamma_{\mathbf{0}} \approx \frac{h_i^2 T^2}{768\pi m_\phi}. \tag{3.16}$$

The quantitative range of validity (3.16) has to be treated with care. It is a consistent approximation to the integral (3.15) for large T (see Fig. 3.1.3), but due to the breakdown of perturbation theory at high temperatures, the validity of (3.15) itself is limited.

However, it can be argued on a qualitative level that contributions to $\Gamma_{\mathbf{q}}$ from scatterings should further increase with T in the nonperturbative regime. The reasons are Bose enhancement due to induced transitions and the fact that scattering processes should become more frequent due to the higher density of the plasma.

3.1.3 Numerical Results

In this section we present a number of plots to demonstrate our previous results. Whenever we take them into account, we model the self-interactions of the bath fields by a quartic coupling,

$$\mathcal{L}_{\chi_i \text{int}} = \frac{\lambda_i}{4!} \chi_i^4. \quad (3.17)$$

The thermal mass M_i is to leading order given by the contribution from the tadpole diagrams shown in Fig. 3.1e), f):

$$M_\chi^2 = m_i^2 + \lambda_i \int \frac{d^3 \mathbf{p}}{(2\pi)^3} \frac{f_B(\omega_i)}{2\omega_i} \approx m_i^2 + \frac{\lambda_i}{24} T^2. \quad (3.18)$$

It is independent of momentum. We estimate the χ_i -width by Lorentz-dilation of the zero-mode approximation (3.16).

Fig. 3.2 shows the contribution to $\Gamma_{\mathbf{q}}$ from the $g\phi\chi_1\chi_2$ coupling, normalised to its vacuum value, as a function of momentum \mathbf{q} and temperature T . The mass hierarchy at $T = 0$ is chosen according to case (a), $m_\phi > m_1 + m_2$. We assumed a relatively strong self-coupling with $\lambda_2 = 0.5$ for χ_2 , but only a weak coupling $\lambda_1 = 0.01$ for χ_1 . We neglected the thermal χ_i widths. Fig. 3.3 compares this result to a computation that neglects χ_i -self-interactions. At low temperature, the mass hierarchy corresponds to case (a) and ϕ receives its width from decays and inverse decays. When the thermal χ_2 -mass correction becomes relevant, it first suppresses and then, above a critical temperature $T_c^{\phi \leftrightarrow 1+2}$ at which $M = M_1 + M_2$, completely blocks those processes. For $T > T_c^{\phi \leftrightarrow 1+2}$, the field ϕ effectively decouples from the plasma. At a much higher temperature $T_c^{2 \leftrightarrow \phi+1}$, when $M_2 > M_1 + M$, decays and inverse decays of χ_2 set in. Neglecting the χ_i self-interactions leads to a dramatic overestimate of the ϕ width in all three regimes, low temperatures excluded. We neglected the mass correction for ϕ which, due to its weak coupling, has much less dramatic effects than that of χ_2 . Taking it into account does not change the picture qualitatively, but only slightly moves the boundaries of the regimes. At low temperatures it is negligible compared to m_ϕ and at high temperatures it is small compared to the thermal χ_2 mass M_2 . The plots extend into the regime of very high temperatures for illustrative purposes. There, the leading order results (3.6) and (3.18) do not give quantitatively correct results. However, the qualitative picture remains valid as long as the system is in the quasiparticle regime.

Fig. 3.4 shows the effect of off-shell processes in the quasiparticle regime. $\chi_{1,2}$ are taken equal in mass $m_{1,2} = m_\chi = 0.4m_\phi$ and have a self interaction of the same strength, $\lambda_{1,2} = \lambda = 0.1$. Then their thermal masses are also equal, $M_1 = M_2 = M_\chi$. There is only one critical temperature T_c .

T_c is defined by the condition (2.149). When neglecting the thermal mass correction

for the very weakly coupled field ϕ one finds

$$T_c^2 \approx \frac{24}{\lambda} \left(\left(\frac{m_\phi}{2} \right)^2 - m_\chi^2 \right). \quad (3.19)$$

The kinematic arguments that forbid the ϕ -decay for $T > T_c$ rely on the quasiparticle nature of the involved particles, namely the smallness of the $\chi_{1,2}$ -width at T_c . We want to estimate for which choices of parameters the suppression is effective. For the $\mathbf{q} = 0$ mode one can approximate, c.f. (3.16),

$$\Gamma_\chi \approx \frac{\lambda^2 T^2}{768\pi M_\chi}. \quad (3.20)$$

Defining narrow width by $\Gamma_\chi \ll M_\chi$ one can formulate the condition

$$\Gamma_\chi(T_c) \approx \frac{\lambda}{64\pi} \frac{m_\phi^2 - 4m_\chi^2}{m_\phi} \ll M_\chi(T_c) = \frac{m_\phi}{2}, \quad (3.21)$$

leading to

$$\frac{\lambda}{32\pi} \left(1 - \left(\frac{2m_\chi}{m_\phi} \right)^2 \right) \ll 1. \quad (3.22)$$

The inequality (3.22) is the criterion for effective ϕ -decay suppression above T_c . The quantitative validity of this result of course relies on the convergence of the perturbative series. The fact that T_c is determined by the difference of the mass squares allows us to bring it into the perturbative regime by choosing a small mass difference. Fig. 3.4 shows that the suppression above T_c is very effective in the quasiparticle regime.

The fields in the Lagrangian (3.1) are also coupled by the $h_i \phi \chi_i^3$ terms. In vacuum and at low temperatures they act via the processes $\phi \leftrightarrow \chi\chi\chi$. For the previous choice of parameters, $m_{1,2} = 0.4m$, these are forbidden. Even if allowed, they are subdominant compared to the process $\phi \leftrightarrow \chi\chi$ at low temperatures due to phase space arguments unless $h_i \gg g/m$. Nevertheless, their contribution increases with temperature, see (3.16) and Fig. 3.1.3, hence they can provide ϕ with a width for $T > T_c$.

It is instructive to estimate how efficiently this compensates for the suppression of the trilinear interaction above T_c . We compare $\Gamma_{\mathbf{q}}$ at $T = T_c$ and $T = 0$ for $\mathbf{q} = 0$, assuming that the former is dominated by $\chi\chi \leftrightarrow \phi\chi$ scatterings and the latter by $\phi \leftrightarrow \chi\chi$ decays and inverse decays. In vacuum, $\Gamma_{\mathbf{q}}$ then is given by¹

$$\Gamma|_{T=0} = \frac{g^2}{8\pi m_\phi} \left(1 - \left(\frac{2m_\chi}{m_\phi} \right)^2 \right)^{\frac{1}{2}}. \quad (3.23)$$

¹Some authors use a definition of $\Gamma_{\mathbf{q}}$ that deviates from ours by a factor $\frac{1}{2}$ and would quote half of our result for decay width in vacuum.

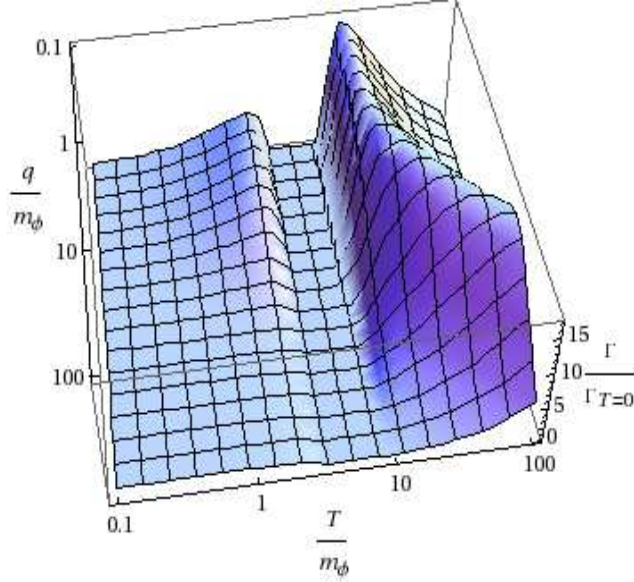


Figure 3.2: $\Gamma/\Gamma|_{T=0}$ in the scalar model as a function of T and $|\mathbf{q}|$ for $g = 0.05m_\phi$, $m_1 = m_2 = 0.4m_\phi$, $h_1 = h_2 = 0$, $\lambda_1 = 0.01$, $\lambda_2 = 0.5$. Corrections to the ϕ -mass are very small and, at this order, increasingly negative for high temperatures.

With (3.20) one finds

$$\frac{\Gamma|_{T=T_c}}{\Gamma|_{T=0}} = \sum_i \left(\frac{h_i m_\phi}{g} \right)^2 \frac{1}{2\lambda} \sqrt{1 - \left(\frac{2m_\chi}{m_\phi} \right)^2}. \quad (3.24)$$

The dependencies in this formula can easily be understood. The quadratic dependence on g and h_i comes from the vertices. Increasing λ decreases T_c . At a lower temperature, the contribution from $\chi\phi \leftrightarrow \chi\chi$ scatterings is smaller because of the smaller density of scattering partners. Therefore increasing λ decreases the ratio (3.24). The dependence on m_ϕ and m_χ follows the same logic, T_c increases with m_ϕ and decreases with m_χ . Fig. 3.1.3 compares the contributions from the different couplings. The parameters are chosen in a way that there is no dissipationless regime.

With the knowledge of the self energies we can plot the various correlation functions². In the following we always set $h_1 = h_2 = 0$ and concentrate on the trilinear coupling. Unless stated differently, we use the value of the coupling constant g such that

$$\frac{\Gamma}{m_\phi} \Big|_{T=m_i=0} = \frac{g^2}{8\pi m_\phi^2} = 0.2$$

² Figs. 3.7, 3.8, 3.9, 3.10, 3.11, 3.12, 3.13, 3.14 and 3.15 are taken from [5]

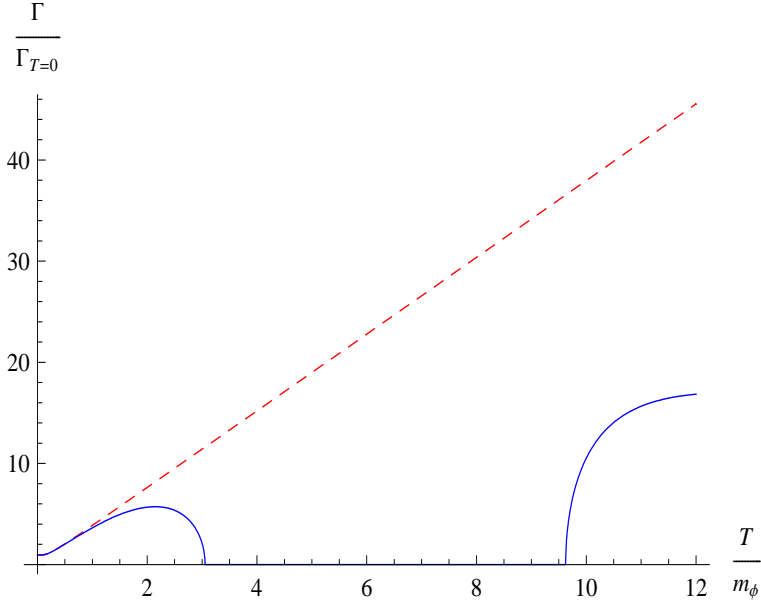


Figure 3.3: $\Gamma/\Gamma|_{T=0}$ in the scalar model as a function of T for $\mathbf{q} = 0$, $g = 0.05$, $m_1 = m_2 = 0.4m_\phi$, $h_1 = h_2 = 0$. For the red dashed curve, χ_i -self-interactions have been neglected ($\lambda_1 = \lambda_2 = 0$), for the solid blue curve the χ_i have been given thermal masses ($\lambda_2 = 0.5 \gg \lambda_1 = 0.01$). Corrections to the ϕ -mass are very small and, at this order, increasingly negative for high temperatures. The three temperature regimes corresponding to case (a), (c) and (b) are clearly visible in the blue curve.

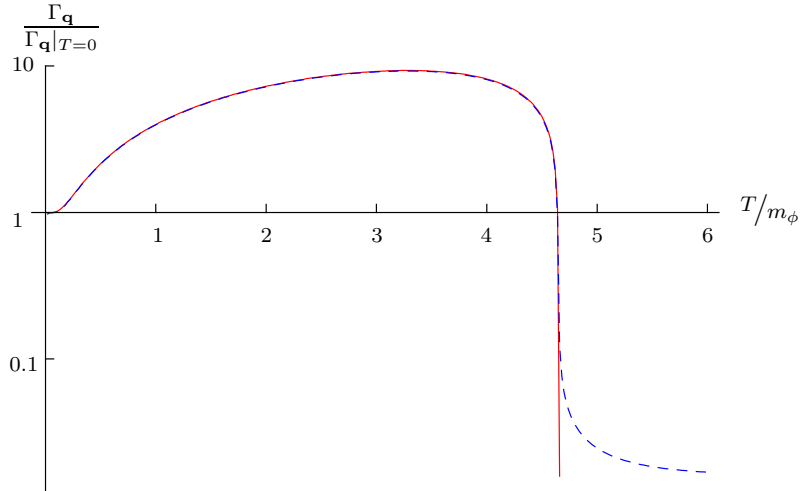


Figure 3.4: $\Gamma/\Gamma|_{T=0}$ in the scalar model to leading order (solid red line) and with resummed propagators (dashed blue line) for $h_1 = h_2 = 0$, $m_{\chi_1} = m_{\chi_2} = m_\chi$, $\frac{m_\chi}{m_\phi} = 0.4$, $\lambda_1 = \lambda_2 = 0.1$. Above a critical temperature T_c , the nonvanishing dissipation is only visible on the logarithmic scale. For these parameters $T_c \approx 4.6m_\phi$.

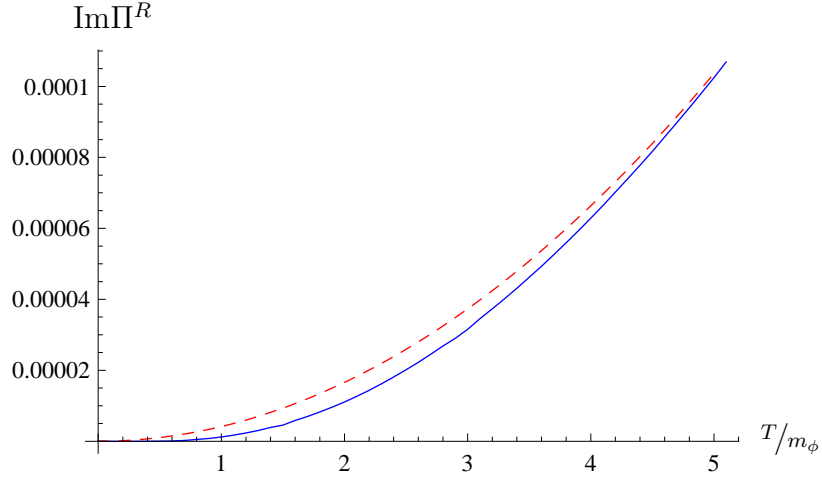


Figure 3.5: Contribution to $\text{Im}\Pi^R$ in the scalar model from the quartic coupling for $h_i = \lambda_i = 0.01$. The numerical evaluation of (3.15), solid blue curve, is compared to the approximation (3.16), dashed red curve.

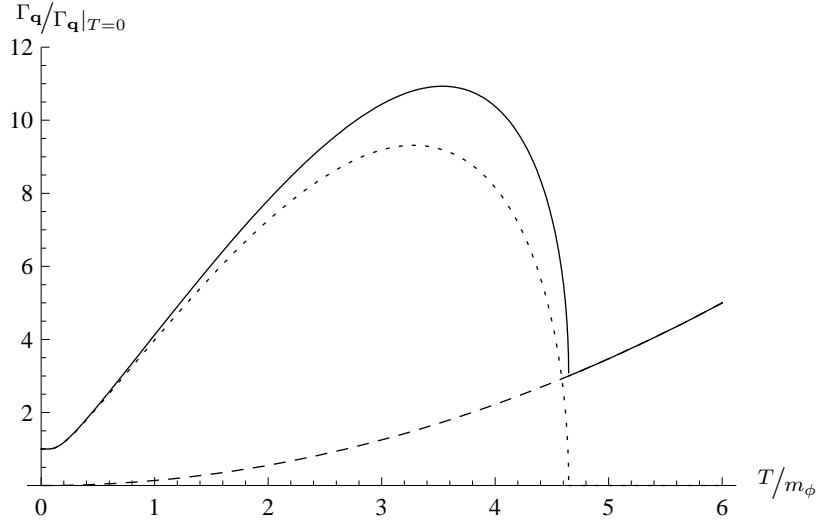


Figure 3.6: Total $\frac{\Gamma_{\mathbf{q}}}{\Gamma_{\mathbf{q}}|_{T=0}}$ (solid) and the contributions from trilinear (dotted) and quartic (dashed) couplings in the scalar model for $\frac{m_\chi}{m_\phi} = 0.4$, $h_i = 2\frac{g}{m_\phi}$ and $\lambda = 0.1$.

and set the quartic couplings $h_{1,2}$ to zero everywhere except in Figs. 3.1.3 and 3.1.3. This relatively large value is chosen for illustrative purposes. Furthermore, we concentrate on the zero mode $\mathbf{q} = 0$. Thermal masses and widths of the bath fields $\chi_{1,2}$ are always neglected.

Figs. 3.7 and 3.8 show the spectral function for ϕ at different temperatures for the cases (a) and (b), respectively. In case (a), when ϕ already has a finite width in the vacuum, the quasiparticle peak “melts” at relatively low temperatures without a significant change in position. In contrast to that, in case (b) the melting is accompanied by a negative mass shift. From the previous discussion, it follows that the broadening in Fig. 3.7 might be much weaker if one takes the thermal masses of the bath fields $\chi_{1,2}$ into account. The peak could even become narrow again, and hence ϕ could enter a second quasiparticle regime at high T , if the system enters a temperature regime in which a thermal mass hierarchy of the type (c) is realised. The mass shift in Fig. 3.8 can be understood from Fig. 3.9. $\text{Re}\Pi^R$ at $\Omega_{\mathbf{q}}$ and can have either sign, depending on the temperature.

Fig. 3.10 shows $\Delta_{\mathbf{q}}^-(y)$, the Fourier transform of $\rho_{\mathbf{q}}(\omega)$. It oscillates with the frequency $\Omega_{\mathbf{q}}$ and a damping $\Gamma_{\mathbf{q}}/2$, see (2.70). The statistical propagator $\Delta_{\mathbf{q}}^+(t_1, t_2)$, given by (2.61), as a function of t_1 and t_2 is displayed in Fig. 3.11. We set all initial conditions in (2.61) to zero to show the memory integral³. The system equilibrates along the diagonal $t = \frac{t_1+t_2}{2}$ -direction and eventually becomes time translation invariant. This can be seen in detail in Fig. 3.12 and 3.13. They show Δ^+ along cuts through the t_1 - t_2 -plane. Fig. 3.12 shows Δ^+ for different fixed $t = \frac{t_1+t_2}{2}$. At all times there are characteristic oscillations in $y = t_1 - t_2$. For late t , Δ^+ as a function of y approaches its equilibrium shape, see Sec. 2.2.3. Fig. 3.13 shows Δ^+ for $y = 0$. The two characteristic features are the asymptotic approach to an equilibrium value and the oscillations in t . The latter are a consequence of the fact that the Kadanoff-Baym equations, in contrast to the Boltzmann equations, are second order differential equations. The amplitude of the oscillations is of order $\Gamma_{\mathbf{q}}$, hence they do not appear in the memory integral term of the leading order approximation (2.71). Fig. 3.14 demonstrates that the approach to equilibrium happens independently of the initial conditions.

The energy density can be computed from Δ^+ at $y = 0$ using (2.104). In Sec. 2.3.1 we pointed out that it deviates from that of a quasiparticle gas. This is shown in Fig. 3.15.

3.2 A Fermion with Yukawa Couplings

We now consider a system of two fermions $\Psi_{1,2}$ and a scalar ϕ . The Lagrangian is

$$\mathcal{L} = \sum_{i=1}^2 i\bar{\Psi}_i (\not{\partial} - m_i) \Psi_i + \frac{1}{2} \partial_\mu \phi \partial^\mu \phi - \frac{1}{2} m_\phi^2 \phi^2 - g\phi (\bar{\Psi}_1 \Psi_2 + \bar{\Psi}_2 \Psi_1). \quad (3.25)$$

³ This does not correspond to a vanishing initial particle number which would be realised by setting $\mathcal{N}_{\mathbf{q}} = 0$ in (2.134).

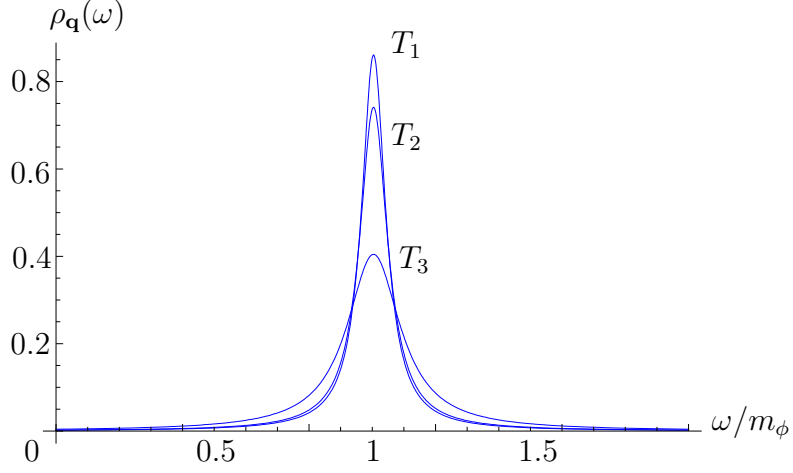


Figure 3.7: Spectral function $\rho_{\mathbf{q}}(\omega)$ in the scalar model for $\mathbf{q} = 0$; case (a) with masses $m_1 = m_2 = 0.2m_\phi$ and temperatures $T_1 = 0.1m_\phi$, $T_2 = 0.2m_\phi$, $T_3 = 0.5m_\phi$.

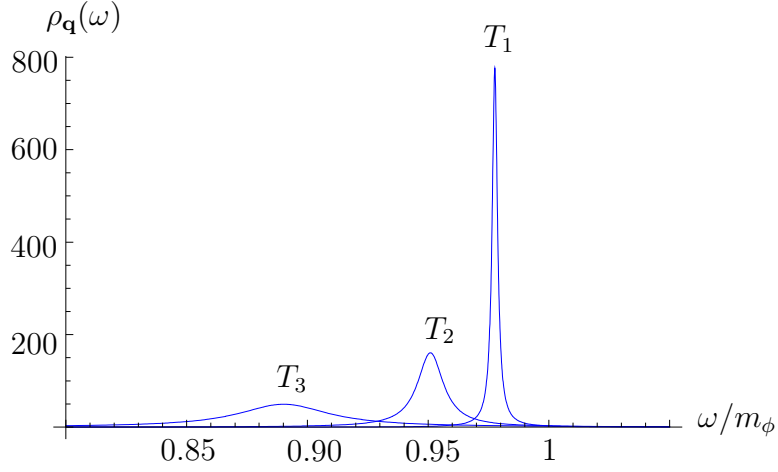


Figure 3.8: Spectral function $\rho_{\mathbf{q}}(\omega)$ in the scalar model for $\mathbf{q} = 0$; case (b) with masses $m_1 = m_\phi$, $m_2 = 5m_\phi$ and temperatures $T_1 = m_\phi$, $T_2 = 2m_\phi$, $T_3 = 5m_\phi$.

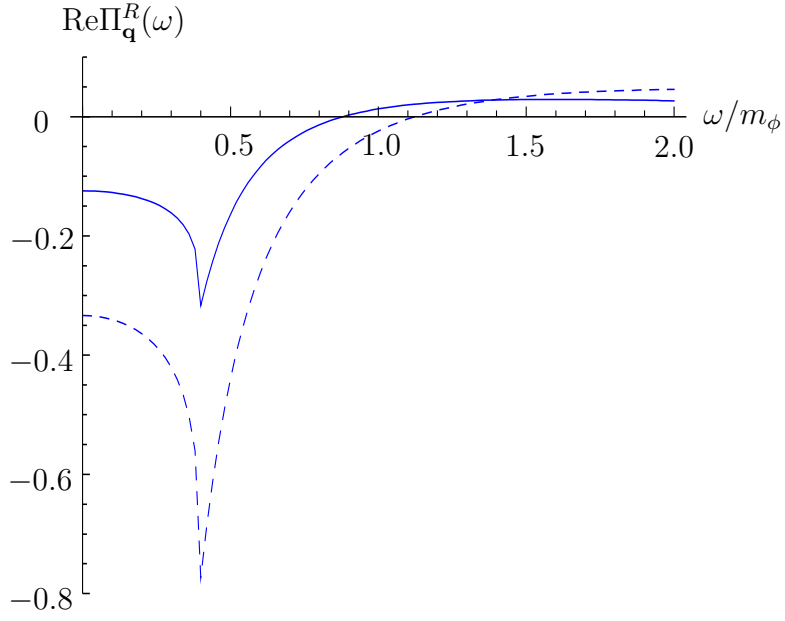


Figure 3.9: Real part of the self-energy $\Pi_{\mathbf{q}}^R(\omega)$ for $\mathbf{q} = 0$; case (a) with masses $m_1 = m_2 = 0.2m_\phi$ and temperatures $T_1 = 0.5m_\phi$ (solid) and $T_2 = m_\phi$ (dashed).

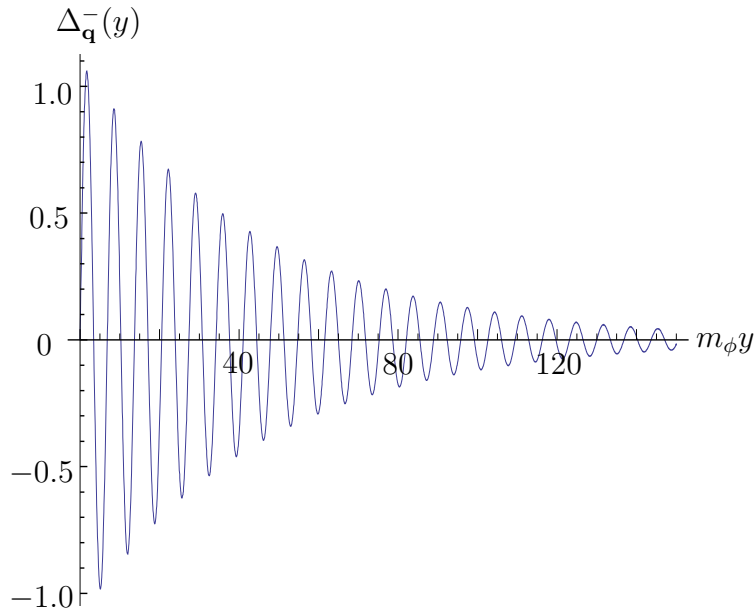


Figure 3.10: Spectral function $\Delta_{\mathbf{q}}^-(y)$ for $\mathbf{q} = 0$; case (b) with masses $m_1 = m_\phi$, $m_2 = 5m_\phi$ and $T = 10m_\phi$.

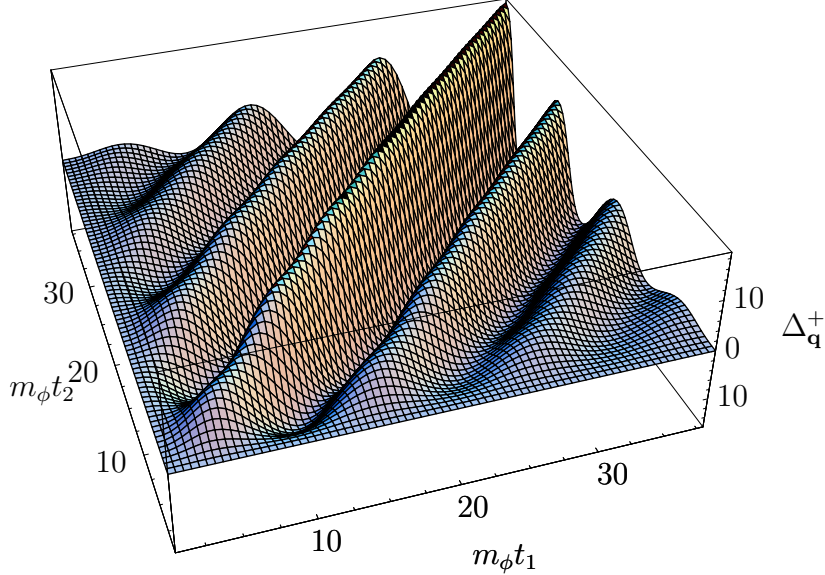


Figure 3.11: Statistical propagator $\Delta_{\mathbf{q},\text{mem}}^+(t_1, t_2)$ for $\mathbf{q} = 0$; case (b) with masses $m_1 = m_\phi$, $m_2 = 5m_\phi$ and $T = 10m_\phi$. Note that only the contribution from the memory integral is plotted, which vanishes for $t_{1,2} = 0$. The boundary conditions for the full function $\Delta_{\mathbf{q}}^+(t_1, t_2)$ depend on the physical initial conditions and generally do not vanish for $t_{1,2} = 0$. If one, for instance, chooses vacuum initial conditions, $\Delta_{\mathbf{q}}^+(t_1, t_2)$ consistently coincides with the non-zero dressed statistical propagator in vacuum for $t_1 = t_2 = 0$.

The coupling constant g in (3.25) is dimensionless. When $\Psi_{1,2}$ form the thermal bath and, as previously, ϕ is out of equilibrium, we can again use the solutions (2.43) and (2.61) for the spectral and statistical propagators Δ^- and Δ^+ , but with a self energy that is computed from diagrams of the form shown in Fig. 3.1k). The leading order result for $\Gamma_{\mathbf{q}}$ with $\mathbf{q} = 0$ in the case of equal fermion masses $m_1 = m_2 = m$ is given by [32]

$$\Gamma_{\mathbf{0}}(\omega) = \frac{g^2 \omega}{8\pi} \left(1 - \left(\frac{2m}{m_\phi} \right)^2 \right)^{\frac{3}{2}} (1 - 2f_F(\omega)) \theta(\omega - m/2). \quad (3.26)$$

It can be compared to (3.13). The most striking difference is that $\Gamma_{\mathbf{q}}$ decreases with increasing temperature due to the factor $1 - 2f_F(\omega)$. The physical reason is that at large temperatures, Pauli suppression decreases the rate of decays $\phi \rightarrow \Psi\Psi$. For bosons in the final state, (3.13) showed that it is increased due to induced transitions.

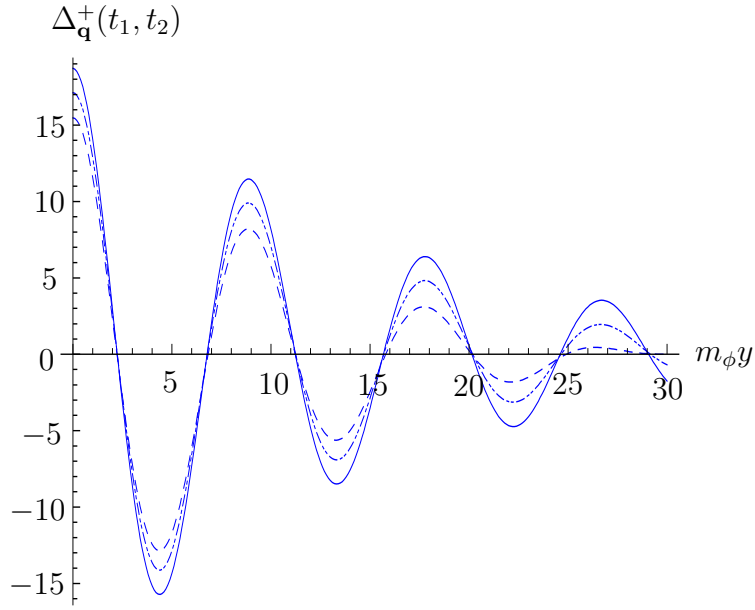


Figure 3.12: Memory integral $\Delta_{\mathbf{q},\text{mem}}^+(t_1, t_2)$ as function of $y = t_1 - t_2$ for $\mathbf{q} = 0$; case (b) with $m_1 = m$, $m_2 = 5m$, $T = 10m$ and three values of $t = (t_1 + t_2)/2$: $m_\phi t = 15$ (dashed line), $m_\phi t = 20$ (dotted-dashed), $m_\phi t = 60$ (solid).

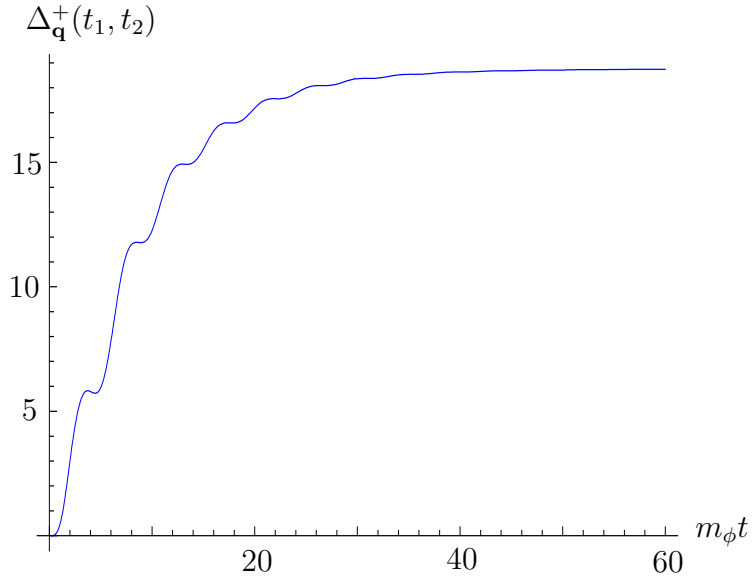


Figure 3.13: Memory integral $\Delta_{\mathbf{q},\text{mem}}^+(t_1, t_2)$ as function of $t = (t_1 + t_2)/2$ for $y = 0$, $\mathbf{q} = 0$; case (b) with masses $m_1 = m_\phi$, $m_2 = 5m_\phi$ and $T = 10m_\phi$.

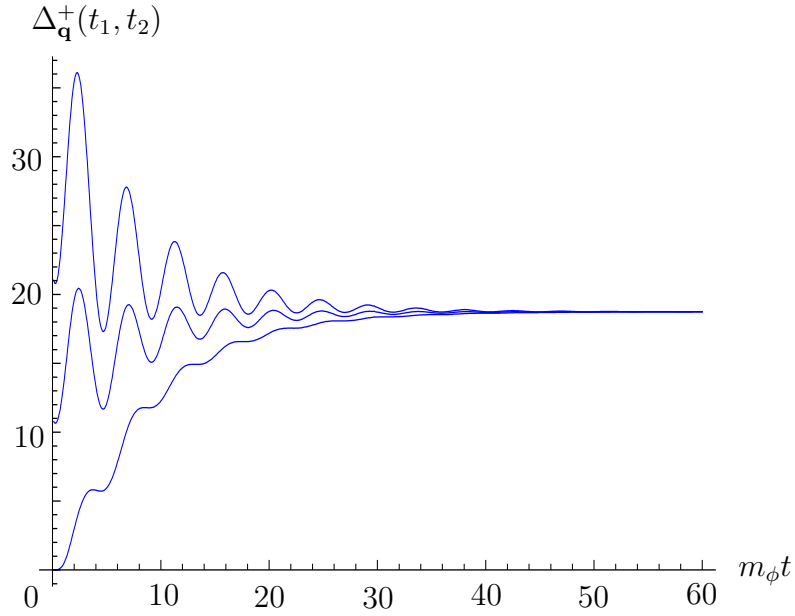


Figure 3.14: Statistical propagator $\Delta_{\mathbf{q}}^+(t_1, t_2)$ with $\mathbf{q} = 0$ as function of $t = (t_1 + t_2)/2$ for $y = 0$ and different initial conditions; case (b) with masses $\mathbf{q} = 0$, $m_1 = m_\phi$, $m_2 = 5m_\phi$ and $T = 10m_\phi$.

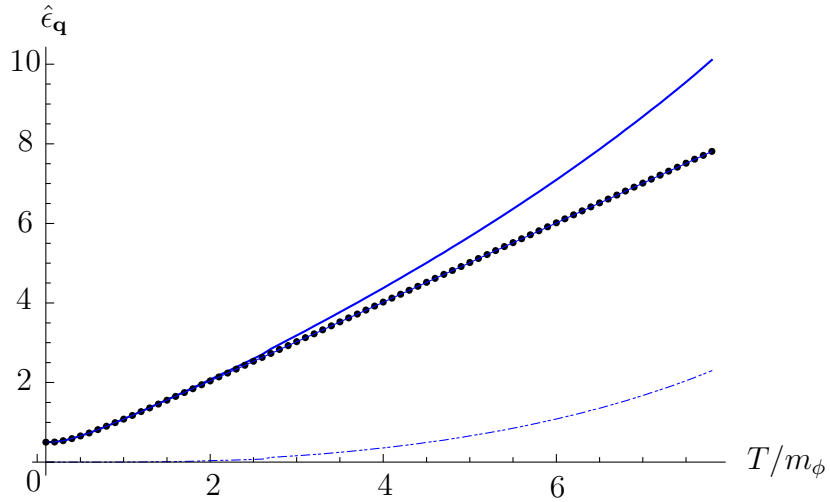


Figure 3.15: Energy density $\hat{\epsilon}_{\mathbf{q}} = \epsilon_{\mathbf{q}}/\omega_{\mathbf{q}}$ in the scalar model as function of temperature for $\mathbf{q} = 0$; case (b) with masses $m_1 = m_\phi$, $m_2 = 5m_\phi$: total energy density (solid), particle and quasi-particle energy densities (dotted), and 'vacuum' energy density (dashed).

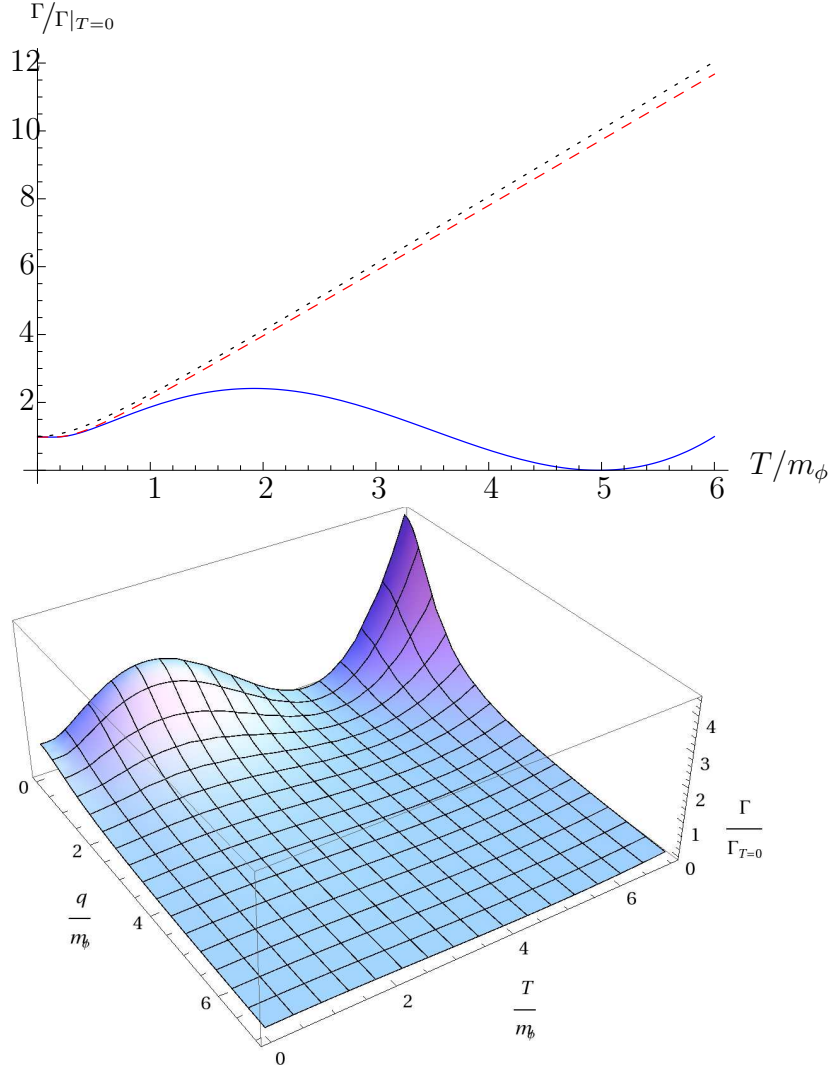


Figure 3.16: Upper plot: $\Gamma/\Gamma|_{T=0}$ in the Yukawa model as a function of temperature for $\mathbf{q} = 0$, $g = 0.1$, $m_\phi = 0.1m_1$. The plot compares the approximation (3.28) (dotted black curve) to the exact solution with negligible bath self interaction (red dashed curve) and the exact solution with a $\frac{\lambda}{4!}\phi^4$ self coupling of strength $\lambda = 0.2$ (blue curve). Since $m_2 = 0$ was assumed, the temperature region corresponding to case (c) shrinks to a point. Γ increases further with T beyond the plotted region and reaches very large values before it asymptotically approaches zero at even larger temperatures, but the quantitative validity of the leading order result is questionable in those temperature regimes. Lower plot: $\Gamma/\Gamma|_{T=0}$ in the Yukawa model as a function of T and $|\mathbf{q}|$ for $g = 0.1$, $m_\phi = 0.1m_1$ with a $\frac{\lambda}{4!}\phi^4$ self coupling of strength $\lambda = 0.2$.

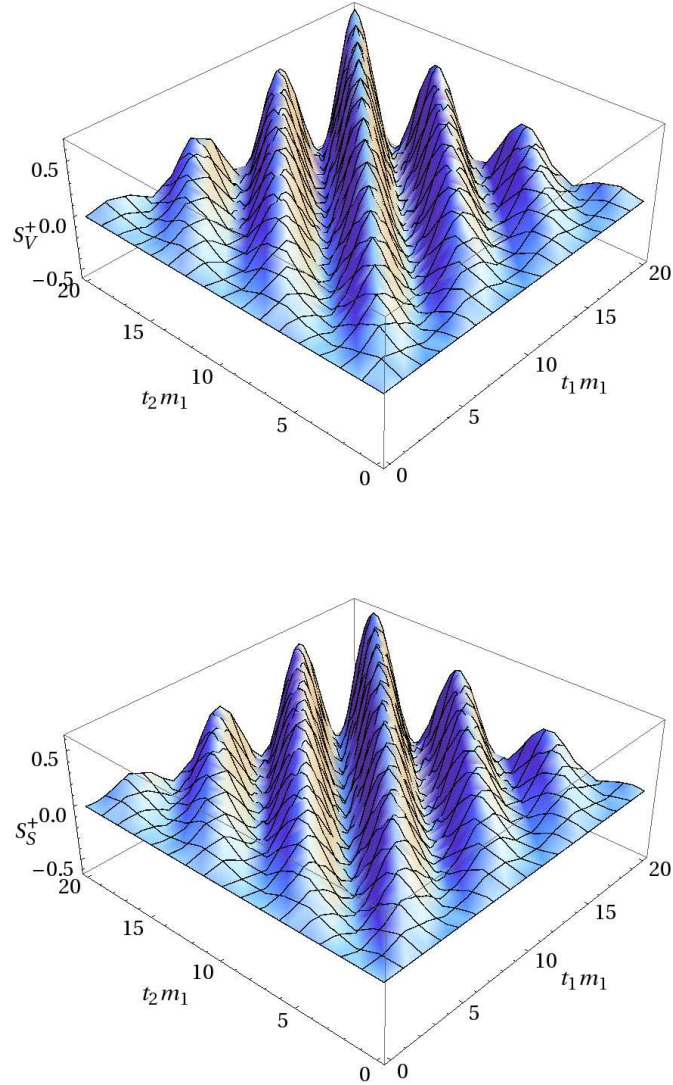


Figure 3.17: Vector and scalar part of $S_{\mathbf{q},\text{mem}}^+(t_1, t_2)$ as functions of t_1 and t_2 for $\mathbf{q} = 0$, $T = 0.5m_1$, $m_2 = m_\phi = 0$. Note that the vector part is symmetric in y while the scalar part is antisymmetric. As in Fig. 3.11, only the memory integral, which vanishes for $t_{1,2} = 0$, is plotted. The full solution (2.87) shows similar oscillations in t as in the scalar case, cf. Fig. 3.11, which are not visible here because we plot the approximate solution (2.94).

We now turn to the case that one of the fermions, Ψ_1 , is out of equilibrium and ϕ and Ψ_2 form the bath. The spectral and statistical propagators S^- and S^+ for Ψ_1 are given by (2.80) and (2.88). The self energy Σ in this case has to be computed from the diagram shown in Fig. 3.1*l*). In Appendix B.2 we present an analytic expression for $\text{Im}\Sigma^R$ in the case of vanishing m_2 mass that is, to the best of our knowledge, so far unknown in the literature. It is in good agreement with numerical plots shown in [72]. The real part can then be computed from

$$\text{Re}\Sigma_{\mathbf{q}}(\omega) = \frac{1}{\pi} \mathcal{P} \int dq_0 \frac{\text{Im}\Sigma_{\mathbf{q}}(q_0)}{q_0 - \omega}. \quad (3.27)$$

The expressions (B.30)-(B.35), (B.79)-(B.86) for $\text{Im}\Sigma^R$ are rather complicated, but the resulting $\Gamma_{\mathbf{q}}$ can be well approximated by

$$\Gamma_{\mathbf{q}} \approx g^2 \frac{m_1^2}{16\pi\omega_{\mathbf{q}}} \left(1 + \left(\frac{2T}{m_1} \right)^2 \right)^{\frac{1}{2}} \quad (3.28)$$

if the coupling is weak, $m_\phi \ll T, m_1$ and $|\mathbf{q}|, T \lesssim m_1$. Here $\omega_{\mathbf{q}}$ has of course to be evaluated with m_1 . Fig. 3.16 compares this approximation to the exact result. The analytic structure and the interpretation of the cuts and poles are the same as in the scalar case. The temperature regimes corresponding to case (a), (b) and (c) can be seen in Fig. 3.16. With the knowledge of Σ we can finally plot the correlation functions. The Lorentz components of $S_{\mathbf{q}}^-(y)$ are damped exponentials, see (2.77), (2.90). The vector and scalar parts of the memory integral in $S_{\mathbf{q}}^+(t_1, t_2)$ in the quasiparticle approximation (2.93) are shown in Fig. 3.17. Note the different symmetry of the scalar and vector part in the relative time coordinate $t_1 - t_2$. As in the scalar case (cf. Fig. 3.11), one observes oscillations in the relative time coordinate y and equilibration in the centre of mass time t . The oscillations in t that are visible in Fig. 3.11 have amplitudes $\mathcal{O}(\Gamma)$. Such oscillations are not visible in Fig. 3.17 because we plot the analytic leading order approximation (2.93) while Fig. 3.11 displays a numerical evaluation of the full result (2.61).

Applications in Cosmology

The overall structure of the observable universe is surprisingly simple.

On scales $> 100\text{Mpc}$ it appears spatially homogeneous and isotropic. Moreover, the cosmic microwave background reveals that the density fluctuations were even smaller before nonlinear galaxy formation created the structures we observe today [73]. Thus, the overall geometry can in good approximation be described by a Friedmann-Robertson-Walker metric,

$$ds^2 = g_{\mu\nu} dx^\mu dx^\nu = dt^2 - a^2(t) \left(\frac{dr^2}{1 - \kappa r^2} + r^2 (d\vartheta^2 + \sin^2 \vartheta d\varphi^2) \right). \quad (4.1)$$

κ determines the overall curvature of space, its sign is determined by the sign of $\Omega - 1$ where $\Omega = \epsilon/\epsilon_{cr}$ with ϵ being the energy density and ϵ_{cr} the critical energy density

$$\epsilon_{cr} = \frac{3H^2}{8\pi G}. \quad (4.2)$$

Here G is Newton's constant and $H = \dot{a}/a$ the Hubble parameter. The time evolution of the scale factor $a(t)$ is governed by the Friedmann equations

$$\ddot{a} = -\frac{4\pi}{3} G(\epsilon + 3p)a \quad (4.3)$$

$$H^2 + \frac{\kappa}{a^2} = \frac{8\pi G}{3} \epsilon. \quad (4.4)$$

Here contributions from a cosmological constant Λ have been included into energy density ϵ and pressure p . Based on various observations, it is possible to determine the composition

of the energy density. The total ϵ is very close to the critical density ϵ_{cr} and the overall geometry of the universe therefore in good approximation flat, $\kappa = 0$. It is composed of three main ingredients, with $\sim 4\%$ baryonic matter, $\sim 23\%$ dark matter and $\sim 73\%$ dark energy¹. In addition, there are small contributions from photons and neutrinos.

Extrapolating (4.3) and (4.4) backwards in time implies that the observable universe originates from a volume that was many orders of magnitude smaller than its current size. At early times, energy density and pressure were much higher than in any human made experiment, making it an excellent laboratory for high energy physics in which the standard model of particle physics and its possible extensions can be probed. In exchange, particle physics can provide an underlying microscopic theory that fills the cosmological parameters deduced from astronomical observations with a meaning. Indeed, many of the observed features can be understood as consequences of nonequilibrium phenomena in the early universe.

Processes in the primordial plasma are canonically studied by means of Boltzmann equations. From the discussion in the previous sections it is clear that this approach becomes increasingly unreliable in early epochs. However, during much of its early history the universe is filled with a slowly cooling plasma in thermal equilibrium. As the plasma cools down, its constituents successively fall out of equilibrium and *freeze out* when their interaction rates become low. If the temperature changes slowly with respect to the time scale associated to the particle reactions, such process can in good approximation be described by the methods we developed in the previous chapters. In this chapter, we apply them to two particular problems. In Sec. 4.2 we discuss thermal leptogenesis as an example for a freezeout process that requires a quantum mechanical description. Before, in Sec. 4.1, we use our results from the scalar model to study the kinematics of the reheating after inflation.

4.1 Inflaton Decay and Reheating

The homogeneity and isotropy of the observable universe on large scales pose a problem in classical cosmology. When extrapolating Eqs. (4.3) and (4.4) backwards in time, with the observed energy content, different patches in the sky correspond to regions in space that have never been causally connected. This leaves the question why they have the same temperature. Furthermore $\epsilon \approx \epsilon_{cr}$ at present time requires ϵ to be extremely close to ϵ_{cr} in the past. Without further assumptions, there is no explanation for this fine tuning. These problems, known as horizon- and flatness-problem, can be explained by the assumption that the universe underwent a phase of accelerated expansion at a very early stage of its evolution². Such an era of cosmic inflation would also explain the absence of topological defects predicted by many theories of particle physics in the observable universe as a result

¹See [2] for detailed numbers.

²For a review, see e.g. [74] and references therein.

of their dilution. The rapid expansion, if it lasted sufficiently long, implies that the entire observable universe originates from a very tiny, causally connected volume. The simplest mechanism that can drive inflation is provided by the potential energy of a scalar field ϕ , the inflaton, which at some point dominated the energy density in the small volume from which the observable universe originates. Here we focus on this scenario of *single field inflation*. During the inflationary phase, while ϕ moves towards its potential minimum, all other forms of energy are diluted and become negligible. When ϕ starts oscillating around the minimum, its energy is released into all other degrees of freedom, to which we collectively refer as \mathcal{X} . This process is known as *reheating* and leaves the universe filled with the hot primordial plasma that forms the initial state of big bang cosmology. The details of the ϕ dissipation and the subsequent thermalisation of the plasma are unknown, and so is the resulting temperature³.

The temperature in the early universe is a very important cosmological parameter. It determines the abundance at which particles are produced thermally. This includes dark matter candidates, leading to upper temperature bounds to avoid overproduction. In supersymmetric theories this is in particular of interest in the context of the so called gravitino problem [76]. In thermal leptogenesis it determines the abundance of heavy right handed neutrinos therefore the amount of baryon asymmetry that can be generated. This implies a lower bound on the temperature. It has also been speculated about the importance of thermal effects for moduli decay [77, 78] or destabilisation of extra dimensions [79], the latter also giving rise to an upper bound on T . In [80] it has been suggested that large thermal masses of the decay products in the primordial plasma imply another upper bound on the temperature. In this section we use our results from Sec. 2.3.3 to analyse the conditions under which this can happen.

In the beginning of the reheating phase almost all energy is stored in the coherent oscillations of the $\mathbf{q} = 0$ mode of the macroscopic field $\langle\phi\rangle$. Therefore $\phi_{0,\text{in}}$ and $\dot{\phi}_{0,\text{in}}$ reach large values while all other contributions to the energy density are small. The energy can be transferred into other degrees of freedom in different ways. In general this is a far-from-equilibrium process. The energy is released either into fluctuations of ϕ itself, which can be interpreted as particles and are characterised by Δ^\pm , or directly into \mathcal{X} s. If $\langle\phi\rangle$ dominates the self energies Π^R of the fields it couples to, effective masses are also dominated by the oscillating field value. In this case, most of the energy transfer happens via *parametric resonance* which dissipates enormous amounts of energy. This process can approximately be described in terms of classical fields, and its collective nature can easily allow the creation of particles with masses larger than m_ϕ [81, 82]. Kinematic restrictions as discussed in Sec. 2.3.3 are certainly not valid because they only apply if the system can be well described by the language of (quasi)particles. If there is no parametric resonance, or if a large amounts of energy have been released into fluctuations of ϕ , further dissipation happens via perturbative decays and scatterings of ϕ quanta. When these processes are

³ For a review, see e.g. [75] and references therein.

responsible for a significant part of the energy transfer, the kinematical considerations from Sec. 2.3.3 can play a crucial role.

The intrinsic mass of ϕ is usually thought to be larger than the intrinsic masses of the \mathcal{X} . On the other hand, it is coupled weakly to all other fields, much weaker than e.g. the Standard Model fields amongst each other. In case the interactions within the bath are strong enough to thermalise it fast on the time scale on which ϕ evolves, the decay happens in the background of a thermal plasma. This can be a reasonable approximation during the late phase of reheating [83, 80, 33] or in scenarios known as warm inflation [84, 71]. Pauli blocking suppresses reactions involving fermions, cf. (3.26), so that most of the energy is dissipated into bosonic degrees of freedom. Under these conditions, the scalar model in Sec. 3.1 can be used to study the influence of thermal masses and widths

During reheating backreaction is of course not negligible and the temperature not constant. $T(t)$ can be a complicated function and is determined by the struggle between cooling by expansion and heating by ϕ decay. However, if the time scale associated with the dynamics of ϕ is much shorter than that of the Hubble expansion, but still long enough for the bath to be considered in equilibrium at any time, one can use the approximation (2.48) for the spectral function and insert equilibrium propagators to compute the dissipation rate $\Gamma_{\mathbf{q}}$ at the given temperature in each moment.

The claim in [80] is that the thermal masses of the decay products increase with T and effectively block further ϕ -decay above a critical temperature T_c . Any cooling of the plasma below T_c by Hubble expansion is compensated by ϕ -decay, and the temperature remains at T_c until ϕ has dissipated its excessive energy. Then, when ϕ is in equilibrium with all other fields, the universe enters the radiation dominated era. Based on our results in Sec. 2.3.3 and 3.1, we can confirm this claim under certain conditions.

It is clear that the arguments related to energy and momentum conservation at vertices connecting resummed propagators can only hold if the involved fields are in the quasiparticle regime. Otherwise reheating can always continue via off-shell processes. In the quasiparticle regime, there can be a critical temperature above which further heating by perturbative decays and scatterings becomes inefficient because ϕ effectively decouples from the bath. Due to off-shell processes, Γ is never strictly zero, but it is suppressed by the smallness of the widths of the resonances when the on-shell decay becomes forbidden. In general, the conditions under which on-shell reactions between the quasiparticles become forbidden have to be extracted from the possibly complicated dispersion relations of all involved plasma waves. A simple rephrasing of these conditions by replacing intrinsic masses by thermal masses as done in [80, 33] is only valid if the free quasiparticle approximation holds and medium corrections to the dispersion relations depend only mildly on the wave vectors. In this case, the inequality (3.22) allows to estimate that for trilinear couplings that can be resembled by the scalar model from Sec. 3.1, the suppression above

T_c is effective if

$$\frac{\lambda}{32\pi} \left(1 - \left(\frac{2m_\chi}{m_\phi} \right)^2 \right) \ll 1.$$

This condition is quantitatively valid if the critical temperature given by (3.19),

$$T_c^2 \approx \frac{24}{\lambda} \left(\left(\frac{m_\phi}{2} \right)^2 - m_\chi^2 \right),$$

is low enough for perturbation theory to hold.

Even if these conditions are fulfilled, $2 \rightarrow 2$ scatterings always provide a channel to transfer energy from ϕ into the bath if ϕ also couples to the bath fields by four-vertices. Their efficiency depends on the coupling strength and on the value of T_c , see discussion following (3.24). The importance of widths in this context has previously been pointed out in [33], but modified dispersion relations and the possibility of scatterings were neglected.

4.2 Thermal Leptogenesis

The observable universe is purely made of matter, with a tiny fraction antimatter present in cosmic rays which can consistently be explained by secondary emission [85]. This requires an excess of matter over antimatter, or baryon asymmetry, in the primordial plasma. The excess can be estimated by the baryon-to-photon ratio $\eta = n_B/n_\gamma$, which can be determined in two ways, either from the CMB [86],

$$\eta_{CMB} = (6.225 \pm 0.170) \times 10^{-10} \quad (4.5)$$

or from the abundance of light elements in the intergalactic medium, thought to be created during big bang nucleosynthesis [87],

$$\eta_{BBN} = (5.5 \pm 1.0) \times 10^{-10}. \quad (4.6)$$

In inflationary cosmology, this number can not be assigned to the initial conditions because any pre-inflationary asymmetry is diluted during the accelerated expansion. Its value would be negligibly small after reheating. Hence baryogenesis, the generation of an $\eta \neq 0$, must have occurred during or after reheating. The details of the baryogenesis mechanism are unknown, and different models have been proposed. Any possible explanation has to be in agreement with the Sakharov conditions, namely it requires a deviation from thermal equilibrium and processes that violate C , CP and baryon number [88]. Here C and P stand for charge and parity conjugation. Baryon number B and lepton number L are quantum numbers for baryons and leptons respectively, with value 1 for particles and -1 for antiparticles.

In principle all these ingredients are provided in the Standard Model by the electroweak interaction [89]. It violates P and C as well as CP through the CKM matrix [11]. Baryon number B and lepton number L are violated by nonperturbative transitions between equivalent topological vacua [89, 90], the sphalerons. Those are negligible at zero temperature, but become relevant near the electroweak phase transition. Hubble expansion brings the plasma out of equilibrium. However, in order to explain the observed η , a first order electroweak phase transition is required. In the Standard Model, this would occur for a Higgs mass $m_H < 45$ GeV [91, 92], which is ruled out by experiment [4]. In addition, the CP violation in the CKM matrix is too small [93]. Thus, successful baryogenesis requires physics beyond the Standard Model. Many possibilities to achieve this have been explored during the past four decades⁴, including GUT baryogenesis [94], Affleck-Dine baryogenesis [95] and leptogenesis [13].

Leptogenesis⁵ provides a particularly attractive scenario because it links the baryon asymmetry to neutrino properties. If the light neutrino masses in the Standard Model are generated by a type-I see-saw mechanism (see appendix A), the CP violating out-of-equilibrium decay of the heavy neutrinos N can generate a matter-antimatter asymmetry in the leptonic sector. In the case that the inverse processes that wash out the asymmetry are efficient, its final value is independent of the initial conditions and given in terms of neutrino properties. The lepton-asymmetry can then partially be transferred to the baryonic sector by sphaleron processes.

Quantitatively, leptogenesis is usually studied by means of classical Boltzmann equations⁶. However, the creation of a lepton asymmetry is a quantum effect as it arises from the interference between tree level decays and higher order corrections. The description of this quantum effect in terms of Boltzmann equations suffers from the basic conceptual problems discussed in the previous sections. Furthermore, most leptogenesis scenarios require a high temperature $T \sim 10^{10}$ GeV to generate sufficiently many heavy neutrinos. At these temperatures thermal effects in the plasma can certainly not be ignored. It is important to understand the range of validity of the Boltzmann equations and estimate the size of the corrections. In recent years, enormous progress has been made towards this goal [49, 99, 50, 53, 54, 51], mostly based on quantum Boltzmann equations.

If leptogenesis takes place after the primordial plasma has thermalised, the simplicity of the setup can make a full quantum treatment possible. The heavy neutrinos N are in good approximation the only fields that are out of equilibrium. They are weakly coupled to a background plasma with slowly changing temperature. Since the number of degrees of freedom in the bath is > 100 and η known to be tiny, backreaction is negligible. The asymmetry only becomes relevant much later in the history of the universe. In this scenario, the propagation and decay of N in the primordial plasma can, with some

⁴For a review, see e.g. [96]

⁵For detailed reviews, see e.g. [97].

⁶For a detailed treatment in terms of Boltzmann equations see e.g. [98]

modifications, be modelled by the Yukawa model from Sec. 3.2. Ψ_1 is identified with N , Ψ_2 with the Standard Model leptons l and ϕ with the Higgs Φ . The main differences can be summarised as

- (1) N is a Majorana fermion.
- (2) Φ and l form weak isospin doublets.
- (3) N and l carry flavour indices. The Yukawa matrix λ is generally non-diagonal in flavour space and has complex entries.
- (4) The temperature is a function of time.

The Kadanoff-Baym equations for the propagators $G_{\alpha\beta}^>(x_1, x_2) = \langle N_\alpha(x_1)N_\beta(x_2) \rangle$ and $G_{\alpha\beta}^<(x_1, x_2) = -\langle N_\beta(x_2)N_\alpha(x_1) \rangle$ of Majorana fermions are given in [49],

$$C(i\partial_1 - M)G^>(x_1, x_2) = - \int d^4x' (\Sigma^>(x_1, x')G^A(x', x_2) + \Sigma^R(x_1, x')G^>(x', x_2)) , \quad (4.7)$$

$$C(i\partial_1 - M)G^<(x_1, x_2) = - \int d^4x' (\Sigma^<(x_1, x')G^A(x', x_2) + \Sigma^R(x_1, x')G^<(x', x_2)) . \quad (4.8)$$

Here C is the charge conjugation matrix, for which we take the representation $i\gamma^2\gamma^0$. Following the steps in Eqs. (1.52)-(1.60), it is straightforward to derive the Kadanoff-Baym equations for the spectral and statistical propagator,

$$C(i\partial_1 - M)G^-(x_1, x_2) = \int d^3\mathbf{x}' \int_{t_2}^{t_1} dt' \Sigma^-(x_1, x')G^-(x', x_2) , \quad (4.9)$$

$$\begin{aligned} C(i\partial_1 - M)G^+(x_1, x_2) &= \int d^3\mathbf{x}' \int_{t_i}^{t_1} dt' \Sigma^-(x_1, x')G^+(x', x_2) \\ &- \int d^3\mathbf{x}' \int_{t_i}^{t_2} dt' \Sigma^+(x_1, x')G^-(x', x_2) . \end{aligned} \quad (4.10)$$

Multiplication with C^{-1} from the left gives Eqs. (4.9) and (4.10) the same shape as the corresponding equations for Dirac fermions (1.88) and (1.89) with the replacements $S^\pm \rightarrow G^\pm$ and $\Sigma \rightarrow C^{-1}\Sigma$. The boundary condition (2.76) is modified to $G_{\mathbf{q}}^-(0) = i\gamma^0 C^{-1}$. Thus, one can find the solutions for Majorana neutrinos from those for Dirac neutrinos by replacement.

In the symmetric phase of the electroweak theory the modification (2) simply means that one has to sum over the components of the weak isospin doublet when computing the self energy. Each term has the same structure.

As a consequence of modification (3), the self energy Σ is generally not diagonal in flavour space. The resummed propagator is a matrix in flavour space, off-diagonal elements describe coherences between different flavours. Furthermore, due to the complex

entries in λ , CP is violated and the Lorentz structure is modified. Σ cannot be decomposed as in (2.81) because it also has pseudo-scalar and axial-vector parts. This makes the inversion of (2.78) technically more difficult, but does not pose a conceptual problem. Usually Σ is split into a left-handed and a right-handed part each of which can be decomposed as in (2.81). If the Majorana masses of the heavy neutrinos are strongly hierarchical, the lepton asymmetry is usually generated by the decay of the lightest flavour. The two heavier fields can then be integrated out to obtain an effective theory with only one flavour.

The biggest challenge is posed by the time dependence of T because the solutions of the Kadanoff-Baym equations were obtained under the assumption of a time translation invariant self-energy. If there is a separation of time scales, one can, analogue to Eqs.(2.47)-(2.48), treat t as an external parameter. Then the spectral propagator is given by

$$G^-(t_1, t_2) = \int \frac{d\omega}{2\pi} e^{-i\omega(t_1-t_2)} \times \left(\frac{1}{\not{q} - M - C^{-1}\Sigma_{\mathbf{q}}^A(\omega, T(t)) - i\omega\epsilon} - \frac{1}{\not{q} - M - C^{-1}\Sigma_{\mathbf{q}}^R(\omega, T(t)) + i\omega\epsilon} \right) C^{-1}. \quad (4.11)$$

This result can be used to compute $G^+(y; t)$ analogue to (2.88),

$$G_{\mathbf{q}}^+(t_1, t_2) = -G_{\mathbf{q}}^-(t_1)C\gamma^0G_{\mathbf{q}}^+(0, 0)\gamma^0C^{-1}G_{\mathbf{q}}^-(-t_2) + \int \frac{d\omega}{2\pi} e^{-i\omega(t_1-t_2)} \left(\int_0^{t_1} dy_1 G_{\mathbf{q}}^-(y_1) e^{i\omega y_1} \right) C^{-1}\Sigma_{\mathbf{q}}^+(\omega) \left(\int_0^{t_2} dy_2 G_{\mathbf{q}}^-(-y_2) e^{-i\omega y_2} \right). \quad (4.12)$$

Here it has been used that the symmetry relations (1.86) and (1.87) for Majorana fermions can be written as $G^{\pm}(x_1, x_2) = \mp (G^{\pm}(x_2, x_1))^T$.

The correlation functions G_{++} , $G^>$, $G^<$ and G_{--} can be obtained from G^{\pm} via the decomposition

$$(G_C(x_1, x_2))_c = G^+(x_1, x_2) - \frac{i}{2} \text{sign}_c(x_1^0 - x_2^0) G^-(x_1, x_2), \quad (4.13)$$

cf. (1.61). Since all Standard Model fields very close to equilibrium, they can be described by thermal (equilibrium) propagators in loop integrals. Those are well-known to leading order. Thus, knowledge of the spectral and statistical nonequilibrium propagators G^{\pm} for N allows to evaluate all relevant Feynman diagrams. In particular, CP -violating contributions to the lepton self energy can be computed. Those are responsible for the generation of a matter-antimatter asymmetry in the leptonic sector. The dressed statistical propagator S_{ij}^+ for leptons, where we have now written the flavour indices i and j explicitly, allows to define the 'lepton number matrix'

$$L_{\mathbf{q}ij}(t, t') = -\text{tr}(\gamma^0 S_{\mathbf{q}ij}^+(t, t')). \quad (4.14)$$

The asymmetry in flavour i as a function of time is then given by $L_{\mathbf{q}ii}(t, t)$. Computation of S_{ij}^+ to fourth order in the Yukawa couplings λ_{ij} in (A.1) provides a full quantum mechanical treatment of leptogenesis⁷. Since the Kadanoff-Baym formalism makes no semi-classical approximations, it inherently avoids a number of complications that computations based on conventional Boltzmann equations have been plagued with. In particular, there is no necessity for a subtraction of real intermediate states. Evaluation of the self energy diagrams automatically includes all on- and off-shell processes at a given order in the correct manner, and no apparent creation of an asymmetry in equilibrium is found. Furthermore, if leptons and Higgs fields in loop corrections are in equilibrium, thermal corrections to the production rates are linear in their distribution functions, as expected from detailed balance considerations⁸.

However, care has to be taken at two points. First, leptogenesis takes place at a very high temperature. Due to the breakdown of perturbation theory at large T the spectrum of the Standard Model in this regime is unknown. The assumption that the Standard Model fields are in the quasiparticle regime and can be described by the well-known leading order or next-to-leading-order propagators for dressed particles is doubtful. These problems are also neglected in all present computations that use Boltzmann or quantum Boltzmann equations and causes an error of unknown size in all computations to date. At the current stage, our results can be used to determine corrections due to quantum and non-Markovian effects by comparison to Boltzmann equations under equal assumptions regarding the spectrum. In the future, provided all relevant self energies at the temperature of interest are known from some other source, they allow the quantitative computation of the generated lepton asymmetry. Second, a realistic computation of course requires a more careful treatment of the dependence on centre of mass time. In particular, the CP violating part of the lepton self energy is not time translation invariant due to the deviation of the N propagators from equilibrium. Both of these aspects go beyond the scope of this work, but will be addressed in the near future⁹.

⁷This applies to the production and washout processes. In realistic leptogenesis, other *spectator processes* in the plasma can have an influence on the final asymmetry [100].

⁸This can be seen explicitly in Eqns. (3.6), (3.15), (3.26) and (B.45) for the models we studied in this work. By the time of printing, it has been confirmed in a realistic model for leptogenesis in [47], contrasting earlier claims made in [55], and is discussed in detail in [51].

⁹By the time of printing, there has been considerable progress towards this goal and a fully quantum mechanical computation of the asymmetry has been published in [47].

Conclusion

Many properties of the universe today can be explained as the result of nonequilibrium processes during its early history. The high energy densities during those epochs also make the early universe an excellent laboratory for the study of physics beyond the Standard Model. Hence, nonequilibrium processes in the primordial plasma are interesting for cosmology as well as particle physics. To date, most computations are based on Boltzmann equations. As classical Markovian equations for phase space distribution functions, these suffer from basic conceptual problems when quantum phenomena like coherent oscillations or memory effects are relevant. While in some cases, e.g. big bang nucleosynthesis or the decoupling of photons, these can in good approximation be neglected, they might be crucial in other situations. For instance, in leptogenesis scenarios, the creation of matter is caused by a quantum interference. Over the past years, evidence has amounted that classical Boltzmann equations may be insufficient to correctly describe this quantum mechanical process. Therefore it is important to understand the range of validity of the Boltzmann equations and estimate the size of the corrections.

Quantum and non-Markovian effects can modify the properties of a dense plasma in various ways. This includes effects that are related to the coherence of the quantum state as well as changes in the spectrum. The Kadanoff-Baym equations offer a tool to perform computations in a full quantum mechanical framework. However, while numerical solutions of Boltzmann equations usually allow a simple qualitative understanding of the results and their dependences on the model parameters, this transparency is often lost when using Kadanoff-Baym equations. When the spectrum of resonances in the plasma is approximately known and simple, one can derive effective Boltzmann equations from the Kadanoff-Baym equations, the quantum Boltzmann equations.

In this thesis we discussed systems in which one can go further and directly solve the

Kadanoff-Baym equations by analytic methods. Many important processes in the early universe can in good approximation be described by quantum fields out of equilibrium that are weakly coupled to a thermal bath. We solved the Kadanoff-Baym equations for scalars and fermions for such systems in full generality, without restrictions regarding the size of the deviation from equilibrium or making an ansatz that parameterises the propagators in terms of distribution functions. The composition of the heatbath need not be specified. The solutions remain valid in good approximation if the bath temperature changes slowly compared to all other timescales. Thus, they can directly be applied to a number of cosmological problems. Furthermore, they improve the conceptual understanding of quantum effects in a hot plasma.

We then performed a detailed comparison of our solutions to results obtained by other methods. First, we showed that the Kadanoff-Baym equations are equivalent to a stochastic Langevin equation. A comparison to Boltzmann equations for particles and quasiparticles revealed how these emerge from the Kadanoff-Baym equations in the limit of weak coupling and low temperature. We then studied the plasma properties with focus on the applicability of Boltzmann equations in different kinematic regimes.

- In the *particle regime*, the effects of the plasma on the properties of resonances are negligible. The standard Boltzmann equations hold and describe the kinematics with a high accuracy. If coherences are important, these can consistently be incorporated by the use of quantum Boltzmann equations.
- In the *quasiparticle regime*, modifications of the spectrum due to the presence of the medium become relevant. Dressed particles receive a thermal mass correction and new resonances, which correspond to collective excitations in the plasma, can appear. As long as all of these have small decay widths, they can effectively be described as quasiparticles. In this regime, quantum corrected Boltzmann equations may be used. They require the knowledge of the spectral function, including collective excitations, as a function of time. The dependence of the dispersion relations and decay widths on temperature and time causes non-Markovian effects. The latter can be parameterised by time-dependent collision terms. To leading order, energy and momentum are conserved in decays and scatterings involving quasiparticles. Hence, quasiparticles react like ordinary particles, but with modified dispersion relations and widths. The dispersion relations can deviate strongly from those of free particles. They change the available phase space volume for processes in a temperature dependent, hence dynamical, way and can have a dramatic influence on production and dissipation rates. A simple parameterisation by thermal masses is only possible if the dependence of the corrections on the wave vector is mild, leading to plasma waves that behave like free quasiparticles. The memory kernel can then be integrated in the narrow width limit, leading to ordinary Boltzmann equations with intrinsic masses replaced by thermal masses. It is important to note that, though the system's approach to equilibrium follows a Boltzmann-type equation,

the equation of state can differ significantly from that of a quasiparticle gas. The additional contributions can be interpreted as a shift in the ground state and can even generate a negative pressure. When coherences in flavour space are relevant, the quantum Boltzmann equations have to be formulated as matrix equations to include correlations between different flavours. Though quantum corrected Boltzmann equations may in principle be used in this regime, they have to be derived consistently either from the Kadanoff-Baym equations or, equivalently, the von Neumann equation for the density matrix. Many often-made assumptions in current computations, including the structure of the spectral function, the parameterisation of the propagators by distribution functions, the smallness of the deviation from equilibrium or the factorisation of the collision terms into a deviation from equilibrium and a time dependent damping rate, are generally not valid and have to be justified individually.

- In the *broad resonance regime*, Boltzmann equations completely fail to describe the system. When the decay width of the resonances is large, their interpretation as (quasi)particles becomes meaningless. Off-shell contributions to gain- and loss rates can be of the same order as on-shell processes or even dominate over them. This behaviour is expected for strong couplings, but can even occur in a weakly coupled theory at sufficiently high temperature.

We illustrated our results in a scalar and a Yukawa model. In both cases an analytic leading order expression for the imaginary part of the self energy, which determines the gain and loss rates, could be found. In case of the Yukawa model, the expression is, to our knowledge, previously unknown in the literature. The nontrivial behaviour of the self-energies as functions of temperature when including higher order corrections shows that the validity of approximations based on resummed leading order perturbation theory is limited.

Finally, we discussed applications of our results in cosmology. They can be used for a quantum mechanical treatment of a wide range of phenomena, in particular freezeout processes. We focused on two examples. In the context of reheating, our analysis allows to understand under which circumstances the appearance of large thermal masses can put an upper bound on the reheating temperature. This is the case if a significant part of the energy transfer from the inflaton modes into the primordial plasma happens via perturbative decay, quanta of the involved fields have dispersion relations corresponding to quasiparticles and Landau damping by scatterings is subdominant. In thermal leptogenesis scenarios, our results provide a toolkit for a full quantum mechanical computation of the generated lepton asymmetry. The full computation goes beyond the scope of this work, but will be addressed in the near future.

A

Right Handed Neutrinos and the Seesaw Mechanism

One of the simplest possible modifications of the Standard Model that can explain the observed neutrino oscillations is provided by its extension by three singlet fermions N_{Ri} , often referred to as right handed neutrinos,

$$\mathcal{L} = \mathcal{L}_{SM} + i\bar{N}_{Ri}\not{\partial}N_{Ri} - \lambda_{ij}\bar{l}_{Li}^I N_{Rj}\tilde{\Phi}^I - \frac{1}{2}M_{ij}\bar{N}_{Ri}^c N_{Rj} + h.c.. \quad (\text{A.1})$$

Here $N_R^c = C\bar{N}_R^T$ and $\tilde{\Phi} = -i(\Phi^\dagger\sigma_2)^T$. i and j are flavour indices and I marks the components of the weak isospin doublet. The fields N_R are usually referred to as right handed neutrinos. Adding them is in agreement with all symmetries of the Standard Model. While the first term after \mathcal{L}_{SM} in the above Lagrangian is simply the kinetic term for the right handed neutrinos, the second and third term provide Yukawa couplings analogue to those of the charged leptons. The last term is a Majorana mass term for the N_{Ri} . In general, it is not possible to diagonalise λ_{ij} , M_{ij} and the Yukawa coupling matrix of the charged leptons simultaneously in flavour space. In the following we chose a flavour base in which M_{ij} and the charged lepton Yukawa couplings are diagonal, the latter corresponding to a mass eigenstate base for the charged leptons after electroweak symmetry breaking. We now write the weak isospin doublet l_{Li}^I as

$$l_{Li} = \begin{pmatrix} \nu_{Li} \\ e_{Li} \end{pmatrix}. \quad (\text{A.2})$$

After electroweak symmetry breaking, ν obtains a Dirac mass term $(m_D)_{ij} = \lambda_{ij}v$ where v is the Higgs expectation value. Then the mass terms for N_R and ν_L can be written as

$$-\frac{1}{2} \begin{pmatrix} \bar{\nu}_L & \bar{N}_R^c \end{pmatrix} \begin{pmatrix} 0 & m_D \\ m_D^T & M \end{pmatrix} \begin{pmatrix} \nu_L^c \\ N_R \end{pmatrix}. \quad (\text{A.3})$$

Here each entry is of course a 3×3 flavour matrix, we suppressed flavour indices for notational simplicity. The physical neutrinos correspond to the mass eigenstates and are superpositions of N_R and ν_L . If one assumes $M \gg m_D$, those superpositions are approximately

$$\nu_i \approx \sum_j (U^T)_{ij} \left((\nu_{Lj} - (\nu_{Lj})^c) - \frac{(m_D)_{ji}}{M_{ii}} (N_{Ri}^c - N_{Ri}) \right) \quad (\text{A.4})$$

and

$$N_i \approx \sum_j \frac{(m_D)_{ji}}{M_{ii}} (\nu_{Lj} + (\nu_{Lj})^c) + (N_{Ri}^c + N_{Ri}) \quad (\text{A.5})$$

where the sum is to be taken over j only and U is the PMNS matrix [101, 102] that relates the neutrino mass and flavour eigenstates. Since $M \gg m_D$, the mass matrix for the states ν_α is approximately

$$m_\nu \approx \frac{m_D^2}{M} \quad (\text{A.6})$$

and are very light compared to the N_i with masses

$$M_i \approx M_{ii}. \quad (\text{A.7})$$

The neutrinos are Majorana particles, meaning they are their own antiparticles in the sense that $N_i^c = N_i$ and $\nu_i^c = -\nu_i$. The fact that large M lead to small m_ν gives the mechanism the name seesaw mechanism. If the $(m_D)_{ij}$ are chosen at the electroweak scale, the experimental data¹ implies $M_{ii} \approx 10^{15}$ GeV. This is close to the expected scale of Grand Unification. Since M is not protected by any symmetry, it is expected to have a value at that scale.

Finally, it should be pointed out that, on experimental ground, at this point it is not necessary to introduce three generations of N_R because only mass differences for the known neutrinos have been measured. If the lightest active neutrino is massless, two N_R are sufficient to explain the observed mass differences.

¹See [4] for recent values.

B

Some explicit Computations

B.1 Time Translation Invariance of Δ^-

In [5] it has been proven that $\Delta^-(x_1, x_2)$ is time translation invariant if it is analytic and the self energy is time translation invariant. Here we present an alternative proof. The initial conditions of $\Delta^-(x_1, x_2)$ do not depend on the initial conditions of the system, but are given by Eqs. (1.66)-(1.68),

$$\begin{aligned}\Delta^-(x_1, x_2)|_{t_1=t_2} &= 0, \\ \partial_{t_1}\Delta^-(x_1, x_2)|_{t_1=t_2} &= -\partial_{t_2}\Delta^-(x_1, x_2)|_{t_1=t_2} = \delta(\mathbf{x}_1 - \mathbf{x}_2), \\ \partial_{t_1}\partial_{t_2}\Delta^-(x_1, x_2)|_{t_1=t_2} &= 0.\end{aligned}$$

$\Pi^-(x_1, x_2)$ is antisymmetric under exchange of the four vectors x_1 and x_2 ,

$$\Pi^-(x_1, x_2) = -\Pi^-(x_2, x_1). \quad (\text{B.1})$$

The thermal bath is invariant under translations in space and time

$$\Pi^-(x_1, x_2) = \Pi^-(x_1 - x_2) \quad (\text{B.2})$$

and its properties are also invariant under the spatial parity transformation $\mathbf{x}_1 \leftrightarrow \mathbf{x}_2$

$$\Pi^-(\mathbf{x}_1 - \mathbf{x}_2, t_1 - t_2) = \Pi^-(\mathbf{x}_2 - \mathbf{x}_1, t_1 - t_2). \quad (\text{B.3})$$

In combination this implies that Π^- is antisymmetric under an exchange of the time components:

$$\Pi^-(\mathbf{x}_1 - \mathbf{x}_2, t_1 - t_2) = -\Pi^-(\mathbf{x}_1 - \mathbf{x}_2, t_2 - t_1). \quad (\text{B.4})$$

From the Kadanoff Baym equation it is know that

$$\Delta^{- (2,0)}(\mathbf{x}_1, t_1; \mathbf{x}_2, t_2) + \omega^2 \Delta^{-}(\mathbf{x}_1, t_1; \mathbf{x}_2, t_2) + \int_{t_2}^{t_1} dt' \Pi^{-}(\mathbf{x}_1 - \mathbf{x}'; t_1 - t') \Delta^{-}(\mathbf{x}', t'; \mathbf{x}_2, t_2) = 0, \quad (\text{B.5})$$

which in a spatially homogeneous system simplifies to

$$\Delta^{- (2,0)}(\mathbf{x}_1 - \mathbf{x}_2; t_1, t_2) + \omega^2 \Delta^{-}(\mathbf{x}_1 - \mathbf{x}_2; t_1, t_2) + \int_{t_2}^{t_1} dt' \Pi^{-}(\mathbf{x}_1 - \mathbf{x}'; t_1 - t') \Delta^{-}(\mathbf{x}' - \mathbf{x}_2; t_1, t_2) = 0. \quad (\text{B.6})$$

A Fourier transform in spatial momentum yields

$$\Delta_{\mathbf{q}}^{- (2,0)}(t_1, t_2) + \omega^2 \Delta_{\mathbf{q}}^{-}(t_1, t_2) + \int_{t_2}^{t_1} dt' \Pi_{\mathbf{q}}^{-}(t_1, t') \Delta_{\mathbf{q}}^{-}(t', t_2) = 0. \quad (\text{B.7})$$

The above properties of Δ^{-} imply

$$\Delta_{\mathbf{q}}^{- (0,0)}(t_1, t_2)|_{t_1=t_2} = 0 \quad (\text{B.8})$$

$$\Delta_{\mathbf{q}}^{- (1,0)}(t_1, t_2)|_{t_1=t_2} = 1 \quad (\text{B.9})$$

$$\Delta_{\mathbf{q}}^{- (0,1)}(t_1, t_2)|_{t_1=t_2} = -1 \quad (\text{B.10})$$

$$\Delta_{\mathbf{q}}^{- (1,1)}(t_1, t_2)|_{t_1=t_2} = 0 \quad (\text{B.11})$$

$$\Delta_{\mathbf{q}}^{- (n,m)}(t_1, t_2)|_{t_1=t_2} = -\Delta_{\mathbf{q}}^{- (m,n)}(t_1, t_2)|_{t_1=t_2} \quad (\text{B.12})$$

Here $\Delta_{\mathbf{q}}^{- (n,m)}$ means that the derivative of $\Delta_{\mathbf{q}}^{-}$ is taken n times with respect to the first time argument and m times with respect to the second. If Δ^{-} is analytic on the real axis it can be Taylor expanded in t_1 and t_2 and is equal to its Taylor series,

$$\Delta_{\mathbf{q}}^{-}(t_1, t_2) = \sum_{m,n=0}^{\infty} \frac{t_1^n t_2^m}{n!m!} \Delta_{\mathbf{q}}^{- (n,m)}(t_1, t_2)|_{t_1=t_2=0} \quad (\text{B.13})$$

In order to prove that Δ^{-} is translation invariant one has to show that it does not depend on the center of mass coordinate, meaning

$$\frac{\partial}{\partial(t_1 + t_2)} \Delta_{\mathbf{q}}^{-}(t_1, t_2) = \Delta_{\mathbf{q}}^{- (1,0)}(t_1, t_2) + \Delta_{\mathbf{q}}^{- (0,1)}(t_1, t_2) \quad (\text{B.14})$$

must vanish for any t_1 and t_2 . Expanding Δ^{-} according to (B.13) yields

$$\begin{aligned} \Delta_{\mathbf{q}}^{- (1,0)}(t_1, t_2) + \Delta_{\mathbf{q}}^{- (0,1)}(t_1, t_2) = \\ \sum_{m,n=0}^{\infty} \frac{t_1^n t_2^m}{n!m!} (\Delta_{\mathbf{q}}^{- (n+1,m)}(t_1, t_2)|_{t_1=t_2=0} + \Delta_{\mathbf{q}}^{- (n,m+1)}(t_1, t_2)|_{t_1=t_2=0}). \end{aligned} \quad (\text{B.15})$$

For the rest of this section we will use the short notation

$$\Delta^{(n,m)}| = \Delta_{\mathbf{q}}^{-(n,m)}(t_1, t_2)|_{t_1=t_2=0}. \quad (\text{B.16})$$

One can see from (B.15) that it is now sufficient to prove that

$$\Delta^{(n+1,m)}| + \Delta^{(n,m+1)}| = 0 \quad (\text{B.17})$$

for all m and n . The advantage of the expansion is that it allows to use the equal time commutation relations. The proof from now on goes along the following line: We assume that

$$\Delta^{(p+1,q)}| + \Delta^{(p,q+1)}| = 0 \quad (\text{B.18})$$

for all $p < n$, $q \leq m$. From that and (B.7) we can then proof that

$$\Delta^{(n+1,m)}| + \Delta^{(n,m+1)}| = 0. \quad (\text{B.19})$$

Applying the operator $\frac{\partial^p}{\partial t_1^p} + \frac{\partial^q}{\partial t_2^q}$ to (B.7) leads to

$$\begin{aligned} \Delta^{(p+2,q)}(t_1, t_2) &= -\omega^2 \Delta^{(p,q)}(t_1, t_2) \\ &\quad - \sum_{u=1}^p \sum_{s=0}^{p-u} \sum_{t=0}^s B_s^{p-u} B_t^s (-1)^{s-t} \Pi^{(u+s-1)}(t_1 - t_1) \Delta^{(p-u-s,q)}(t_1, t_2) \\ &\quad + \sum_{k=1}^q \sum_{l=0}^{q-k} \sum_{r=0}^l B_l^{q-k} B_r^l (-1)^{q-k-l} \Pi^{(p+q-k-l)}(t_1 - t_2) \Delta^{(l-r, k+r-1)}(t_2, t_2) \\ &\quad + \int_{t_2}^{t_1} dt' \left(\frac{\partial^p}{\partial t_1^p} + \frac{\partial^q}{\partial t_2^q} \right) \left(\Pi_q^-(t_1 - t') \Delta_q^-(t', t_2) \right). \end{aligned} \quad (\text{B.20})$$

Here B_j^i is the binomial coefficient $\binom{i}{j}$. The integral term will vanish for $t_1 = t_2$. It follows that

$$\begin{aligned} \Delta^{(n+1,m)}| + \Delta^{(n,m+1)}| &= -\omega^2 \left(\Delta^{\Delta^{(n-1,m)}| + (n-2, m+1)}| \right) \\ &\quad + \sum_{k=1}^m \sum_{l=0}^{m-k} \sum_{r=0}^l \left(B_l^{m-k} B_r^l (-1)^{m-k-l} \Pi^{(n-1+m-k-l)}(t_1 - t_2) \Delta^{(l-r, k+r-1)}(t_2, t_2) \right) \Big|_{t_1=t_2} \\ &\quad + \sum_{k=1}^{m+1} \sum_{l=0}^{m+1-k} \sum_{r=0}^l \left(B_l^{m+1-k} B_r^l (-1)^{m+1-k-l} \Pi^{(n-2+m+1-k-l)}(t_1 - t_2) \Delta^{(l-r, k+r-1)}(t_2, t_2) \right) \Big|_{t_1=t_2} \\ &\quad - \sum_{u=1}^{n-2} \sum_{s=0}^{n-2-u} \sum_{t=0}^s \left(B_s^{n-2-u} B_t^s (-1)^{s-t} \Pi^{(u+s-1)}(t_1 - t_1) \Delta^{(n-2-u-s, m+1)}(t_1, t_2) \right) \Big|_{t_1=t_2} \\ &\quad - \sum_{u=1}^{n-1} \sum_{s=0}^{n-1-u} \sum_{t=0}^s \left(B_s^{n-1-u} B_t^s (-1)^{s-t} \Pi^{(u+s-1)}(t_1 - t_1) \Delta^{(n-1-u-s, m)}(t_1, t_2) \right) \Big|_{t_1=t_2}. \end{aligned}$$

The $k = m + 1$ term in the third line and the $u = n - 1$ term in the fifth line cancel each other. The first line is zero by assumption (B.18). Therefore the whole expression can be rewritten as

$$\begin{aligned}
& \sum_{k=1}^m \left(\sum_{l=0}^{m-k} \sum_{r=0}^l B_l^{m-k} B_r^l (-1)^{m-k-l} \Pi^{(n-1+m-k-l)}(t_1 - t_2) \Delta^{(l-r, k+r-1)}(t_2, t_2) \right. \\
& \quad \left. + \sum_{l=0}^{m+1-k} \sum_{r=0}^l B_l^{m+1-k} B_r^l (-1)^{m+1-k-l} \Pi^{(n-2+m+1-k-l)}(t_1 - t_2) \Delta^{(l-r, k+r-1)}(t_2, t_2) \right) \Big|_{t_1=t_2} \\
& - \sum_{u=1}^{n-2} \left(\sum_{s=0}^{n-2-u} \sum_{t=0}^s B_s^{n-2-u} B_t^s (-1)^{s-t} \Pi^{(u+s-1)}(t_1 - t_1) \Delta^{(n-2-u-s, m+1)}(t_1, t_2) \right. \\
& \quad \left. + \sum_{s=0}^{n-1-u} \sum_{t=0}^s B_s^{n-1-u} B_t^s (-1)^{s-t} \Pi^{(u+s-1)}(t_1 - t_1) \Delta^{(n-1-u-s, m)}(t_1, t_2) \right) \Big|_{t_1=t_2}
\end{aligned} \tag{B.21}$$

Now the sum over t in the last two lines can be performed. It can be checked that

$$\sum_{t=0}^s (-1)^{s-t} B_t^s = \begin{cases} 1 & \text{for } s = 0 \\ 0 & \text{otherwise} \end{cases} . \tag{B.22}$$

Using this one can see that the last two lines never contribute due to (B.18). The upper two lines can now be summarized as

$$\begin{aligned}
& \sum_{k=1}^m \left(\sum_{l=0}^{m-k} \sum_{r=0}^l B_r^l \Pi^{(n-1+m-k-l)}(t_1 - t_2) \Delta^{(l-r, k+r-1)}(t_2, t_2) \left((-1)^{m-k-l} B_l^{m-k} \right. \right. \\
& \quad \left. \left. + (-1)^{m-k-l+1} B_l^{m-k+1} \right) \right. \\
& \quad \left. + \sum_{r=0}^{m-k+1} B_r^{m+1-k} \Pi^{(n-2)}(t_1 - t_2) \Delta^{(m-k+1-r, k+r-1)}(t_2, t_2) \right) \Big|_{t_1=t_2}
\end{aligned} \tag{B.23}$$

which equals

$$\begin{aligned}
& \sum_{k=1}^m \left(\Pi^{(n-2)}(t_1 - t_2) \left(\frac{\partial^{m-k+1}}{\partial t_2^{m-k+1}} \Delta^{(0,k-1)}(t_2, t_2) \right) \right. \\
& + \sum_{l=0}^{m-k} \left(\frac{\partial^{m-k-l+1}}{\partial t_2^{m-k-l+1}} \Pi^{(n-2)}(t_1 - t_2) \right) \left(\frac{\partial^l}{\partial t_2^l} \Delta^{(0,k-1)}(t_2, t_2) \right) B_l^{m-k+1} \\
& \left. - \sum_{l=0}^{m-k} \left(\frac{\partial^{m-k-l+1}}{\partial t_2^{m-k-l+1}} \Pi^{(n-2)}(t_1 - t_2) \right) \left(\frac{\partial^l}{\partial t_2^l} \Delta^{(0,k-1)}(t_2, t_2) \right) B_l^{m-k} \right) \Big|_{t_1=t_2}. \quad (\text{B.24})
\end{aligned}$$

This can be simplified to

$$\begin{aligned}
& \sum_{k=1}^m \left(\frac{\partial^{m-k+1}}{\partial t_2^{m-k+1}} (\Pi^{(n-2)}(t_1 - t_2) \Delta^{(0,k-1)}(t_2, t_2)) \right. \\
& \left. + \frac{\partial}{\partial t_1} \sum_{l=0}^{m-k} \left(\frac{\partial^{m-k-l}}{\partial t_2^{m-k-l}} \Pi^{(n-2)}(t_1 - t_2) \right) \left(\frac{\partial^l}{\partial t_2^l} \Delta^{(0,k-1)}(t_2, t_2) \right) B_l^{m-k} \right) \Big|_{t_1=t_2} \quad (\text{B.25})
\end{aligned}$$

and furthermore

$$\begin{aligned}
& \sum_{k=1}^m \left(\frac{\partial^{m-k+1}}{\partial t_2^{m-k+1}} (\Pi^{(n-2)}(t_1 - t_2) \Delta^{(0,k-1)}(t_2, t_2)) \right. \\
& \left. + \frac{\partial}{\partial t_1} \left(\frac{\partial^{m-k}}{\partial t_2^{m-k}} (\Pi^{(n-2)}(t_1 - t_2) \Delta^{(0,k-1)}(t_2, t_2)) \right) \right) \Big|_{t_1=t_2} \quad (\text{B.26})
\end{aligned}$$

which is equal to

$$\left(\frac{\partial}{\partial t_1} + \frac{\partial}{\partial t_2} \right) \sum_{k=1}^m \frac{\partial^{m-k}}{\partial t_2^{m-l}} (\Pi^{(n-2)}(t_1 - t_2) \Delta^{(0,k-1)}(t_2, t_2)) \Big|_{t_1=t_2}. \quad (\text{B.27})$$

This equals

$$\sum_{k=1}^m \frac{\partial^{m-k}}{\partial t_2^{m-l}} (\Pi^{(n-2)}(t_1 - t_2) (\Delta^{(1,k-1)}(t_2, t_2) + \Delta^{(0,k)}(t_2, t_2))) \Big|_{t_1=t_2}. \quad (\text{B.28})$$

The sum in the bracket is zero due to (B.18). Therefore

$$\Delta^{(n+1,m)}| + \Delta^{(n,m+1)}| = 0 \quad (\text{B.29})$$

Obviously the whole proof relies on (B.18). This is certainly true for $p = 0, q = 0$. It can also be verified easily for $p = 1, q = 0$. From (B.20) it can be seen that (B.18) only needs

to be fulfilled for all $p < n$. Therefore (B.20) allows to conclude that (B.29) is fulfilled for $n + 1$ if it is known to be true for n . Starting from $\Delta^{(0,0)}$, $\Delta^{(1,0)}$, and $\Delta^{(1,0)}$ it can be proven for all

$$\Delta^{(n+1,0)} + \Delta^{(n,1)},$$

meaning one can "go up" in derivatives with respect to the first argument. In contrast to that it relies on (B.18) for all $q \leq m$. To prove the statement for a certain order derivative in the second argument it has to be known to be valid for that order derivative and not only for lower orders. Hence one cannot recursively conclude for (or "go up" to) higher derivatives in the second argument. But due to

$$\Delta^{(n,m)} = -\Delta^{(m,n)}$$

one can find arbitrary $\Delta^{(0,n+1)}$ and $\Delta^{(1,n)}$ and then again proceed step by step to higher order derivatives in the first argument. This way it becomes clear that all coefficients in the Taylor series (B.15) are zero and $\Delta_q^-(t_1, t_2)$ is really time translation invariant.

B.2 The Fermion Self Energy

We translate the parameterisation (2.81)

$$\Sigma_{(V)}^R = a_{\mathbf{q}}(\omega) \not{q} + b_{\mathbf{q}}(\omega) \not{\psi}, \quad \Sigma_{(S)}^R = c_{\mathbf{q}}(\omega)$$

into the quantities

$$A = \left(\frac{1}{4} \text{tr} (q \Sigma_{\mathbf{q}}^R(\omega)) \right) \tag{B.30}$$

$$B = \left(\frac{1}{4} \text{tr} (\psi \Sigma_{\mathbf{q}}^R(\omega)) \right) \tag{B.31}$$

$$C = \left(\frac{1}{4} \text{tr} (\Sigma_{\mathbf{q}}^R(\omega)) \right) \tag{B.32}$$

from which one can obtain $a_{\mathbf{q}}(\omega)$, $b_{\mathbf{q}}(\omega)$ and $c_{\mathbf{q}}(\omega)$ via

$$a = \frac{Bqu - Au^2}{(qu)^2 - q^2u^2} \tag{B.33}$$

$$b = \frac{-Bq^2 + Aqu}{(qu)^2 - q^2u^2} \tag{B.34}$$

$$c = C \tag{B.35}$$

where $qu = q_\mu u^\mu$ etc. The quantities defined above are generally complex scalars that can be decomposed as $a = a_R + ia_I$ etc., where a_I is defined via the discontinuity.

$$a_I = \text{Im} a_{\mathbf{q}}(\omega) = \frac{1}{2i} (a_{\mathbf{q}}(\omega + i\epsilon) - a_{\mathbf{q}}(\omega - i\epsilon)) \tag{B.36}$$

We perform the computation in the rest frame of the bath where $u = (1, 0, 0, 0)$. From (1.106) it follows that

$$S^>(p) = (1 - f_F(p_0))\rho_\Psi(p) \quad (\text{B.37})$$

$$\Delta^>(p) = (1 + f_B(p_0))\rho_\phi(p). \quad (\text{B.38})$$

From the KMS condition (1.104) and the relation (B.99) one obtains

$$\text{disc}\Sigma_{\mathbf{q}}^R(\omega) = (e^{-\beta\omega} + 1)\Sigma_{\mathbf{q}}^>(\omega), \quad (\text{B.39})$$

leading to

$$\begin{aligned} \text{disc}\Sigma_{\mathbf{q}}^R(\omega) &= -ig^2(e^{-\beta\omega} + 1) \int \frac{d^4p}{(2\pi)^4} S^>(p)\Delta^>(q-p) \\ &= -ig^2 f_F(-\omega)^{-1} \int \frac{d^4p}{(2\pi)^2} (1 - f_F(p_0))(1 + f_B(\omega - p_0)) \text{sign}(p_0) \text{sign}(\omega - p_0) (\not{p} + m_2) \\ &\quad \times \delta(p^2 - m_2^2) \delta((q-p)^2 - m_\phi^2) \\ &= -ig^2 f_F(-\omega)^{-1} \int \frac{d^4p}{(2\pi)^2} \frac{1}{2\omega_1 2\omega_2} (1 - f_F(p_0))(1 + f_B(\omega - p_0)) \text{sign}(p_0) \text{sign}(\omega - p_0) (\not{p} + m_2) \\ &\quad \times (\delta(p_0 - \omega_1) + \delta(p_0 + \omega_1)) (\delta(\omega - p_0 - \omega_2) + \delta(\omega - p_0 + \omega_2)) \end{aligned} \quad (\text{B.40})$$

with $\omega_1 = (\mathbf{p}^2 + m_2^2)^{\frac{1}{2}}$ and $\omega_2 = ((\mathbf{q} - \mathbf{p})^2 + m_\phi^2)^{\frac{1}{2}}$. Performing the p_0 integration leads to

$$\begin{aligned} &-ig^2 f_F(-\omega)^{-1} \int \frac{d^3\mathbf{p}}{(2\pi)^2} \frac{1}{2\omega_1 2\omega_2} \\ &\quad \left((1 - f_F(\omega_1))(1 + f_B(\omega - \omega_1)) \text{sign}(\omega - \omega_1) (\omega_1 \gamma^0 - \boldsymbol{p}\boldsymbol{\gamma} + m_2) \right. \\ &\quad \quad \times (\delta(\omega - \omega_1 - \omega_2) + \delta(\omega - \omega_1 + \omega_2)) \\ &\quad - (1 - f_F(-\omega_1))(1 + f_B(\omega + \omega_1)) \text{sign}(\omega + \omega_1) (-\omega_1 \gamma^0 - \boldsymbol{p}\boldsymbol{\gamma} + m_2) \\ &\quad \quad \left. \times (\delta(\omega + \omega_1 - \omega_2) + \delta(\omega + \omega_1 + \omega_2)) \right) \end{aligned} \quad (\text{B.41})$$

Each δ -function can only be non-zero for one sign of $\omega - \omega_1$. Now we define

$$n_B(\omega) = f_B(|\omega|), \quad n_F(\omega) = f_F(|\omega|). \quad (\text{B.42})$$

We use

$$f_B(-w) + f_B(w) = -1 \quad (\text{B.43})$$

$$f_F(-w) + f_F(w) = 1 \quad (\text{B.44})$$

and relations as $\text{sign}(\omega - \omega_1)f(\omega - \omega_1)\delta(\omega - \omega_1 - \omega_2) = f(\omega_2)\delta(\omega - \omega_1 - \omega_2)$ etc. to rewrite

$$\begin{aligned} \text{disc}\Sigma_{\mathbf{q}}^R(\omega) = & -ig^2 \int \frac{d^3\mathbf{p}}{(2\pi)^2} \frac{1}{2\omega_1 2\omega_2} \\ & \left((1 - n_F(\omega_1) + n_B(\omega_2)) \left((\omega_1\gamma^0 - \mathbf{p}\boldsymbol{\gamma} + m_2)\delta(\omega - \omega_1 - \omega_2) \right. \right. \\ & \quad \left. \left. + (\omega_1\gamma^0 + \mathbf{p}\boldsymbol{\gamma} - m_2)\delta(\omega + \omega_1 + \omega_2) \right) \right. \\ & \left. + (n_F(\omega_1) + n_B(\omega_2)) \left((\omega_1\gamma^0 - \mathbf{p}\boldsymbol{\gamma} + m_2)\delta(\omega - \omega_1 + \omega_2) \right. \right. \\ & \quad \left. \left. + (\omega_1\gamma^0 + \mathbf{p}\boldsymbol{\gamma} - m_2)\delta(\omega + \omega_1 - \omega_2) \right) \right) \end{aligned} \quad (\text{B.45})$$

This expression can be compared to (3.6) and agrees with (3.6) in [72]¹. With an application in thermal leptogenesis in mind, we can set $m_2 = 0$, leading to

$$c_I = C_I = \left(\hat{\Sigma}_{(S)} \right)_I = 0. \quad (\text{B.46})$$

From this one can find for A_I

$$\begin{aligned} A_I = & -g^2 \int \frac{d^3\mathbf{p}}{(2\pi)^3} \frac{2\pi}{8\omega_1\omega_2} \left((1 - n_1 + n_2) \left((\omega\omega_1 - \mathbf{q}\mathbf{p})\delta(\omega - \omega_1 - \omega_2) \right. \right. \\ & \quad \left. \left. + (\omega\omega_1 + \mathbf{q}\mathbf{p})\delta(\omega + \omega_1 + \omega_2) \right) \right. \\ & \left. + (n_1 + n_2) \left((\omega\omega_1 - \mathbf{q}\mathbf{p})\delta(\omega - \omega_1 + \omega_2) \right. \right. \\ & \quad \left. \left. + (\omega\omega_1 + \mathbf{q}\mathbf{p})\delta(\omega + \omega_1 - \omega_2) \right) \right) \end{aligned} \quad (\text{B.47})$$

with the notation $n_1 = n_F(\omega_1)$ and $n_2 = n_B(\omega_2)$. This expression is as a whole antisymmetric in ω and allows to rewrite

$$\begin{aligned} A_I = & -g^2 \int \frac{d^3\mathbf{p}}{(2\pi)^3} \frac{2\pi}{8\omega_1\omega_2} \left(\omega\omega_1 \left((1 - n_1 + n_2)(\delta_1 + \delta_2) + (n_1 + n_2)(\delta_3 + \delta_4) \right) \right. \\ & \left. - \text{sign}(\omega)\mathbf{q}\mathbf{p} \left((1 - n_1 + n_2)(\delta_1 - \delta_2) + (n_1 + n_2)(\delta_4 - \delta_3) \right) \right) \end{aligned} \quad (\text{B.48})$$

where

$$\begin{aligned} \delta_1 = \delta(|\omega| - \omega_1 - \omega_2), \quad \delta_2 = \delta(|\omega| + \omega_1 + \omega_2), \\ \delta_3 = \delta(|\omega| + \omega_1 - \omega_2), \quad \delta_4 = \delta(|\omega| - \omega_1 + \omega_2) \end{aligned} \quad (\text{B.49})$$

¹Eq. (B.45) differs from (2.22) in [7] by a difference in the projectors, probably due to a typo.

At this point it is already clear that δ_2 can not contribute. We change to spherical coordinates $\varphi, \vartheta, |\mathbf{p}|$. The φ integration is trivial and due to $m_2 = 0$ one has $|\mathbf{p}| = \omega_1$. Introducing $x = |\mathbf{p}||\mathbf{q}| \cos(\vartheta) = \mathbf{p}\mathbf{q}$ one can write

$$A_I = \frac{-g^2}{16\pi|\mathbf{q}|} \int_0^\infty d\omega_1 \int_{-\omega_1|\mathbf{q}|}^{\omega_1|\mathbf{q}|} dx \left(\begin{aligned} &\delta(x - x_{01})(\omega\omega_1(1 - n_1 + n_2) - \text{sign}(\omega)x(1 - n_1 + n_2)) \\ &+ \delta(x - x_{03})(\omega\omega_1(n_1 + n_2) + \text{sign}(\omega)x(n_1 + n_2)) \\ &+ \delta(x - x_{04})(\omega\omega_1(n_1 + n_2) - \text{sign}(\omega)x(n_1 + n_2)) \end{aligned} \right) \quad (\text{B.50})$$

where we used $\delta_i = \omega_2 \delta(x - x_{0i})$. The x_{0i} can easily be determined as

$$x_{01} = \frac{1}{2}(\mathbf{q}^2 - \omega^2 + m_\phi^2) + \omega_1|\omega| \quad (\text{B.51})$$

$$x_{03} = \frac{1}{2}(\mathbf{q}^2 - \omega^2 + m_\phi^2) - \omega_1|\omega| \quad (\text{B.52})$$

$$x_{04} = x_{01}. \quad (\text{B.53})$$

This allows to perform the x integration,

$$A_I = \frac{-g^2}{16\pi|\mathbf{q}|} \left(\int_1 d\omega_1 (\omega f_1 + g_1) + \int_3 d\omega_1 (\omega f_3 - g_3) + \int_4 d\omega_1 (\omega f_4 + g_4) \right). \quad (\text{B.54})$$

Here the subscript at the \int_i indicates which δ_i determines integration limits for the ω_1 integration. The f_i and g_i are given by

$$f_1 = \omega_1(1 - n_F(\omega_1) + n_B(|\omega| - \omega_1)) \quad (\text{B.55})$$

$$f_3 = \omega_1(n_F(\omega_1) + n_B(|\omega| + \omega_1)) \quad (\text{B.56})$$

$$f_4 = \omega_1(n_F(\omega_1) + n_B(\omega_1 - |\omega|)) \quad (\text{B.57})$$

$$g_1 = \text{sign}(\omega) \left(\frac{1}{2}(\omega^2 - \mathbf{q}^2 - m_\phi^2) - \omega_1|\omega| \right) (1 - n_F(\omega_1) + n_B(|\omega| - \omega_1)) \quad (\text{B.58})$$

$$g_3 = \text{sign}(\omega) \left(\frac{1}{2}(\omega^2 - \mathbf{q}^2 - m_\phi^2) + \omega_1|\omega| \right) (n_F(\omega_1) + n_B(|\omega| + \omega_1)) \quad (\text{B.59})$$

$$g_4 = \text{sign}(\omega) \left(\frac{1}{2}(\omega^2 - \mathbf{q}^2 - m_\phi^2) - \omega_1|\omega| \right) (n_F(\omega_1) + n_B(\omega_1 - |\omega|)) \quad (\text{B.60})$$

$$(\text{B.61})$$

It is easy to see from Eqs. (B.30), (B.31) and (B.50) that

$$B_I = \frac{-g^2}{16\pi|\mathbf{q}|} \left(\int_1 d\omega_1 f_1 + \int_3 d\omega_1 f_3 + \int_4 d\omega_1 f_4 \right) \quad (\text{B.62})$$

f_1 and g_1 are contributions from decay and inverse decays $\Psi_1 \leftrightarrow \Psi_2\phi$ and can lead to a zero temperature part if $m_1 > m_\phi$. f_3, f_4, g_3 and g_4 come from scatterings in the plasma. It is interesting to note that

$$f_1 = f_4 \quad (\text{B.63})$$

$$g_1 = g_4 \quad (\text{B.64})$$

despite the fact that they originate from different processes². The f_i are symmetric in ω , the g_i antisymmetric. In the rest frame of the bath (B.33 ff) can be written as

$$a = \frac{B\omega - A}{\mathbf{q}^2} \quad (\text{B.65})$$

$$b = \frac{\omega(A - B\omega)}{\mathbf{q}^2} + B \quad (\text{B.66})$$

$$c = C \quad (\text{B.67})$$

B_I is symmetric in ω while A_I is antisymmetric. As a consequence, a_I is antisymmetric while b_I is symmetric which is consistent with [103]. The stem functions of all f_i, g_i are known analytically, so the only remaining difficult task is the determination of the proper integration limits. This shall be done now.

$\delta(|\omega| - \omega_1 - \omega_2)$: In order for x_{01} to be a zero point, the condition

$$|\omega| - \omega_1 > 0 \quad (\text{B.68})$$

has to be fulfilled. In any case,

$$\omega_1 > m_2 = 0. \quad (\text{B.69})$$

In order for the x -integral to be non-zero it requires

$$|x_{01}| < \omega_1 |\mathbf{q}|. \quad (\text{B.70})$$

The solutions to $|x_{01}| = \omega_1 |\mathbf{q}|$ are

$$\omega_\pm = \frac{1}{2} \frac{q^2 - m_\phi^2}{q^2} (|\omega| \pm |\mathbf{q}|) \quad (\text{B.71})$$

with $q^2 = \omega^2 - \mathbf{q}^2$. One has to distinguish three different regimes: For $0 < |\omega| < |\mathbf{q}|$ and $\omega_1 > 0$ only ω_+ is a solution, and it puts a lower bound on ω_1 in order for the inequality (B.70) to be fulfilled, leading to $\omega_1 > \omega_+$. On the other hand the condition (B.68) has

²Note that despite the equalities (B.63) and (B.64) the Landau damping terms f_4, g_4 never lead to a contribution to Σ at zero temperature while the decay and inverse decay parts f_1 and g_1 can contribute as expected. The reason lies in the different integration limits, see (B.68) and (B.77)

to be fulfilled, and since for $|\omega| < |\mathbf{q}|$ always $\omega_+ > |\omega|$, there is no contribution to the integral from this region. For $|\mathbf{q}| < |\omega| < (\mathbf{q}^2 + m_\phi^2)^{\frac{1}{2}}$ both $\omega_\pm < 0$ and non of them makes (B.75) an equality. For $|\omega| > (\mathbf{q}^2 + m_\phi^2)^{\frac{1}{2}}$ both ω_\pm are always smaller than $|\omega|$ and (B.75) leads to $\omega_- < |\omega| < \omega_+$. Therefore

$$\int_1 d\omega_1 = \theta(q^2 - m_\phi^2) \int_{\omega_-}^{\omega_+} d\omega_1 \quad (\text{B.72})$$

$\delta(|\omega| + \omega_1 - \omega_2)$: Here the three conditions

$$|\omega| + \omega_1 > 0 \quad (\text{B.73})$$

$$\omega_1 > m_2 = 0 \quad (\text{B.74})$$

$$|x_{03}| < \omega_1 |\mathbf{q}| \quad (\text{B.75})$$

have to be fulfilled. In this case (B.75) is made an equality for $\omega_1 = -\omega_\pm$. Again the same regimes have to be distinguished. For $|\omega| < |\mathbf{q}|$ only $-\omega_-$ makes (B.75) an equality while $-\omega_+$ is negative and not a solution. $-\omega_-$ is positive as required by (B.74) and forms a lower bound. For $|\mathbf{q}| < |\omega| < (\mathbf{q}^2 + m_\phi^2)^{\frac{1}{2}}$ both $-\omega_\pm$ are positive and solutions. Due to its first order pole at $|\omega| = |\mathbf{q}|$ the solution $-\omega_+$ is now the larger one and forms an upper limit, leading to $-\omega_- < \omega_1 < -\omega_+$. For $|\omega| > (\mathbf{q}^2 + m_\phi^2)^{\frac{1}{2}}$ both $-\omega_\pm$ are negative and not solutions of (B.75) as an equality. Then there is no contribution to the integral from that region. Therefore

$$\int_3 d\omega_1 = \theta(-q^2) \int_{-\omega_-}^{\infty} d\omega_1 + \theta(q^2) \theta(m_\phi^2 - q^2) \int_{-\omega_-}^{-\omega_+} d\omega_1 \quad (\text{B.76})$$

$\delta(|\omega| - \omega_1 + \omega_2)$: The situation here is exactly the same as for δ_1 , in particular $x_{04} = x_{01}$, except that the condition $|\omega| - \omega_1 > 0$ has to be replaced by

$$|\omega| - \omega_1 < 0, \quad (\text{B.77})$$

enforcing $\omega_1 > |\omega|$. Again for $|\omega| < |\mathbf{q}|$ only ω_+ fulfils (B.70), imposing a lower bound on ω_1 and for $|\omega| > (\mathbf{q}^2 + m_\phi^2)^{\frac{1}{2}}$ both ω_\pm are solutions. ω_+ is the upper and ω_- the lower bound here. For $0 < q^2 < m_\phi^2$ none of ω_\pm is a valid solution. This time the condition (B.77) selects out the region $q^2 < 0$, hence the integral is

$$\int_4 d\omega_1 = \theta(-q^2) \int_{\omega_+}^{\infty} d\omega_1 \quad (\text{B.78})$$

The combined expressions are

$$\begin{aligned}
A_I &= \frac{-g^2}{16\pi|\mathbf{q}|} \left(\theta(q^2 - m_\phi^2) \left[\omega F_1 + G_1 \right]_{\omega_-}^{\omega_+} \right. \\
&\quad + \theta(-q^2) \left[\omega F_3 - G_3 \right]_{-\omega_-}^{\infty} + \theta(q^2) \theta(m_\phi^2 - q^2) \left[\omega F_3 - G_3 \right]_{-\omega_-}^{-\omega_+} \\
&\quad \left. + \theta(-q^2) \left[\omega F_4 + G_4 \right]_{\omega_+}^{\infty} \right) \tag{B.79}
\end{aligned}$$

and

$$\begin{aligned}
B_I &= \frac{-g^2}{16\pi|\mathbf{q}|} \left(\theta(q^2 - m_\phi^2) \left[F_1 \right]_{\omega_-}^{\omega_+} \right. \\
&\quad + \theta(-q^2) \left[F_3 \right]_{-\omega_-}^{\infty} + \theta(q^2) \theta(m_\phi^2 - q^2) \left[F_3 \right]_{-\omega_-}^{-\omega_+} \\
&\quad \left. + \theta(-q^2) \left[F_4 \right]_{\omega_+}^{\infty} \right) \tag{B.80}
\end{aligned}$$

with

$$F_1 = \frac{\omega_1}{\beta} \left(\ln(e^{\beta\omega_1} + 1) - \ln(1 - e^{\beta(\omega_1 - |\omega|)}) \right) + \frac{1}{\beta^2} \left(\text{Li}_2(-e^{\beta\omega_1}) - \text{Li}_2(e^{\beta(\omega_1 - |\omega|)}) \right) \tag{B.81}$$

$$F_3 = \frac{\omega_1}{\beta} \left(\ln(1 - e^{\beta(\omega_1 + |\omega|)}) - \ln(e^{\beta\omega_1} + 1) \right) + \frac{1}{\beta^2} \left(\text{Li}_2(e^{\beta(\omega_1 + |\omega|)}) - \text{Li}_2(-e^{\beta\omega_1}) \right) \tag{B.82}$$

$$F_4 = F_1 \tag{B.83}$$

and

$$\begin{aligned}
G_1 &= \text{sign}(\omega) \frac{m_\phi^2 - q^2}{2\beta} \left(-\ln(1 + e^{\beta\omega_1}) + \ln(e^{\beta\omega_1} - e^{\beta|\omega|}) \right) \\
&\quad + \frac{\omega\omega_1}{\beta} \left(\ln(1 - e^{\beta(\omega_1 - |\omega|)}) - \ln(1 + e^{\beta\omega_1}) \right) \\
&\quad + \frac{\omega}{\beta^2} \left(\text{Li}_2(e^{\beta(\omega_1 - |\omega|)}) - \text{Li}_2(-e^{\beta\omega_1}) \right) \tag{B.84}
\end{aligned}$$

$$\begin{aligned}
G_3 &= \text{sign}(\omega) \frac{m_\phi^2 - q^2}{2\beta} \left(\ln(1 + e^{\beta\omega_1}) - \ln(e^{\beta(\omega_1 + |\omega|)} - 1) \right) \\
&\quad + \frac{\omega\omega_1}{\beta} \left(\ln(1 - e^{\beta(\omega_1 + |\omega|)}) - \ln(1 + e^{\beta\omega_1}) \right) \\
&\quad + \frac{\omega}{\beta^2} \left(\text{Li}_2(e^{\beta(\omega_1 + |\omega|)}) - \text{Li}_2(-e^{\beta\omega_1}) \right) \tag{B.85}
\end{aligned}$$

$$G_4 = G_1. \quad (\text{B.86})$$

Li_2 is the dilogarithm function. The F_i as displayed here are not real in all areas of the parameter space due to the choice of different branches of the (di)logarithms, but the imaginary terms always cancel since the choice of branch is always the same at both integration limits in (B.79), (B.80). This analytic result for $\text{Im}\Sigma^R$ is in agreement with numerical plots shown in [72] as well as our own numerical cross-checks. The θ -functions are, as in (3.7), a consequence of energy- and momentum conservation. We have neglected interactions within the bath by using bare Ψ_2 - and ϕ -propagators. In the quasiparticle regime, those can to leading order be included by the replacement $m_\phi \rightarrow M_\phi(T)$, cf. Sec. 3.1.1 and the discussion in Sec.2.3.3. Note that the analytic structure we find disagrees with [7]. The author there claims that $\text{Im}\Sigma_{\mathbf{q}}^R(\omega) = 0$ for $q^2 < -|m_\phi^2 - m_2^2|$. We cannot confirm this.

B.3 Analytic Properties of Propagators and Self Energies

In the following we list a number of well-known, but convention-dependent relations for the propagators and self energies in equilibrium. All relations are not affected by the three-dimensional Fourier transform. We therefore drop the argument \mathbf{q} or \mathbf{x} . The properties of the fermionic propagators S and self-energies Σ are analogue.

Propagators:

$$\Delta^-(\omega)^* = -\Delta^-(\omega), \quad (\text{B.87})$$

$$\Delta^+(\omega)^* = \Delta^+(\omega), \quad (\text{B.88})$$

$$\Delta^A(\omega) = \frac{i}{2}\Delta^-(\omega) - \mathcal{P} \int_{-\infty}^{\infty} \frac{d\omega'}{2\pi} \frac{\Delta^-(\omega')}{\omega' - \omega}, \quad (\text{B.89})$$

$$\Delta^R(\omega) = -\frac{i}{2}\Delta^-(\omega) - \mathcal{P} \int_{-\infty}^{\infty} \frac{d\omega'}{2\pi} \frac{\Delta^-(\omega')}{\omega' - \omega}, \quad (\text{B.90})$$

$$\text{Re}\Delta^A(\omega) = -\text{Re}\Delta^R(\omega) = \frac{i}{2}\Delta^-(\omega), \quad (\text{B.91})$$

$$\text{Im}\Delta^A(\omega) = \text{Im}\Delta^R(\omega) = -\mathcal{P} \int_{-\infty}^{\infty} \frac{d\omega'}{2\pi i} \frac{\Delta^-(\omega')}{\omega' - \omega}, \quad (\text{B.92})$$

$$\Delta^A(-\omega) = \Delta^R(\omega). \quad (\text{B.93})$$

Self-energies:

$$\Pi^-(\omega)^* = -\Pi^-(\omega), \quad (\text{B.94})$$

$$\Pi^+(\omega)^* = \Pi^+(\omega), \quad (\text{B.95})$$

$$\Pi^A(\omega) = -\frac{1}{2}\Pi^-(\omega) + \mathcal{P} \int \frac{d\omega'}{2\pi i} \frac{\Pi^-(\omega')}{\omega' - \omega}, \quad (\text{B.96})$$

$$\Pi^R(\omega) = \frac{1}{2}\Pi^-(\omega) + \mathcal{P} \int \frac{d\omega'}{2\pi i} \frac{\Pi^-(\omega')}{\omega' - \omega}, \quad (\text{B.97})$$

$$\text{Re}\Pi^A(\omega) = \text{Re}\Pi^R(\omega) = \mathcal{P} \int \frac{d\omega'}{2\pi i} \frac{\Pi^-(\omega')}{\omega' - \omega}, \quad (\text{B.98})$$

$$\text{Im}\Pi^A(\omega) = -\text{Im}\Pi^R(\omega) = \frac{i}{2}\Pi^-(\omega), \quad (\text{B.99})$$

$$\Pi^A(-\omega) = \Pi^R(\omega). \quad (\text{B.100})$$

Relation to the Laplace transform:

$$\tilde{\Pi}^-(s = -i\omega + \epsilon) = \Pi_{\mathbf{q}}^R(\omega) \quad (\text{B.101})$$

$$\tilde{\Pi}^-(s = -i\omega - \epsilon) = \Pi_{\mathbf{q}}^A(\omega) \quad (\text{B.102})$$

B.4 S^+ in the narrow Width Limit and the use of Cauchy's Theorem

When performing the ω integration, all terms can be dissected into pieces that, as functions of ω , are proportional to expressions of the form

$$\int_{-\infty}^{\infty} \frac{d\omega}{2\pi} \frac{e^{\pm it\omega} \omega^k}{((\omega + i\Gamma)^2 - \omega_{\mathbf{q}}^2)((\omega - i\Gamma)^2 - \omega_{\mathbf{q}}^2)} \tanh\left(\frac{\beta\omega}{2}\right), \quad (\text{B.103})$$

where k can be zero, one or two and \pm indicate different alternatives. The integrand is finite along the real axis. Along the imaginary axis, the first factor grows on one side and falls on the other due to the exponential. The tanh has an infinite number of poles along the imaginary axis. To tackle the problem, we expand it in an infinite series,

$$\int_{-\infty}^{\infty} \frac{d\omega}{2\pi} \sum_{n=0}^{\infty} \frac{e^{\pm it\omega} \omega^k}{((\omega + i\Gamma)^2 - \omega_{\mathbf{q}}^2)((\omega - i\Gamma)^2 - \omega_{\mathbf{q}}^2)} \frac{\beta\omega}{(\frac{\beta\omega}{2})^2 + (\frac{\pi}{2} + n\pi)^2}. \quad (\text{B.104})$$

All poles are of first order. In addition to the four poles $\pm\omega_{\mathbf{q}} \pm i\Gamma$ there are infinitely many poles at $\pm\frac{i}{\beta}(1 + 2n)\pi$. To determine the integral along the real axis, we apply Cauchy's theorem. The exponential determines in which halfplane the contour has to be close, and

out of the four poles $\pm\omega_{\mathbf{q}} \pm i\Gamma$ always two contribute. For even k their contribution to the integral is

$$\frac{i}{4\Gamma\omega_{\mathbf{q}}}\text{Im}\left(e^{it(\pm\omega_{\mathbf{q}}+i\Gamma)}(\omega_{\mathbf{q}}\pm i\Gamma)^{k-1}\tanh\left(\frac{\beta(\omega_{\mathbf{q}}\pm i\Gamma)}{2}\right)\right) \quad (\text{B.105})$$

Here the \pm in the three places at which it shows up in (B.105) has to be chosen in accordance with the sign of the exponential in (B.103). For odd k the contribution is

$$\frac{1}{4\Gamma\omega_{\mathbf{q}}}\text{Re}\left(e^{it(\pm\omega_{\mathbf{q}}+i\Gamma)}(\omega_{\mathbf{q}}\pm i\Gamma)^{k-1}\tanh\left(\frac{\beta(\omega_{\mathbf{q}}\pm i\Gamma)}{2}\right)\right). \quad (\text{B.106})$$

In addition there is an infinite number of contributions from the poles of the tanh which are represented by the terms in (B.104). The contribution from the n -th term is

$$\pm i \frac{2}{\beta} \frac{e^{\pm i\omega_n t} \omega_n^k}{((\omega_n + i\Gamma)^2 - \omega_{\mathbf{q}}^2) ((\omega_n - i\Gamma)^2 - \omega_{\mathbf{q}}^2)} \quad (\text{B.107})$$

$$\omega_n = \pm \frac{i}{\beta} \pi(1 + 2n). \quad (\text{B.108})$$

This allows to determine the integral with arbitrary precision by taking into account sufficiently many terms. Obviously their contribution decreases sharply with increasing n . Numerical checks show that for $\Gamma_{\mathbf{q}} \ll m$, the contributions from the poles of the tanh are always many orders of magnitude smaller than those from $\pm\omega_{\mathbf{q}} \pm i\Gamma$. Simply using the latter gives results in very good agreement with exact numerical solutions.

Bibliography

- [1] V. Mukhanov, *Physical Foundations of Cosmology*, Cambridge University Press, Cambridge, 2005.
- [2] O. Lahav and A. R. Liddle, *The Cosmological Parameters*, arXiv:1002.3488 [astro-ph.CO].
- [3] E. W. Kolb and M. S. Turner, *The Early Universe*, (Addison-Wesley, Menlo Park, Ca., 1990).
- [4] C. Amsler *et al.* [Particle Data Group], *Review of Particle Physics*, Phys. Lett. B **667**, 1 (2008).
- [5] A. Anisimov, W. Buchmuller, M. Drewes and S. Mendizabal, *Nonequilibrium Dynamics of Scalar Fields in a Thermal Bath*, Annals Phys. **324** (2009) 1234 [arXiv:0812.1934 [hep-th]].
- [6] L. D. Landau, *The Theory of a Fermi Liquid*, Soviet Phys. JETP. 3, 920 (1957).
- [7] H. A. Weldon, *Simple Rules for Discontinuities in Finite Temperature Field Theory*, Phys. Rev. D **28** (1983) 2007.
- [8] J. Berges, *Introduction to Nonequilibrium Quantum Field Theory*, AIP Conf. Proc. **739** (2005) 3 [hep-ph/0409233].
- [9] D. Boyanovsky, K. Davey and C. M. Ho, *Particle Abundance in a thermal Plasma: Quantum Kinetics vs. Boltzmann Equation*, Phys. Rev. D **71** (2005) 023523 [arXiv:hep-ph/0411042].
- [10] M. Le Bellac, *Thermal Field Theory*, Cambridge University Press 1996
- [11] M. Kobayashi and T. Maskawa, *CP Violation in the Renormalizable Theory of Weak Interaction*, Prog. Theor. Phys. **49** (1973) 652.

- [12] T. Yanagida, in Proc. of the Workshop on *The Unified Theory and the Baryon Number in the Universe*, Tsukuba, Japan, Feb. 13-14, 1979, p. 95, eds. O. Sawada and S. Sugamoto, (KEK Report KEK-79-18, 1979, Tsukuba); Progr. Theor. Phys. **64**, 1103 (1980); P. Ramond, in Talk given at the Sanibel Symposium, Palm Coast, Fla., Feb. 25-Mar. 2, 1979, preprint CALT-68-709.u!
- [13] M. Fukugita and T. Yanagida, *Baryogenesis Without Grand Unification*, Phys. Lett. B **174** (1986) 45.
- [14] R. N. Mohapatra and G. Senjanovic, *Neutrino Masses and Mixings in Gauge Models with Spontaneous Parity Violation*, Phys. Rev. D **23** (1981) 165.
- [15] R. Foot, H. Lew, X. G. He and G. C. Joshi, *Seesaw Neutrino Masses induced by a Triplet of Leptons*, Z. Phys. C **44** (1989) 441.
E. Ma, *Pathways to Naturally Small Neutrino Masses*, Phys. Rev. Lett. **81** (1998) 1171 [arXiv:hep-ph/9805219].
- [16] A. Abada, S. Davidson, A. Ibarra, F. X. Josse-Michaux, M. Losada and A. Riotto, *Flavour matters in Leptogenesis*, JHEP **0609** (2006) 010 [arXiv:hep-ph/0605281].
E. Nardi, Y. Nir, E. Roulet and J. Racker, *The Importance of Flavor in Leptogenesis*, JHEP **0601** (2006) 164 [arXiv:hep-ph/0601084].
R. Barbieri, P. Creminelli, A. Strumia and N. Tetradis, *Baryogenesis through Leptogenesis*, Nucl. Phys. B **575** (2000) 61 [hep-ph/9911315];
T. Endoh, T. Morozumi and Z. h. Xiong, *Primordial Lepton Family Asymmetries in Seesaw Model*, Prog. Theor. Phys. **111** (2004) 123 [hep-ph/0308276];
A. Abada, S. Davidson, F. X. Josse-Michaux, M. Losada and A. Riotto, *Flavour Issues in Leptogenesis*, JCAP **0604** (2006) 004 [hep-ph/0601083];
S. Blanchet, P. Di Bari and G. G. Raffelt, *Quantum Zeno Effect and the Impact of Flavor in Leptogenesis*, JCAP **0703** (2007) 012 [hep-ph/0611337].
- [17] L. P. Kadanoff and G. Baym, *Quantum Statistical Mechanics*, Benjamin, New York, 1962.
- [18] J. S. Schwinger, *Brownian Motion of a Quantum Oscillator*, J. Math. Phys. **2**, 407 (1961).
- [19] P. M. Bakshi and K. T. Mahanthappa, *Expectation Value Formalism in Quantum Field Theory. 1*, J. Math. Phys. **4**, 1 (1963).
- [20] P. M. Bakshi and K. T. Mahanthappa, *Expectation Value Formalism in Quantum Field Theory. 2*, J. Math. Phys. **4**, 12 (1963).
- [21] L. V. Keldysh, *Diagram Technique for Nonequilibrium Processes*, Zh. Eksp. Teor. Fiz. **47**, 1515 (1964) [Sov. Phys. JETP **20**, 1018 (1965)].

- [22] K. c. Chou, Z. b. Su, B. l. Hao and L. Yu, *Equilibrium and Nonequilibrium Formalisms made unified*, Phys. Rept. **118** (1985) 1.
- [23] G. Sigl and G. Raffelt, *General kinetic Description of relativistic mixed Neutrinos*, Nucl. Phys. B **406** (1993) 423.
- [24] J. M. Cornwall, R. Jackiw and E. Tomboulis, *Effective Action for Composite Operators*, Phys. Rev. D **10** (1974) 2428.
- [25] A. Hohenegger, A. Kartavtsev and M. Lindner, *Deriving Boltzmann Equations from Kadanoff-Baym Equations in Curved Space-Time*, arXiv:0807.4551 [hep-ph].
- [26] J. Berges, A. Rothkopf and J. Schmidt, *Non-thermal Fixed Points: Effective weak-coupling for strongly correlated Systems far from Equilibrium*, Phys. Rev. Lett. **101** (2008) 041603 [arXiv:0803.0131 [hep-ph]].
- [27] W. Israel, *Nonstationary Irreversible Thermodynamics: A Causal Relativistic Theory*, Annals Phys. **100** (1976) 310.
- [28] H. A. Weldon, *Covariant Calculations at finite Temperature: The Relativistic Plasma*, Phys. Rev. D **26** (1982) 1394.
- [29] N. P. Landsman and C. G. van Weert, *Real and Imaginary Time Field Theory at Finite Temperature and Density*, Phys. Rept. **145** (1987) 141.
- [30] F. Bloch, *Zur Theorie des Austauschproblems und der Remanenzerscheinung der Ferromagnetika* Z.Physik **74** (1932) 295.
- [31] T. Matsubara, *A new Approach to Quantum Statistical Mechanics*, Prog. Theor. Phys. **14** (1955) 351.
- [32] J. Yokoyama, *Fate of oscillating scalar Fields in the thermal Bath and their cosmological Implications*, Phys. Rev. D **70** (2004) 103511 [arXiv:hep-ph/0406072].
- [33] J. Yokoyama, *Can oscillating scalar Fields decay into Particles with a large thermal Mass?*, Phys. Lett. B **635** (2006) 66 [arXiv:hep-ph/0510091].
- [34] J. Zinn-Justin, *Quantum Field Theory and Critical Phenomena*, Int. Ser. Monogr. Phys. **85** (1993) 1.
- [35] M. Morikawa, *Classical Fluctuations in dissipative Quantum Systems*, Phys. Rev. D **33** (1986) 3607.
- [36] M. Yamaguchi and J. Yokoyama, *Numerical Approach to the Onset of the Electroweak Phase Transition*, Phys. Rev. D **56** (1997) 4544 [arXiv:hep-ph/9707502].

- [37] C. Greiner and B. Muller, *Classical Fields near thermal Equilibrium*, Phys. Rev. D **55** (1997) 1026 [arXiv:hep-th/9605048].
- [38] M. Gleiser and R. O. Ramos, *Microphysical Approach to Nonequilibrium Dynamics of Quantum Fields*, Phys. Rev. D **50** (1994) 2441 [arXiv:hep-ph/9311278].
- [39] C. Greiner and S. Leupold, *Stochastic Interpretation of Kadanoff-Baym Equations and their Relation to Langevin Processes*, Annals Phys. **270** (1998) 328 [arXiv:hep-ph/9802312].
- [40] M. Drewes, Diplomarbeit, DESY 2006 *Damping of the Oscillations of a scalar Field in a bosonic Plasma*, (in German, hardcopy at DESY)
- [41] S. Borsanyi and U. Reinosa, *Renormalised Nonequilibrium Quantum Field Theory: Scalar Fields*, arXiv:0809.0496 [hep-th].
- [42] M. Garny and M. M. Muller, *Kadanoff-Baym Equations with Non-Gaussian Initial Conditions: The Equilibrium Limit*, arXiv:0904.3600 [hep-ph].
- [43] J. Berges, S. Borsanyi and C. Wetterich, *Prethermalization*, Phys. Rev. Lett. **93** (2004) 142002 [arXiv:hep-ph/0403234].
- [44] D. I. Podolsky, G. N. Felder, L. Kofman and M. Peloso, *Equation of State and Beginning of Thermalization after Preheating*, Phys. Rev. D **73**, 023501 (2006) [arXiv:hep-ph/0507096].
- [45] D. Zubarev, V. Morozov, Gerd Röpke, *Statistical Mechanics of Nonequilibrium Processes*, Akademie Verlag 1996
Esteban A. Calzetta, Bei-Lok B. Hu, *Nonequilibrium Quantum Field Theory*, Cambridge University Press 2008
- [46] T. Altherr and D. Seibert, *Problems of Perturbation Series in Nonequilibrium Quantum Field Theories*, Phys. Lett. B **333** (1994) 149 [arXiv:hep-ph/9405396].
- [47] A. Anisimov, W. Buchmuller, M. Drewes and S. Mendizabal, *Leptogenesis from Quantum Interference in a Thermal Bath*, accepted by Phys. Rev. Lett. , arXiv:1001.3856 [hep-ph].
- [48] Zhou Guang-Zhao (K.C.Chou) and Su Zhao-Bin, Ch.5 in *Progress in Statistical Physics* (in Chinese), eds., Bai-Jin Hao et.al.. (Science Press, Beijing, 1981) p.268
- [49] W. Buchmuller and S. Fredenhagen, *Quantum Mechanics of Baryogenesis*, Phys. Lett. B **483** (2000) 217 [arXiv:hep-ph/0004145].

- [50] A. De Simone and A. Riotto, *Quantum Boltzmann Equations and Leptogenesis*, JCAP **0708** (2007) 002 [arXiv:hep-ph/0703175].
By the time of printing, a computation based on a similar approach has been published in:
M. Beneke, B. Garbrecht, M. Herranen and P. Schwaller, *Finite Number Density Corrections to Leptogenesis*, arXiv:1002.1326 [hep-ph].
- [51] M. Garny, A. Hohenegger, A. Kartavtsev and M. Lindner, *Systematic approach to Leptogenesis in nonequilibrium QFT: Vertex Contribution to the CP-violating Parameter*, Phys. Rev. D **80** (2009) 125027 [arXiv:0909.1559 [hep-ph]].
By the time of printing, this work has been continued in:
M. Garny, A. Hohenegger, A. Kartavtsev and M. Lindner, *Systematic approach to Leptogenesis in nonequilibrium QFT: Self-Energy Contribution to the CP-violating Parameter*, arXiv:0911.4122 [hep-ph].
M. Garny, A. Hohenegger and A. Kartavtsev, *Medium corrections to the CP-violating parameter in leptogenesis*, arXiv:1002.0331 [hep-ph].
- [52] M. Lindner and M. M. Müller, *Comparison of Boltzmann Equations with Quantum Dynamics for scalar Fields*, Phys. Rev. D **73** (2006) 125002 [arXiv:hep-ph/0512147].
- [53] A. De Simone and A. Riotto, *On Resonant Leptogenesis*, JCAP **0708** (2007) 013 [arXiv:0705.2183 [hep-ph]].
- [54] V. Cirigliano, A. De Simone, G. Isidori, I. Masina and A. Riotto, *Quantum Resonant Leptogenesis and minimal Lepton Flavour Violation*, JCAP **0801** (2008) 004 [arXiv:0711.0778 [hep-ph]].
- [55] L. Covi, N. Rius, E. Roulet and F. Vissani, *Finite Temperature Effects on CP violating Asymmetries*, Phys. Rev. D **57** (1998) 93 [arXiv:hep-ph/9704366].
G. F. Giudice, A. Notari, M. Raidal, A. Riotto and A. Strumia, *Towards a complete Theory of thermal Leptogenesis in the SM and MSSM*, Nucl. Phys. B **685** (2004) 89 [arXiv:hep-ph/0310123].
- [56] R. E. Cutkosky, *Singularities and Discontinuities of Feynman Amplitudes*, J. Math. Phys. **1** (1960) 429.
- [57] R. Kobes, G. Semenoff, *Cutkosky Rules for Condensed-Matter Systems*, Phys. Rev. B **34**, 4338-4341
- [58] E. Braaten and R. D. Pisarski, *Resummation and Gauge Invariance of the Gluon Damping Rate in Hot QCD*, Phys. Rev. Lett. **64** (1990) 1338.
E. Braaten and R. D. Pisarski, *Soft Amplitudes in Hot Gauge Theories: A General Analysis*, Nucl. Phys. B **337**, 569 (1990).

- [59] R. Baier, D. Schiff and B. G. Zakharov, *Energy Loss in perturbative QCD*, Ann. Rev. Nucl. Part. Sci. **50** (2000) 37 [arXiv:hep-ph/0002198].
M. Gyulassy, I. Vitev, X. N. Wang and B. W. Zhang, *Jet Quenching and radiative Energy Loss in dense nuclear Matter*, arXiv:nucl-th/0302077.
- [60] E. Braaten and R. D. Pisarski, *Calculation of the Gluon Damping Rate in Hot QCD*, Phys. Rev. D **42** (1990) 2156.
- [61] U. Kraemmer and A. Rebhan, *Advances in perturbative Thermal Field Theory*, Rept. Prog. Phys. **67** (2004) 351 [arXiv:hep-ph/0310337].
- [62] R. Arnaldi *et al.* [NA60 Collaboration], *First Measurement of the Rho Spectral Function in High-Energy Nuclear Collisions*, Phys. Rev. Lett. **96** (2006) 162302 [arXiv:nucl-ex/0605007].
- [63] F. Karsch and E. Laermann, *Thermodynamics and In-Medium Hadron Properties from Lattice QCD*, arXiv:hep-lat/0305025.
O. Philipsen, *Lattice QCD at finite Temperature and Density*, Eur. Phys. J. ST **152** (2007) 29 [arXiv:0708.1293 [hep-lat]].
- [64] M. Laine, O. Philipsen and M. Tassler, *Wilson Loop in Classical Lattice Gauge Theory and the Thermal Width of Heavy Quarkonium*, PoS **LAT2007** (2007) 230 [arXiv:0710.0504 [hep-lat]].
- [65] J. M. Maldacena, *The large N Limit of Superconformal Field Theories and Supergravity*, Adv. Theor. Math. Phys. **2** (1998) 231 [Int. J. Theor. Phys. **38** (1999) 1113] [arXiv:hep-th/9711200].
- [66] D. T. Son and A. O. Starinets, *Minkowski-Space Correlators in AdS/CFT Correspondence: Recipe and Applications*, JHEP **0209**, 042 (2002) [arXiv:hep-th/0205051].
C. P. Herzog and D. T. Son, *Schwinger-Keldysh Propagators from AdS/CFT Correspondence*, JHEP **0303** (2003) 046 [arXiv:hep-th/0212072].
P. K. Kovtun and A. O. Starinets, *Quasinormal Modes and Holography*, Phys. Rev. D **72** (2005) 086009 [arXiv:hep-th/0506184].
- [67] J. Erdmenger, N. Evans, I. Kirsch and E. Threlfall, *Mesons in Gauge/Gravity Duals - A Review*, Eur. Phys. J. A **35** (2008) 81 [arXiv:0711.4467 [hep-th]].
J. Babington, J. Erdmenger, N. J. Evans, Z. Guralnik and I. Kirsch, *Chiral Symmetry Breaking and Pions in non-supersymmetric Gauge / Gravity Duals*, Phys. Rev. D **69** (2004) 066007 [arXiv:hep-th/0306018].
- [68] R. R. Parwani, *Resummation In A Hot Scalar Field Theory*, Phys. Rev. D **45** (1992) 4695 [Erratum-ibid. D **48** (1993) 5965] [arXiv:hep-ph/9204216].

- [69] S. Jeon, *Hydrodynamic Transport Coefficients in relativistic Scalar Field Theory*, Phys. Rev. D **52**, 3591 (1995) [arXiv:hep-ph/9409250].
- [70] E. k. Wang, U. W. Heinz and X. f. Zhang, *Spectral functions for composite Fields and Viscosity in Hot Scalar Field Theory*, Phys. Rev. D **53** (1996) 5978 [arXiv:hep-ph/9509331].
- [71] A. Berera, M. Gleiser and R. O. Ramos, *Strong dissipative Behavior in Quantum Field Theory*, Phys. Rev. D **58** (1998) 123508 [arXiv:hep-ph/9803394].
- [72] M. Kitazawa, T. Kunihiro and Y. Nemoto, *Novel Collective Excitations and the Quasi-Particle Picture of Quarks coupled with a massive Boson at finite Temperature*, Prog. Theor. Phys. **117** (2007) 103 [arXiv:hep-ph/0609164].
- [73] E. Komatsu *et al.* [WMAP Collaboration], *Five-Year Wilkinson Microwave Anisotropy Probe Observations: Cosmological Interpretation*, Astrophys. J. Suppl. **180** (2009) 330 [arXiv:0803.0547 [astro-ph]].
- [74] A. Linde, *Inflationary Cosmology*, Lect. Notes Phys. **738** (2008) 1 [arXiv:0705.0164 [hep-th]].
- [75] L. Kofman, A. D. Linde and A. A. Starobinsky, *Towards the Theory of Reheating after Inflation*, Phys. Rev. D **56** (1997) 3258 [arXiv:hep-ph/9704452].
R. Allahverdi, R. Brandenberger, F. Y. Cyr-Racine and A. Mazumdar, *Reheating in Inflationary Cosmology: Theory and Applications*, arXiv:1001.2600 [hep-th].
- [76] T. Moroi, H. Murayama and M. Yamaguchi, *Cosmological Constraints on the light stable Gravitino*, Phys. Lett. B **303** (1993) 289.
- [77] J. Yokoyama, *Thermal Background can solve the Cosmological Moduli Problem*, Phys. Rev. Lett. **96** (2006) 171301 [arXiv:hep-ph/0601067].
- [78] D. Bodeker, *Moduli Decay in the hot Early Universe*, JCAP **0606** (2006) 027 [arXiv:hep-ph/0605030].
- [79] W. Buchmuller, K. Hamaguchi, O. Lebedev and M. Ratz, *Dilaton Destabilization at high Temperature*, Nucl. Phys. B **699** (2004) 292 [arXiv:hep-th/0404168],
W. Buchmuller, K. Hamaguchi, O. Lebedev and M. Ratz, *Maximal Temperature in Flux Compactifications*, JCAP **0501** (2005) 004 [arXiv:hep-th/0411109].
- [80] E. W. Kolb, A. Notari and A. Riotto, *On the Reheating Stage after Inflation*, Phys. Rev. D **68** (2003) 123505 [arXiv:hep-ph/0307241].
- [81] E. W. Kolb, A. D. Linde and A. Riotto, *GUT Baryogenesis after Preheating*, Phys. Rev. Lett. **77** (1996) 4290 [arXiv:hep-ph/9606260].

- [82] E. W. Kolb, A. Riotto and I. I. Tkachev, *GUT Baryogenesis after Preheating: Numerical Study of the Production and Decay of X-Bosons*, Phys. Lett. B **423** (1998) 348 [arXiv:hep-ph/9801306].
- [83] G. N. Felder and L. Kofman, *The Development of Equilibrium after Preheating*, Phys. Rev. D **63** (2001) 103503 [arXiv:hep-ph/0011160].
- [84] A. Berera, *Warm Inflation*, Phys. Rev. Lett. **75** (1995) 3218 [arXiv:astro-ph/9509049].
 J. Yokoyama and A. D. Linde, *Is warm Inflation possible?*, Phys. Rev. D **60** (1999) 083509 [arXiv:hep-ph/9809409].
 A. Berera, I. G. Moss and R. O. Ramos, *Warm Inflation and its Microphysical Basis*, Rept. Prog. Phys. **72** (2009) 026901 [arXiv:0808.1855 [hep-ph]].
- [85] A. S. Beach *et al.*, *Measurement of the Cosmic-Ray Antiproton to Proton Abundance Ratio between 4-GeV and 50-GeV*, Phys. Rev. Lett. **87** (2001) 271101 [arXiv:astro-ph/0111094].
- [86] J. Dunkley *et al.* [WMAP Collaboration], *Five-Year Wilkinson Microwave Anisotropy Probe (WMAP) Observations: Likelihoods and Parameters from the WMAP Data*, Astrophys. J. Suppl. **180** (2009) 306 [arXiv:0803.0586 [astro-ph]].
- [87] B. Fields and S. Sarkar, *Big-Bang Nucleosynthesis* (PDG mini-review), arXiv:astro-ph/0601514.
- [88] A. D. Sakharov, *Violation of CP Invariance, c Asymmetry, and Baryon Asymmetry of the Universe*, Pisma Zh. Eksp. Teor. Fiz. **5** (1967) 32 [JETP Lett. **5** (1967) 34, 392-393.1991 UFNAA,161,61-64.1991) 24].
- [89] V. A. Rubakov and M. E. Shaposhnikov, *Electroweak Baryon Number Non-Conservation in the Early Universe and in High-Energy Collisions*, Usp. Fiz. Nauk **166** (1996) 493 [Phys. Usp. **39** (1996) 461] [arXiv:hep-ph/9603208].
- [90] G. 't Hooft, *Symmetry Breaking through Bell-Jackiw Anomalies*, Phys. Rev. Lett. **37** (1976) 8.
- [91] K. Jansen, *Status of the Finite Temperature Electroweak Phase Transition on the Lattice*, Nucl. Phys. Proc. Suppl. **47** (1996) 196 [arXiv:hep-lat/9509018].
- [92] M. E. Shaposhnikov, *Baryon Asymmetry of the Universe in Standard Electroweak Theory*, Nucl. Phys. B **287** (1987) 757.
- [93] M. B. Gavela, P. Hernandez, J. Orloff and O. Pene, *Standard Model CP-Violation and Baryon Asymmetry*, Mod. Phys. Lett. A **9** (1994) 795 [arXiv:hep-ph/9312215].

- [94] M. Yoshimura, *Unified Gauge Theories and the Baryon Number of the Universe*, Phys. Rev. Lett. **41** (1978) 281 [Erratum-ibid. **42** (1979) 746].
D. Toussaint, S. B. Treiman, F. Wilczek and A. Zee, *Matter - Antimatter Accounting, Thermodynamics, and Black Hole Radiation*, Phys. Rev. D **19** (1979) 1036.
S. Weinberg, *Cosmological Production Of Baryons*, Phys. Rev. Lett. **42** (1979) 850. S. Dimopoulos and L. Susskind, *On the Baryon Number of the Universe*, Phys. Rev. D **18** (1978) 4500.
- [95] I. Affleck and M. Dine, *A New Mechanism for Baryogenesis*, Nucl. Phys. B **249** (1985) 361.
- [96] A. Riotto and M. Trodden, *Recent Progress in Baryogenesis*, Ann. Rev. Nucl. Part. Sci. **49** (1999) 35 [arXiv:hep-ph/9901362].
- [97] W. Buchmuller, P. Di Bari and M. Plumacher, *Leptogenesis for Pedestrians*, Annals Phys. **315** (2005) 305 [arXiv:hep-ph/0401240].
W. Buchmuller, R. D. Peccei and T. Yanagida, *Leptogenesis as the Origin of Matter*, Ann. Rev. Nucl. Part. Sci. **55** (2005) 311 [arXiv:hep-ph/0502169].
- [98] F. Hahn-Woernle, M. Plumacher and Y. Y. Y. Wong, *Full Boltzmann Equations for Leptogenesis including Scattering*, JCAP **0908** (2009) 028 [arXiv:0907.0205 [hep-ph]].
- [99] M. Lindner and M. M. Muller, *Comparison of Boltzmann Kinetics with Quantum Dynamics for a Chiral Yukawa Model far from Equilibrium*, Phys. Rev. D **77** (2008) 025027 [arXiv:0710.2917 [hep-ph]].
- [100] W. Buchmuller and M. Plumacher, *Spectator Processes and Baryogenesis*, Phys. Lett. B **511**, 74 (2001) [arXiv:hep-ph/0104189].
- [101] B. Pontecorvo, *Inverse Beta Processes and Nonconservation of Lepton Charge*, Sov. Phys. JETP **7** (1958) 172 [Zh. Eksp. Teor. Fiz. **34** (1957) 247].
- [102] Z. Maki, M. Nakagawa and S. Sakata, *Remarks on the Unified Model of Elementary Particles*, Prog. Theor. Phys. **28** (1962) 870.
- [103] J. Morales, C. Quimbay and F. Fonseca, *Fermionic Dispersion Relations at finite Temperature and non-vanishing Chemical Potentials in the Minimal Standard Model*, Nucl. Phys. B **560** (1999) 601 [arXiv:hep-ph/9906207].